CONTINUOUS RESERVOIR SIMULATION MODEL UPDATING AND FORECASTING USING A MARKOV CHAIN MONTE CARLO METHOD

A Thesis

by

Chang Liu

Submitted to the Office of Graduate Studies of
Texas A&M University
in partial fulfillment of the requirements for the degree of

MASTER OF SCIENCE

December 2008

Major Subject: Petroleum Engineering

CONTINUOUS RESERVOIR SIMULATION MODEL UPDATING AND FORECASTING USING A MARKOV CHAIN MONTE CARLO METHOD

A Thesis

by

Chang Liu

Submitted to the Office of Graduate Studies of
Texas A&M University
in partial fulfillment of the requirements for the degree of

MASTER OF SCIENCE

Approved by:

Chair of Committee,	Duane A. McVay
Committee Members,	Akhil Datta-Gupta
	Jianhua Huang
Head of Department,	Stephen A. Holditch

December 2008

Major Subject: Petroleum Engineering

ABSTRACT

Continuous Reservoir Simulation Model Updating and Forecasting Using a Markov Chain Monte Carlo Method.

(December 2008)

Chang Liu, B.A., Peking University, China

Chair of Advisory Committee: Dr. Duane A. McVay

Currently, effective reservoir management systems play a very important part in exploiting reservoirs. Fully exploiting all the possible events for a petroleum reservoir is a challenge because of the infinite combinations of reservoir parameters. There is much unknown about the underlying reservoir model, which has many uncertain parameters. MCMC (Markov Chain Monte Carlo) is a more statistically rigorous sampling method, with a stronger theoretical base than other methods. The performance of the MCMC method on a high dimensional problem is a timely topic in the statistics field.

This thesis suggests a way to quantify uncertainty for high dimensional problems by using the MCMC sampling process under the Bayesian frame. Based on the improved method, this thesis reports a new approach in the use of the continuous MCMC method for automatic history matching. The assimilation of the data in a continuous process is done sequentially rather than simultaneously. In addition, by doing a continuous process, the MCMC method becomes more applicable for the industry. Long periods of time to run just one realization will no longer be a big problem during the sampling process. In

addition, newly observed data will be considered once it is available, leading to a better estimate.

The PUNQ-S3 reservoir model is used to test two methods in this thesis. The methods are: STATIC (traditional) SIMULATION PROCESS and CONTINUOUS SIMULATION PROCESS. The continuous process provides continuously updated probabilistic forecasts of well and reservoir performance, accessible at any time. It can be used to optimize long-term reservoir performance at field scale.

DEDICATION

To all my friends who have always stood by me

ACKNOWLEDGEMENTS

I would like to thank my parents for their continuing support of my pursuit of knowledge.

TABLE OF CONTENTS

Page

Page

LIST OF TABLES

Page

LIST OF FIGURES

Page

Page

Page

Page

INTRODUCTION

Determining how to effectively exploit oil and gas reservoirs is a central goal in reservoir management (Thakur 1996). Today's competitive economic situation requires cost-effective production technology to profitability produce marginal petroleum reservoirs. Reservoir simulation is regarded as a critical tool in modern reservoir management (Thomas 1986). It enables assessment of reservoir properties and, when a forecast run is made, an assessment of future production and reserves. These assessments feed directly into the decision-making process.

Capen (1976) demonstrated thirty years ago that people in the petroleum industry often significantly underestimate uncertainty in their assessments. In keeping with this tendency, reservoir simulation engineers traditionally take only limited consideration of uncertainty and in many cases do not try to quantify it at all. Quantifying uncertainty in production forecasts is not a trivial undertaking. When quantifying the uncertainties, all possible outcomes of uncertain events should be considered and assigned probabilities in order to build up a probability density function of the result of interest, e.g., reserves (Howard 2005). Expressing results in term so probability

---

This thesis follows the style of *SPE Journal*.

distributions enables better decision making. However, the decision may be poor if the uncertainty quantification in a forecast is incomplete, or nonexistent. For this reason it is necessary to rigorously quantify uncertainty in production forecast.

Unfortunately, fully assessing all the possible events for a petroleum reservoir is a quite challenging because the reservoir parameter space, the set of all possible combinations of reservoir parameters, is literally infinite. Recent study, e.g., Floris et al. (2001), has shown that, even when we explicitly try to quantify uncertainty in simulation studies, we still tend to underestimate it. Therefore, it is worthwhile to explore reservoir simulation techniques aimed at better quantifying uncertainty in forecasts.

Because of the time and manpower required to tune each parameter in order to history match a simulation model, reservoir studies are usually expensive. Traditional simulation studies are usually done only at discrete points in the life of a reservoir, e.g., when considering a major investment. As such, smaller reservoir management decisions typically do not warrant the expense of a simulation study and thus must proceed without simulation results. As a result, uncalibrated forecasts or no forecasts at all could lead to sub-optimal operations and significant economic consequences. Clearly, reservoir management would benefit if a calibrated simulation model was available at any time.

BACKGROUND

Uncertainty Quantification Techniques

In the past few years, significant work on developing more rigorous uncertainty quantification has been presented in the literature. Specifically, in the PUNQ work, which is probably the most thorough treatment of uncertainty quantification in production forecasts, several industrial and academic partners used different methods to quantify the uncertainties. The overall objective of the PUNQ project was to determine whether a methodology can be developed that propagates the combined reservoir modeling, reservoir parameter and well observation uncertainties to production forecasting uncertainty in a formally unbiased way.

In this study, we will try to quantify the uncertainty of the reservoir associate with observed history data, which is called history matching. The main process of performing a history matching method includes three steps. First, the reservoir is defined in terms of a reservoir parameter set describing the geometry and flow properties. Next, the uncertainty parameters of the reservoir are determined by assigning with probabilistic distributions. Finally, based on the sampled reservoir model, we compare the data from the simulator with the actual observed data to minimize the objective function, which is used in the reservoir simulation process to quantify the difference between simulation results and observed data. Lots of methods exist for searching reasonable models. I will describe some of them below.

Gradient Methods

Gradient methods are used for minimizing the objective function. The Steepest Descent Method(Bos 1999), the Coordinate Descent Method, and the Conjugate Gradient Method are three methods widely used to find the direction of variables. Every one of them uses an iterative formula that contains the gradient of the objective function to find the minimum, hence the name "Gradient Methods." The goal of these methods is optimization, which means the result usually comes out to be just one best reservoir model that fits observation. The method can be stopped when the maximum number of iterations is exceeded or the requested accuracy is obtained for the solution.

The limitation of the gradient method is that we are usually concerned with getting a range of what will happen in the future with associated probabilities. Specifically, the optimum case may not fit our objective in case when we want to get an uncertainty range instead of one optimum model. Also, the gradient method only works well for smooth functions. As the reservoir model is usually complicated, the function we are trying to optimize is usually not smooth. Using gradient methods can lead to biased optimization.

MCMC Method

The Markov Chain Monte Carlo (MCMC) method has been widely used as a strong tool to sample from a complicated distribution function, especially when we do not know the exact form of that function. This method originated in physics as a tool for exploring equilibrium distributions of interacting molecules. In statistical applications, it is used to

generate pseudo-random draws from multidimensional and otherwise intractable probability distributions via Markov chains. A Markov chain is a sequence of random variables in which each element depends only on the value of the previous one. In MCMC simulation, one constructs a Markov chain long enough for the distribution of the elements to stabilize to a stationary distribution, which is the distribution of interest. By repeatedly simulating steps of the chain, the method simulates draws from the distribution of interest.

In reservoir modeling research, MCMC has been applied as a method for exploring posterior distributions in Bayesian inference. The final distribution is simply generated from a set of samples, which are reservoir models in our study. First, a randomly sampled model is built up from a prior distribution. It is also the start point of the Markov chain. Then, the next model is randomly chosen with some constraints related to the previous model which is already in the chain. After the chain is run long enough, we are able to use the models in the chain to generate the posterior distribution. Once the distribution is generated, it is easy to get the range of uncertain parameters with specific probabilities.

Another related method for generating an unknown distribution is called Genetic Algorithm (Goldberg 1989), which has a variety of applications. Genetic algorithms (GAs) are a broad class of optimization algorithms based loosely upon the rules that govern genetics in nature. In a GA, “generations” of unique reservoir models are created by mixing parameter values of previously run models in a process known as “breeding.” Finally, all generations are used to generate a distribution (Holmes et al. 2007).

Compared to GAs, MCMC is statistically more rigorous by working under the Bayesian frame. It can also be considered to be a type of GA because the next model relies on some properties of the previous one, which can be regarded as its parent in GAs.

Although the Markov Chain Monte Carlo methodology is straightforward, how to efficiently generate the posterior distribution can be quite challenging. The chain often converges too slowly in history matching, especially when the parameter space is large. A two-stage MCMC method (Ma et al. 2006) has been used to solve this particular problem by enhancing the acceptance rate of the next model. Also, Holden (1998) has suggested an adaptive MCMC method by using all the previous models which are already in the chain to generate the next one.

Real-Time Data and Ensemble Kalman Filter

Ensemble Kalman Filter (EnKF) techniques are widely used in both statistical field and petroleum industry field to utilize all available data in order to make probabilistic forecasts. The EnKF is a Monte Carlo approach, which is promising with respect to achieving uncertainty quantification through continuous model updating and reservoir monitoring (Nævdal et al. 2003; Gu and Oliver 2004; Bianco et al. 2007; Devegowda et al. 2007). The assimilation of data in EnKF is done sequentially rather than simultaneously as is done in traditional history matching. By doing so the reservoir models are always kept up to date.

The EnKF starts with an ensemble of reservoir models conditioned to all available static

data, e.g., cores, well logs and structural information (Devegowda et al. 2007). These geologic models constitute the initial ensemble and represent the variability in the underlying reservoir properties. As and when data become available, the EnKF updates each of these model realizations using statistical information derived from the ensemble of models and model predicted data, specifically the cross-covariance between the data and the model variables. This step is repeated when more data become available. The underlying algorithm is computationally efficient because the computation of gradients or sensitivities is eliminated and the updates depend solely on statistical information. Consequently, the EnKF generates a suite of plausible model realizations conditioned to production history and, in theory, should honor prior static or geologic information. However, due to the inherent noise in any statistical measure that is dependent on the number of samples or model realizations, the EnKF updates can lead to geologically-inconsistent realizations for small ensemble sizes. Therefore, while the final realizations may honor historical production data, the models do not conform to the prior geologic information (Devegowda et al. 2007). The use of a larger ensemble size may mitigate some of the difficulties in the implementation of the EnKF, but for field-scale problems this may be computationally expensive. For very small ensemble sizes, the individual ensemble members tend to converge to a single realization and progressively ignore future observations. The literature shows examples of the EnKF applied to field studies (Devegowda et al. 2007), but many of the problems described above remain unresolved. Some techniques attempt to improve EnKF performance through better estimates of the cross-covariance matrix using covariance localization techniques. Others have used the gradient of an appropriately defined objective function to derive other

variants of the EnKF. However, the EnKF is still a topic of active research for history matching purposes and the technique is evolving to address many of the difficulties in its implementation.

Justification for Continuous Approach

Because of the limitation of geological information, the reservoir parameter uncertainty space is usually extremely large, even with a coarse parameterization. Obviously, we cannot test every possible model by making simulation runs. So, the techniques presented in the PUNQ study (Bos 1999) attempt to quantify uncertainty with relatively few runs. Techniques like gradient methods attempt to quantify uncertainty using a few hundred runs, where MCMC and GA applications typically employ one thousand to several thousand runs to get a better range of uncertainty. Even with MCMC techniques, however, there are practical limitations. This is because each of these applications has been treated as a one-time study (fixed period of history data and fixed prediction period). When we do a one-time study, it has a time limitation issue. We cannot explore the uncertainty parameter space in a limited time before new available data come out. The problem becomes more severe for real world simulation models, as it takes hours or even days to run simulations with complicated reservoir models on powerful servers. If we can incorporate new data into simulation runs as soon as possible, and the program can run continuously through the whole span of a reservoir's life, then our parameter space would be better explored. Even with large simulation models this offers the potential to make tens of thousands of simulation runs over the life of the reservoir. These thousands of runs should yield a more thorough exploration of the parameter space and better

probabilistic forecasts. Holmes et al. (2007) demonstrates a continuous updating process on both PUNQ synthetic reservoir and also a live field test. The production forecast of his study on PUNQ reservoir does bracket the truth case and also shows a similar uncertainty range compared to other studies published before (Bos 1999). But unfortunately, the sampling methodology used in his study is not statistically rigorous compared to MCMC sampling method. Thus, it would be useful to investigate a statistically rigorous method which could also cooperate with history data continuously.

OBJECTIVE

Based on traditional MCMC, develop an improved continuous MCMC simulation case, which is more statistically rigorous, by incorporating the data frequently in a continuous history matching process to evaluate its practicality and effectiveness in generating probabilistic forecasts. The built-up process will be tested on the PUNQ synthetic reservoir.

By achieving this objective, I will first implement the traditional MCMC history matching method on PUNQ as a one-time study. Then, in order to evaluate the continuous method, I will break up the history data into several parts and add them sequentially into the history matching process. It is a scenario which imitates the live field case that we should incorporate with new observed data when it becomes available.

STATIC SIMULATION PROCESS

Overview

History matching and generating probabilistic forecasts with the MCMC method requires the combination of several components. First, the reservoir uncertain parameters and their associated uncertainties must be determined. Second, as uncertainty in future reservoir performance is usually evaluated from the simulated performance of a set of reservoir models, a method of sampling the parameter space and generating reservoir models is needed. In turn this requires code to automatically run the simulations and read the production forecast of each single sample. The Markov Chain Monte Carlo Monte method (MCMC) is applied here to explore the uncertainty parameter space. Finally, the results of individual runs are combined into probabilistic forecasts. Below, I will describe the details of each of these components.

Parameter Space

Before doing any simulations, it is necessary to first determine which uncertain parameters should be considered. In general this is a manual process and relies on the ability of the reservoir engineer to make assessments based on the available data (Holmes et al. 2007). In the PUNQ-S3 model simulated here, the parameters considered are porosity and permeability. Once we identify the parameters of interest, we assign the prior distributions (usually continuous) to quantitatively represent the uncertainty in these parameters. The type of distribution that would be appropriate is usually based on

reservoir characterization data. In our study of the PUNQ-S3 model, we assume that permeability adheres to log-normal distribution. Porosity adheres to normal distribution. This process for identifying uncertain parameters and assigning prior distributions is fairly consistent with what is traditionally done when assessing input uncertainty in a simulation study.

Posterior Distribution

The posterior distribution is the refined distribution considering observed data from our prior distribution. It represents the whole uncertainty with all possible realizations. In this study, a posterior probability function is built under the Bayesian frame:

$$P(m|d_{obs}) \propto P(d_{obs}|m)P(m) \quad \text{..... (1)}$$

where d_{obs} represents the observed dynamic data from the real field and m represents the uncertain parameters. $P(m)$ represents the prior probability distribution of uncertain parameters determined before. $P(d_{obs}|m)$ is the likelihood function related to our observed data and $P(m|d_{obs})$ is our posterior distribution. In particular, if we assume that the prior model and the data errors follow a Gaussian distribution, then our posterior distribution $P(m|d_{obs})$ becomes the following form (Howard 2005):

$$P(m|d_{obs}) \propto \exp\left\{-\frac{1}{2}(m-\mu)^T C_m^{-1}(m-\mu)+\left(-\frac{1}{2}[g(m)-d_{obs}]^T C_D^{-1}[g(m)-d_{obs}]\right)\right\} \quad \text{.... (2)}$$

where $g(m)$ is the simulated reservoir response, such as water cut, corresponding to the

proposed m. C_m is the parameter covariance and C_D is the data covariance. A more detailed posterior distribution will be described later in the static case and continuous case study.

The posterior distribution is typically defined on a high-dimensional parameter space and often has multiple modes. The Metropolis-Hasting MCMC approach is often applied (Hastings 1970) to sample from this complicated posterior distribution. The main objective of the MCMC method is to construct a Markov chain whose stationary distribution matches the posterior distribution.

Metropolis-Hasting MCMC Algorithm

Metropolis-Hasting MCMC method is used to sample models from our posterior distribution. Assume we want to sample from the distribution $\pi(m)$, the posterior distribution in our study (Hastings 1970).

- Step 1. At state m_n generate m from a specified proposal distribution $q(m|m_n)$
- Step 2. Accept m as a sample with the probability

$$R(m_n, m) = \min\left(1, \frac{q(m_n|m)\pi(m)}{q(m|m_n)\pi(m_n)}\right)$$

In order for the MCMC process to be practical, simulation runs must run automatically without human interaction. In this study, a commercial simulator, Eclipse, was used. I did not have access to the source code, which required the creation of a "wrapper" around the simulator. This entailed writing additional code to create a file for each run, submit it to the simulator and read the results. This process obviously could be streamlined by working directly with the simulator source code. The code flow chart is listed below (**Fig. 1**):

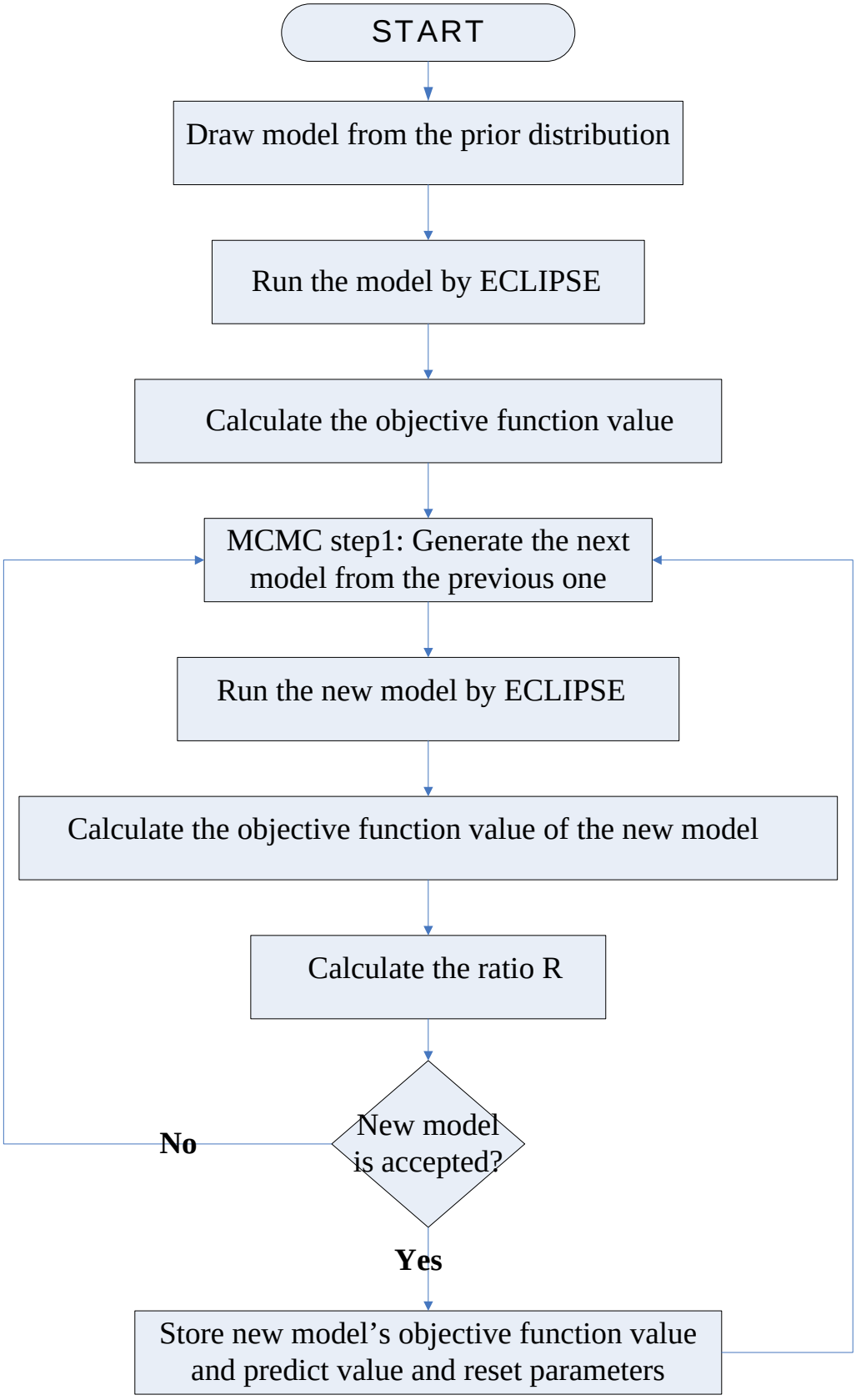

Fig. 1 - Code flow chat

Objective Function

An objective function is used to quantitatively evaluate how well an individual model reproduces the observed data from the field. This term is defined as a part of the posterior distribution function as

$$O(m) = (m-\mu)^T C_m^{-1}(m-\mu) + [g(m) - d_{obs}]^T C_D^{-1}[g(m) - d_{obs}] \quad \text{..... (3)}$$

In **Eq. 3**, $(m-\mu)^T C_m^{-1}(m-\mu)$ is called the prior term and $[g(m) - d_{obs}]^T C_D^{-1}[g(m) - d_{obs}]$ is called the likelihood term. As a result, our objective function is a combination of prior information and observed information. This is a consequence of the posterior distribution construction under the Bayesian frame. Also, we can tell from the posterior distribution expression (**Eq.2**) that when the value of a model's objective function goes down, our posterior distribution value goes up. This results in a higher possibility model in our posterior distribution. The acceptance ratio R is defined as the ratio of the posterior values between the new model and the previous model. The new model with a smaller objective function would have a higher possibility to be accepted.

Good Mixing and Convergence

The most important influence during the MCMC sampling process is how to choose the proposal distribution. Good proposal distributions can greatly enhance the performance of

the Metropolis-Hastings algorithm. A well-chosen proposal distribution produces candidate values that cover the parameter space of the posterior distribution in a reasonable number of iterations. It similarly produces candidate values that are not accepted or rejected too frequently (Greenberg and Chib 1995). If the proposal distribution is too diffuse relative to the target distribution, the candidate values will be rejected frequently. Thus, the chain will require much iteration to adequately explore the space of the target distribution. If the proposal distribution is too focused (e.g., has too small a variance), then the chain will remain in one small region of the target distribution for many iterations. In the meantime, other regions of the target distribution will not be adequately explored. Thus, a proposal distribution whose spread is either too small or too large can produce a chain that requires many iterations to cover the parameter space of the posterior distribution (Givens and Hoeting 2005). Unfortunately, the proper proposal function is really difficult to choose, especially on a high-dimensional problem. In practice, the variance of the proposal distribution can be selected through an informal iterative process. Start a chain and monitor the proportion of proposals that have been accepted. Then, adjust the spread of the proposal distribution accordingly. Once a predetermined acceptance rate is achieved, restart the chain using the appropriately scaled proposal distribution. In this study, we use the random walk method as our proposal distribution. By applying an informal iterative process, the acceptance rate was less than10%. I then modified the scale factor to get a reasonable acceptance rate, on the order of 40%. More details about how to choose a proper scalar will be shown in the static case study.

Another critical problem that needs to be considered is the burn-in time and run length of

the chain. With a generated MCMC chain, the iterations may not be enough for the correct marginal distribution and the dependence on the chain starting point may remain strong. To reduce the severity of this problem, the early group of elements of the chain is typically discarded as a burn-in period. The determination of an appropriate burn-in period and run length is still an active area of research. A commonly used approach is presented by Gelman and Rubin (1992) but there is potential difficulty with their approach. For example, selecting suitable starting values in cases of multimodal posterior distribution may be difficult. Using multiple MCMC chains will not work if all of chains become stuck in the same sub-region or mode. In our study, we simply cut off the first group of models, whose objective function's value is significantly high and use the rest of the models to generate our posterior distribution. **Fig. 2** shows an objective function curve in my study, where the first 7,000 models that have high values are considered as the burn-in period.

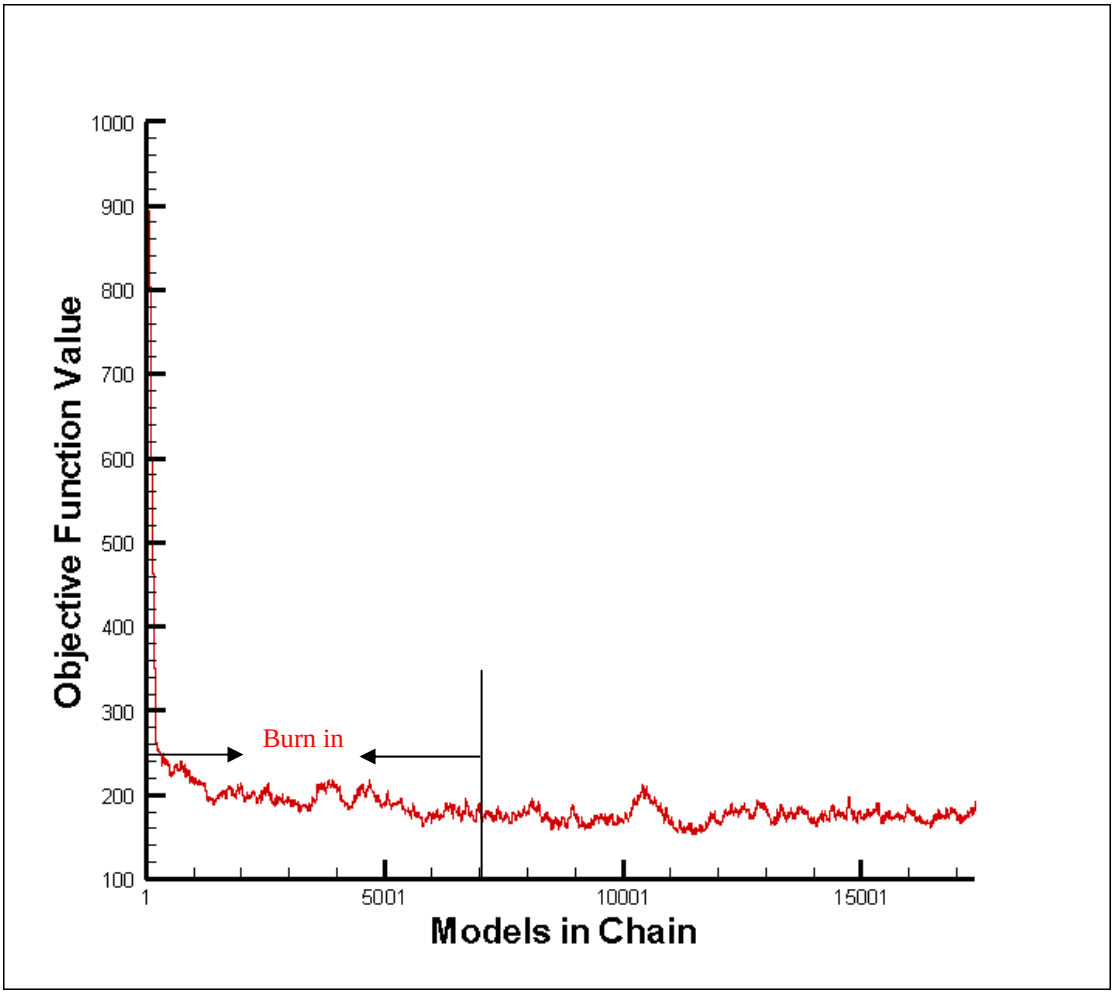

Fig. 2 - Objective function vs. models of a MCMC chain in static case

Forecasting

The final step in the static simulation process is to combine the production forecasts of all the samples into probabilistic forecasts. We use all mixed-well sampled models in the chain to quantify the uncertainty in future oil production. We use all the models in **Fig. 2** except for the first 7,000 models, whose objective function value is significantly high. Unfortunately, even though the MCMC method is a rigorous way of drawing samples from an unknown probability distribution, the implementation may not give the "correct" uncertainty range. This is due to two critical problems: First, the MCMC chains may not

be long enough to fully explore the parameter space or to achieve convergence. This problem becomes even more difficult to handle as there are too many uncertain parameters considered in the updating process. Secondly, the choice of the history match quality definition (*i.e.*, likelihood function) is also crucial. Barker et al. (2001) provide an alternative approach to create probabilistic forecasts which they claim is statistically rigorous. Barker models uncertainty using the exponential likelihood function as

$$L = c \times \exp\left[-\frac{1}{2} \sum_{1}^{n} \left[\frac{y_i^{calc} - y_i^{obs}}{\sigma_i} \right]^2 \right] \quad \text{..... (4)}$$

Eq. 4 requires that the production data are independent measurements with normally distributed error, as stated in the paper. Unfortunately, the authors neither reference nor provide a derivation of this formula. However, **Eq. 4** appears to be an adaptation of the likelihood function for normal distributions, given by Vose (2000) as:

$$L(\mu, \sigma) = \left(\frac{1}{\sqrt{2\pi\sigma^2}} \right)^n \exp\left[-\sum_{i=1}^{n} \frac{(x_i - \mu)^2}{2\sigma^2} \right] \quad \text{..... (5)}$$

where x_i is the observation from an independent experiment. The major problem with adapting this formula for use in production forecasts is the assumption of independent measurements with normally distributed error. In production forecasts the same observation (such as the pressure in a given well) is made at multiple points in time. Obviously, the pressure in a well is not completely independent from the pressure at an

earlier or later point in time. When dependant data points such as these are used in the likelihood function, the assumption of independence is violated and the statistical validity of the approach is called into question. Without any guidance from the authors in the form of a derivation or reference, this issue cannot be reconciled. In our study, we simply consider that the observed data are independent of each other. Thus, we use **Eq.4** as our likelihood function, in line with previous researchers.

CONTINUOUS SIMULATION PROCESS

Overview

Conducting simulation in the continuous manner is similar to the static case with the exception of changes made to the objective function. The same initial model is used in the continuous case. The parameter space is also set to be the same as the static case, in order to do reasonable comparisons. On the other hand, as we are doing the continuous history matching process, new data comes from the real field and is added to the objective function. The updated objective function is then involved in subsequent simulation runs. Finally, the results of individual runs are combined into probabilistic forecasts.

Continuous Data and Changed Objective Function

At various points in time during the continuous simulation process, new data from the field become available. It is advantageous to include new data in the process as quickly as possible, as it is generally assumed that more information from the field leads to better forecasts and assessments of uncertainty. As more data are added, **Eq. 4** will include more observed data points and simulation data points. As a result, the observed data misfit term in our objective function will increase. Even though the way changing the objective function is not statistically rigorous, our objective here is to investigate the impact of the violation by comparing the forecast results with other researchers. **Fig. 3** shows the change of the objective function curve when carrying out the continuous

process in my study.

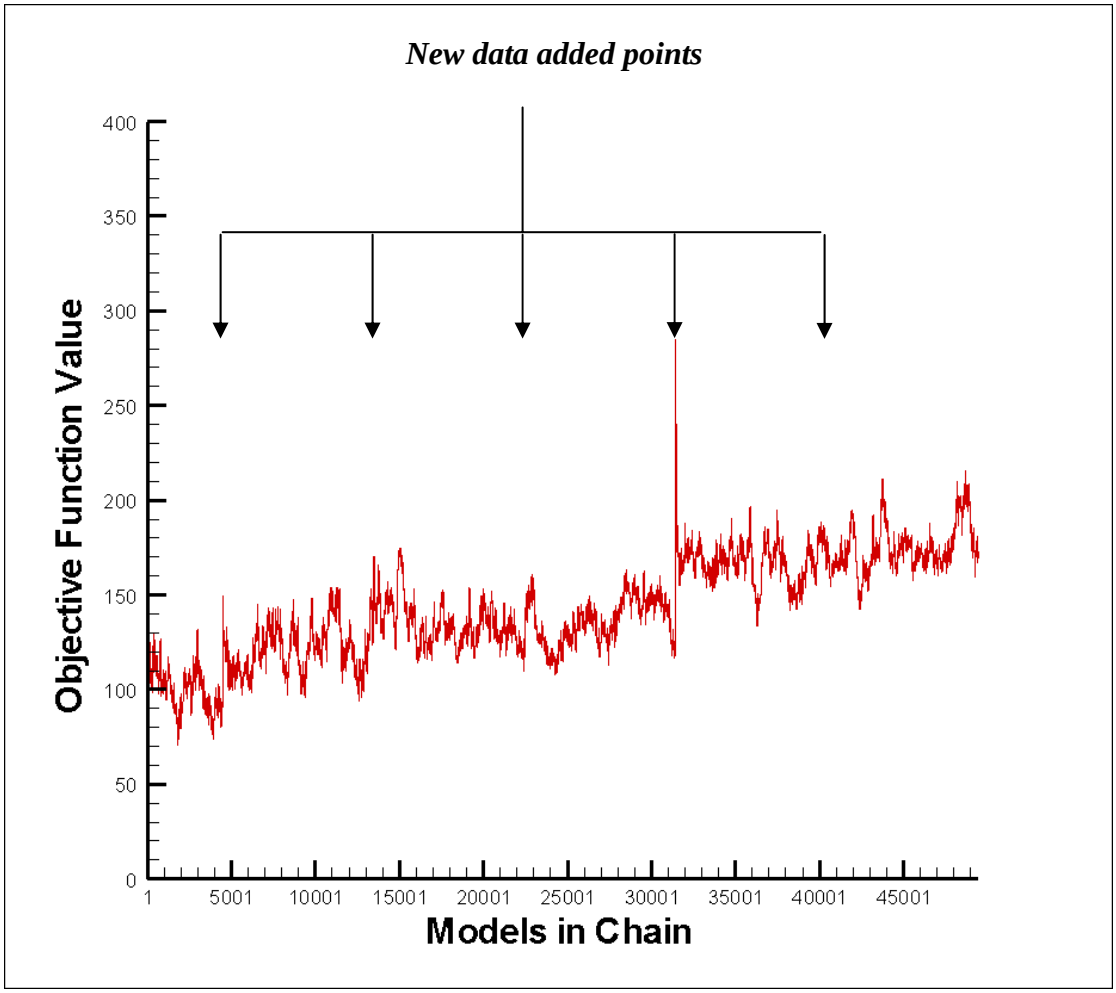

Fig. 3 - Objective function vs. models of a MCMC chain in continuous case

Once the new observed data are incorporated, the current last model in the chain should be recalculated with a revised objective function. This leads to a bigger objective function and causes a shift of our objective function curve shown in **Fig. 3**. New data come in at model number points 4,500; 13,500; 22,500; 31,500; and 40,500.

Forecasting

Combining the results of the simulation runs into probabilistic forecasts in the continuous

simulation process is much similar to the static case. In contrast, the continuous case forecasting can be done at any time by using sampled models in previous years. For example, in this PUNQ-S3 study we divided the history data into six parts. The process first starts with all the history data before year 4.5. Then, we add to the history data sequentially at the 5^{th}, 6^{th}, 7^{th}, 8^{th} and 9^{th} years. If we want to forecast the cumulative 16.5-year oil production at the end of the 9^{th} year, we can simply forecast with the models sampled in the 9^{th} year.

PRIOR MODEL

Overview

Before carrying out the static and continuous MCMC tests on the PUNQ-S3 model, we first built up the initial model and the prior distribution. The two tests use the same prior distribution during the history matching process. The PUNQ-S3 synthetic reservoir has been used in probably the most thorough treatment of uncertainty quantification in production forecasts. Several industrial and academic partners used different methods to test a number of history matching techniques. The objectives of the PUNQ project were to research whether or not a methodology can be developed that propagates the combined reservoir modeling, reservoir parameter and well observation uncertainties into forecast uncertainty in a formally unbiased way. The true total oil recovery after the simulation period is $3.87 \times 10^6 Sm^3$.

The project provides noisy well porosities and permeabilities and noisy synthetic production history of the first eight years. This history of the reservoir life includes 1 year of well testing, 3 years of field shut-in and 4 years of actual field production. The synthetic production data consisted of the Bottom Hole Pressure (BHP), Water Cut (WCT) and Gas Oil Ratio (GOR) for each of the 6 wells. Also, within the history period, two wells show a gas breakthrough and one well shows the onset of water breakthrough (Bos 1999).

In our methology, instead of using porosity and permeability values directly, the uncertain parameters used in our study are porosity and permeability multipliers. These multipliers are applied to permeability and porosity base maps when running the simulation. The effect is the same as if porosity and permeability values were used directly, but this approach simplifies the implementation. As a result, the process for building up the initial distribution generally breaks into three steps:

1. Construct the initial model.
2. Determine uncertain parameters (multipliers).
3. Build up the prior distributions for uncertain parameters.

Construct the Initial Model

The PUNQ-S3 reservoir model is a five-layer, three-phase synthetic reservoir based on an actual field operated by Elf. By most standards the PUNQ-S3 reservoir is a small model with just 1,761 active cells. On a modern desktop computer a single simulation run takes less than a minute, which is advantageous for making a large number of runs. Based on available information from the truth case, some properties of the reservoir such as PVT properties, well information, and schedules were generated. These parts are the same as the truth case in our initial model.

The truth case's structure map (**Fig. 4**) and porosity, horizontal and vertical permeability maps are shown in **Figs. 5-20**. Since we consider porosity and permeability as our unknown parameters, the prior model should be set up with a different porosity and permeability from the truth case for testing purposes.

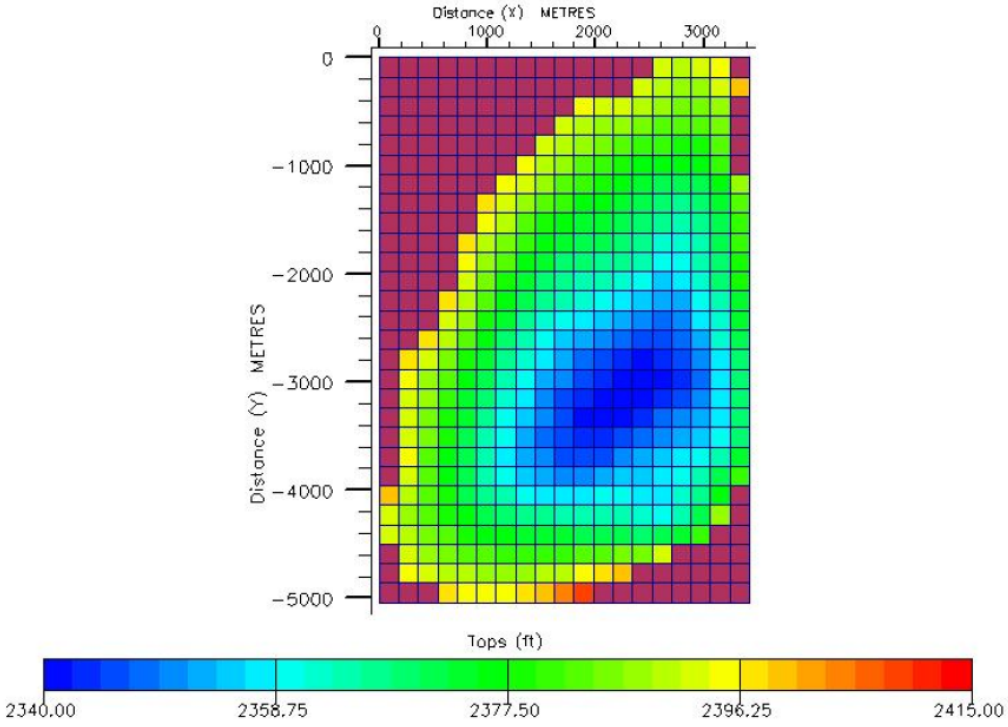

Fig. 4 - Structure of the PUNQ synthetic reservoir

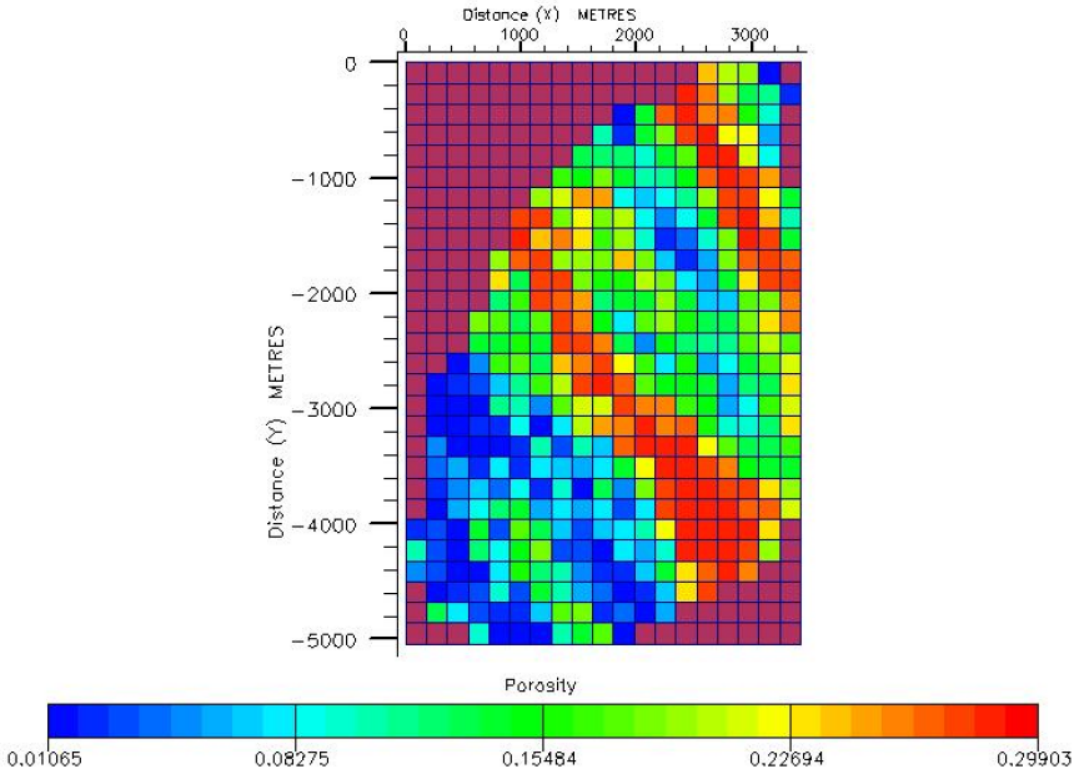

Fig. 5 - Truth case porosity of Layer 1

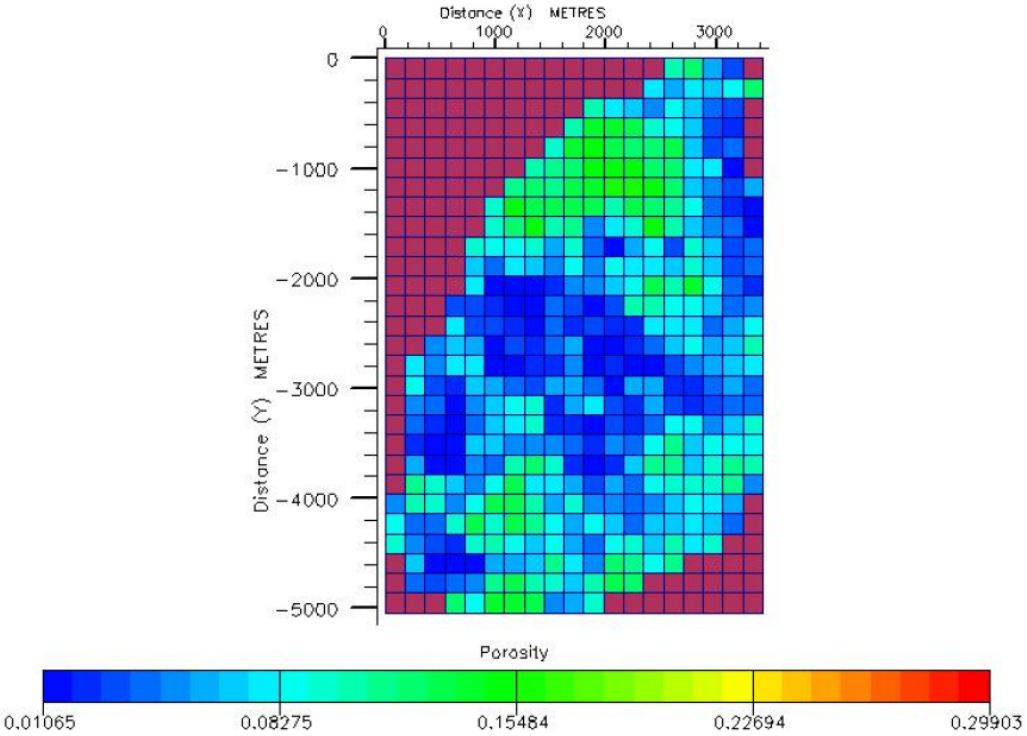

Fig. 6 - Truth case porosity of Layer 2

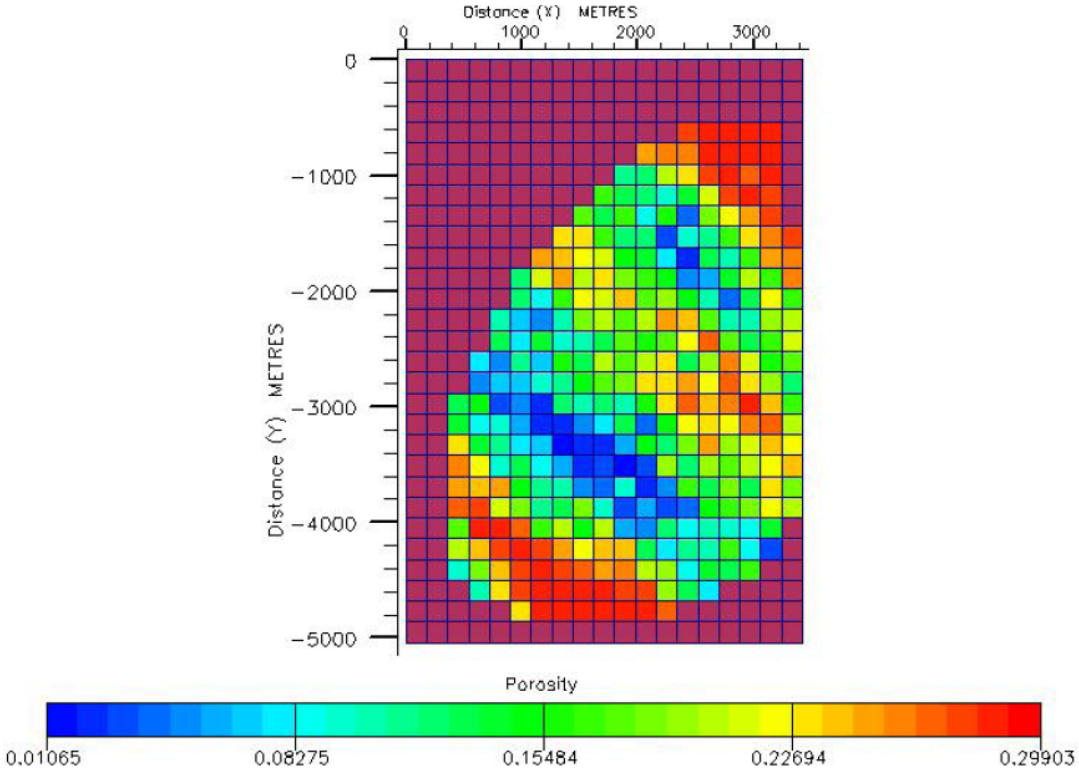

Fig. 7 - Truth case porosity of Layer 3

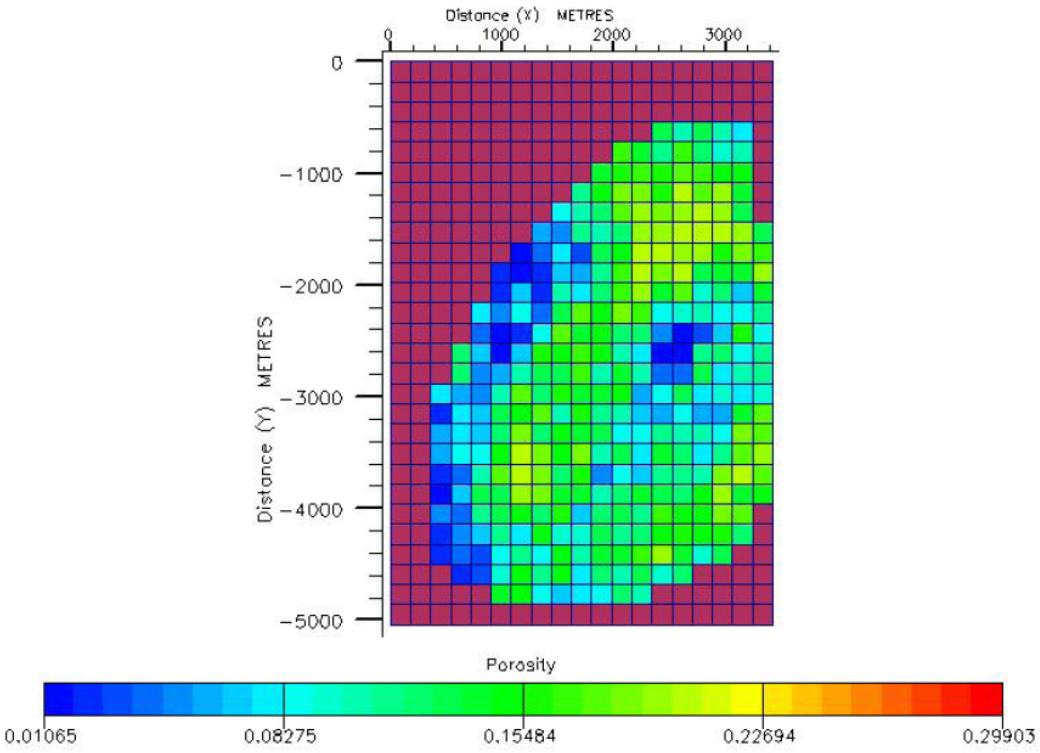

Fig. 8 - Truth case porosity of Layer 4

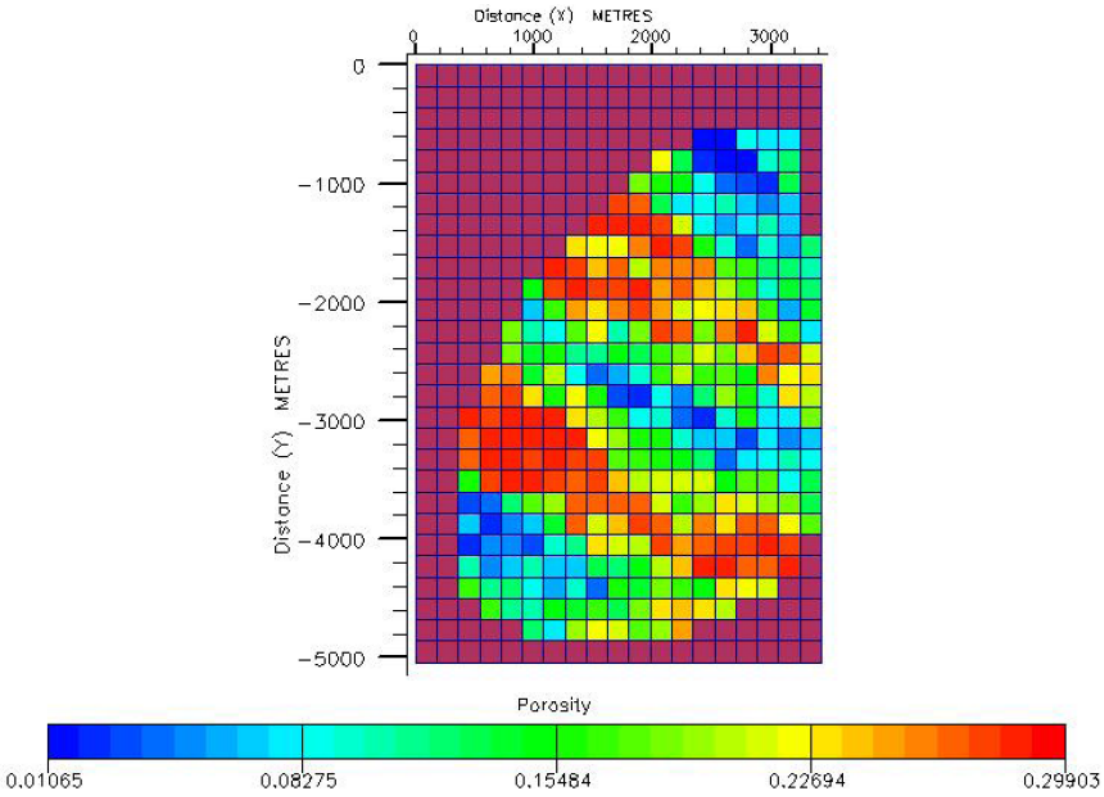

Fig. 9 - Truth case porosity of Layer 5

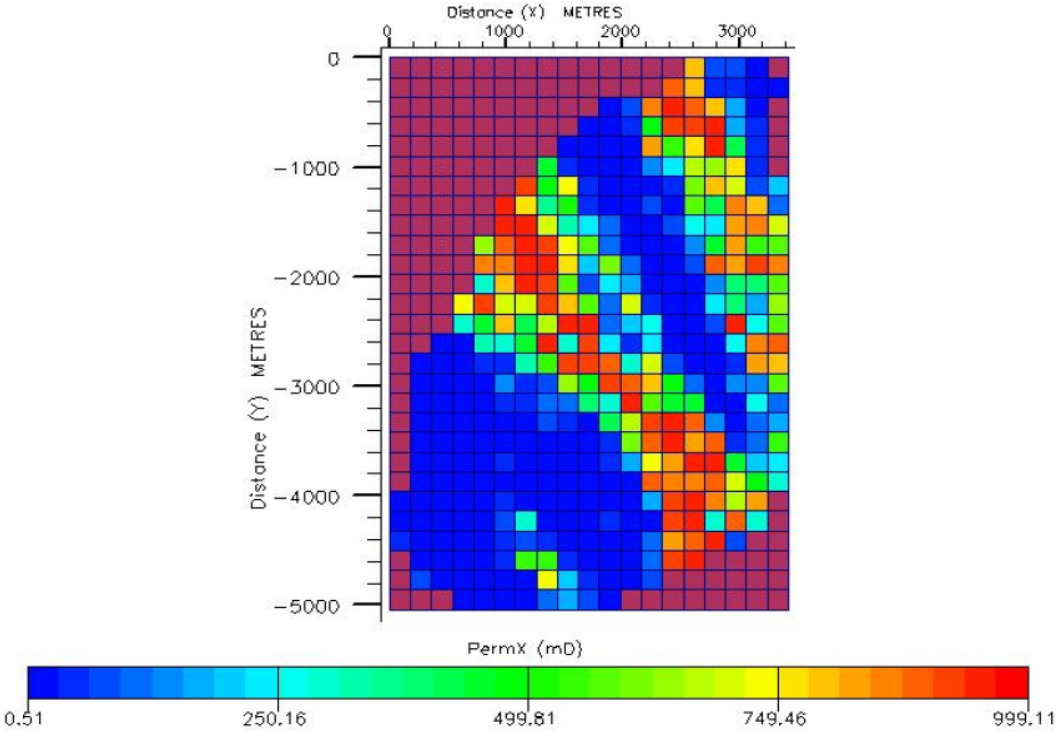

Fig. 10 - Truth case horizontal permeability of Layer 1

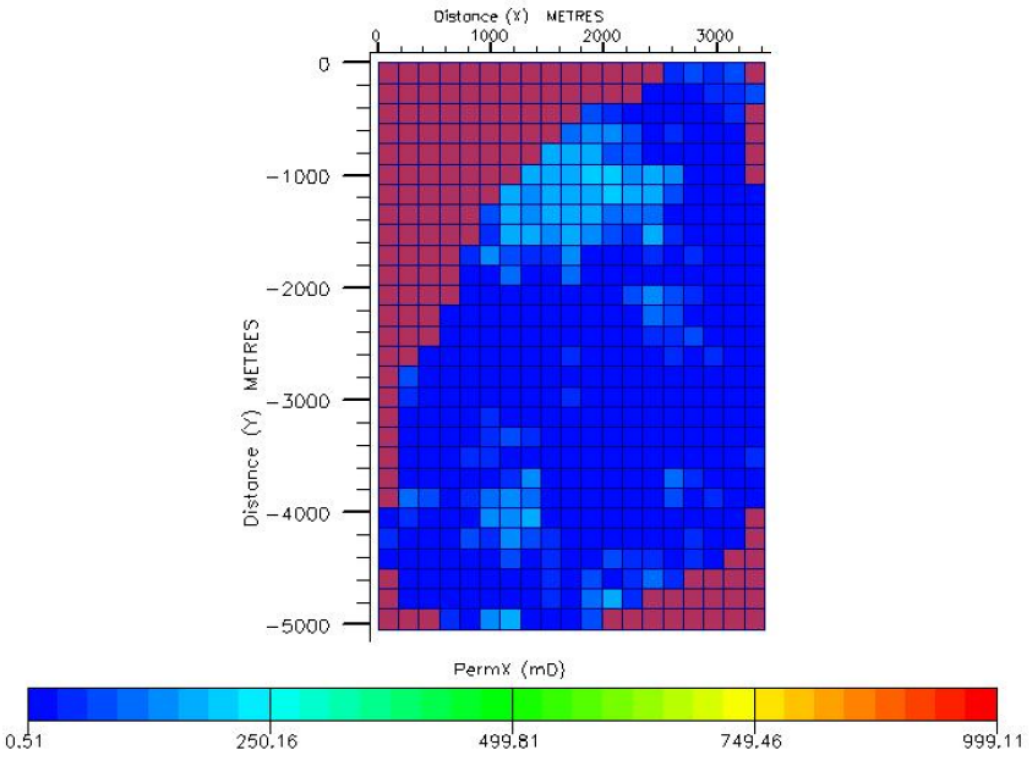

Fig. 11 - Truth case horizontal permeability of Layer 2

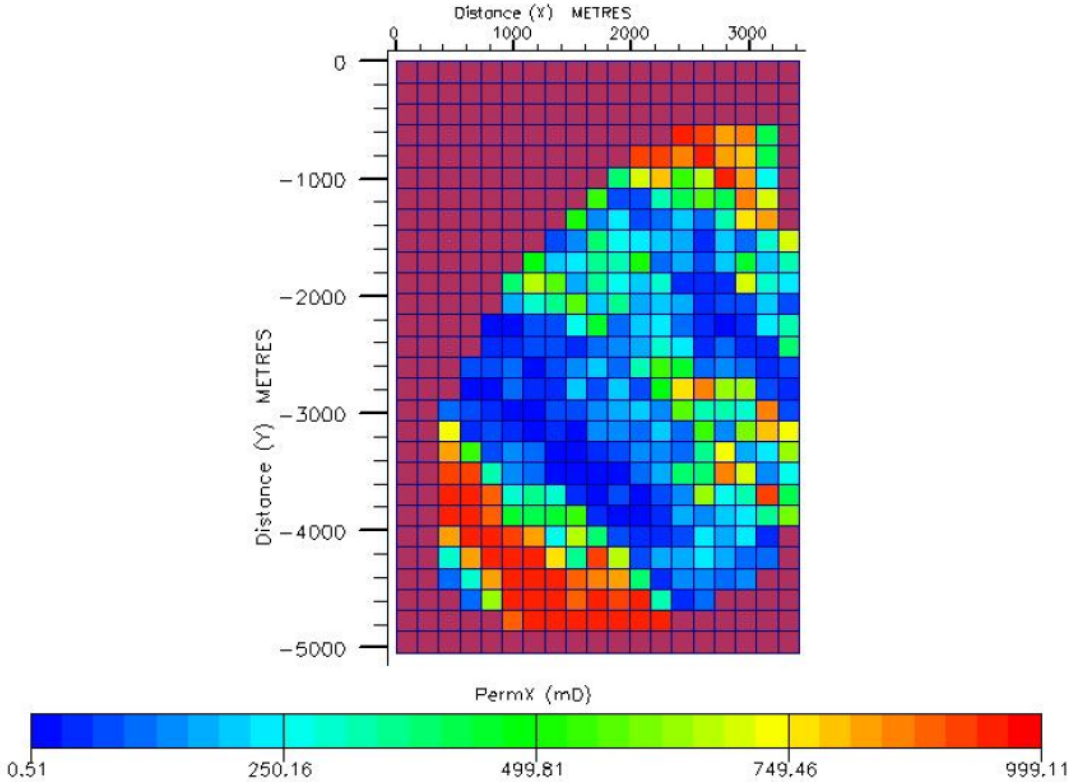

Fig. 12 - Truth case horizontal permeability of Layer 3

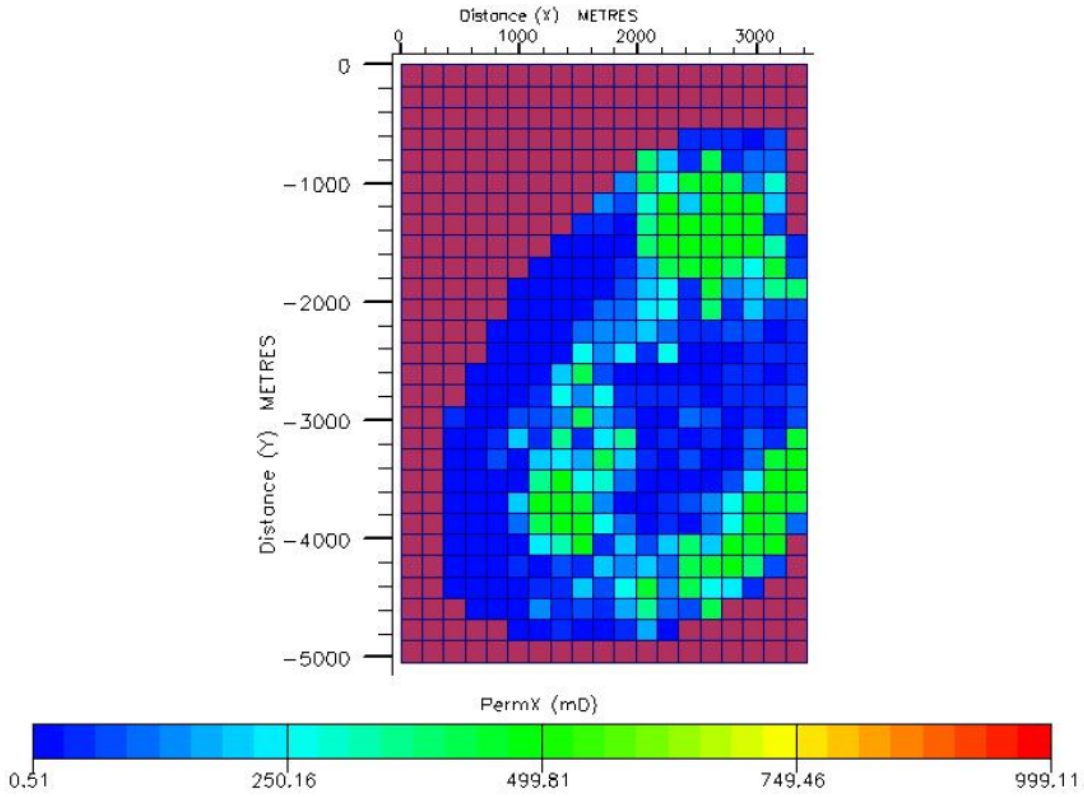

Fig. 13 - Truth case horizontal permeability of Layer 4

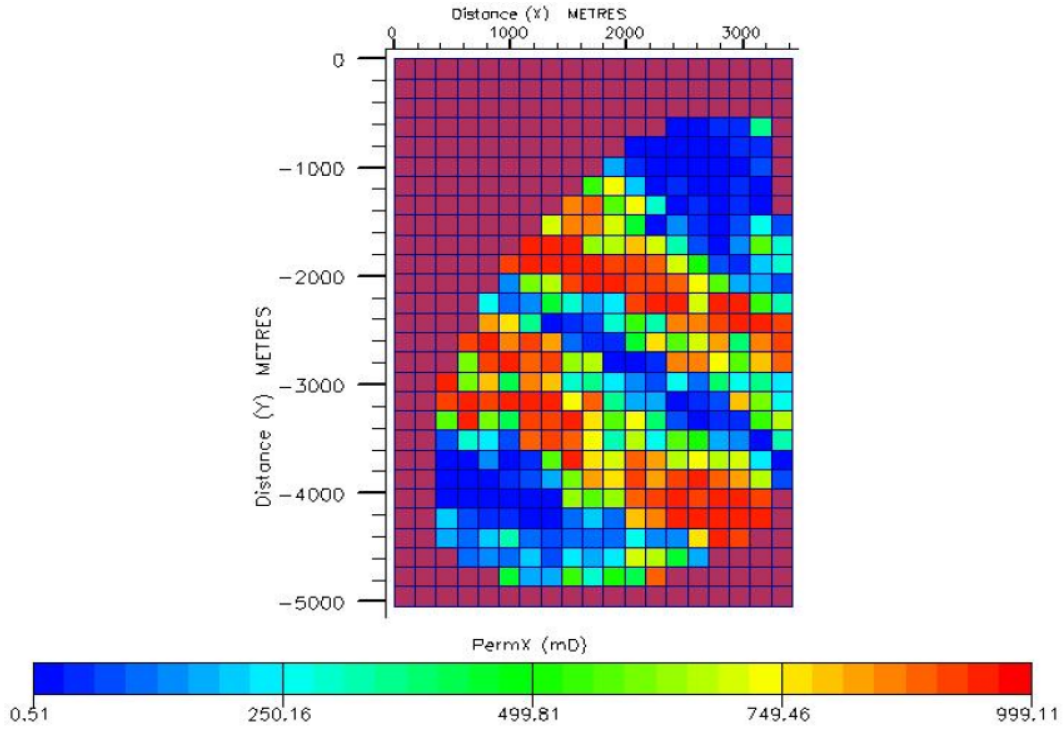

Fig. 14 - Truth case horizontal permeability of Layer 5

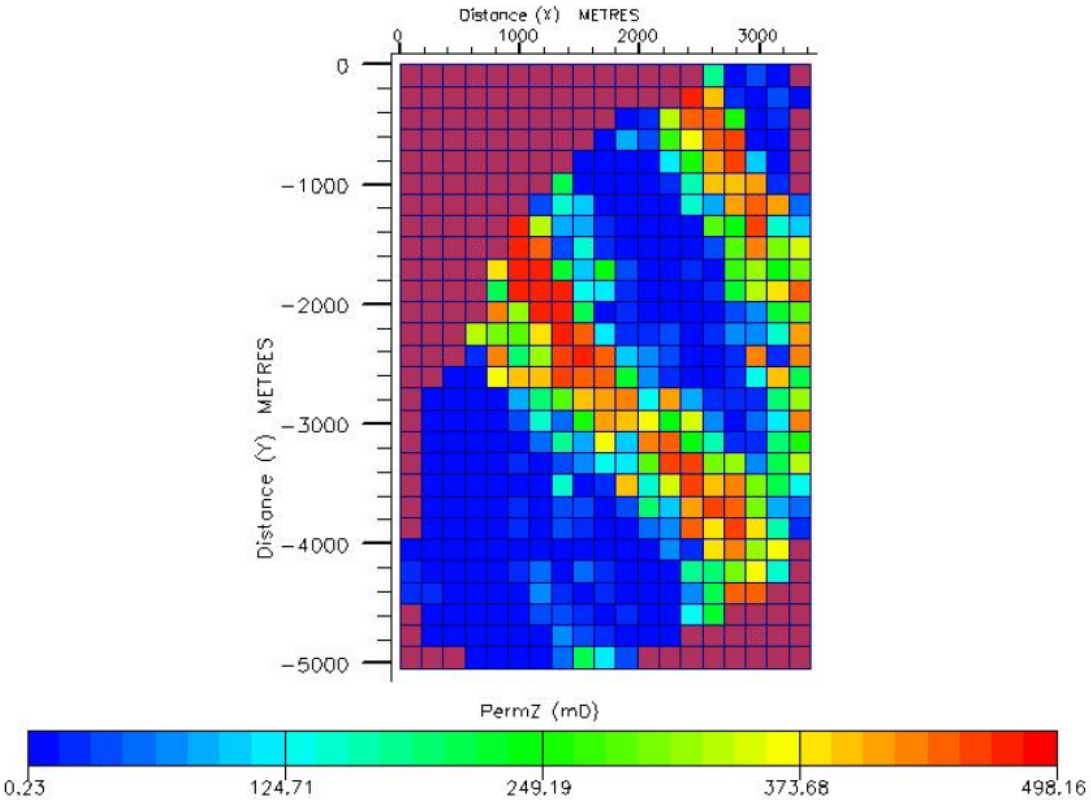

Fig. 15 - Truth case vertical permeability of Layer 1

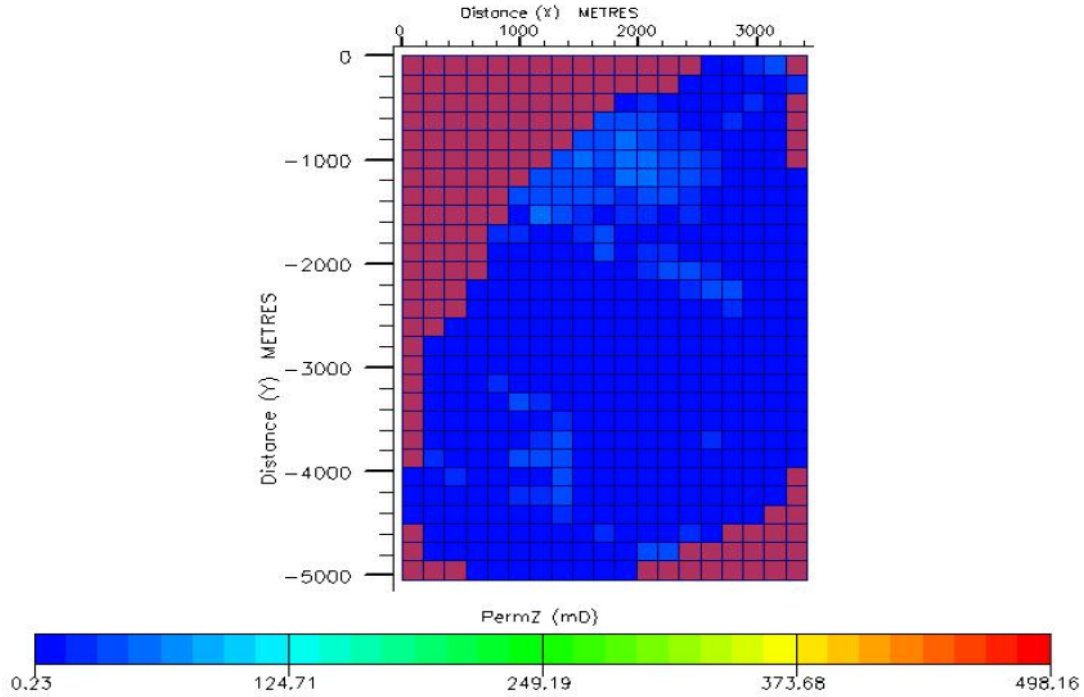

Fig. 16 - Truth case vertical permeability of Layer 2

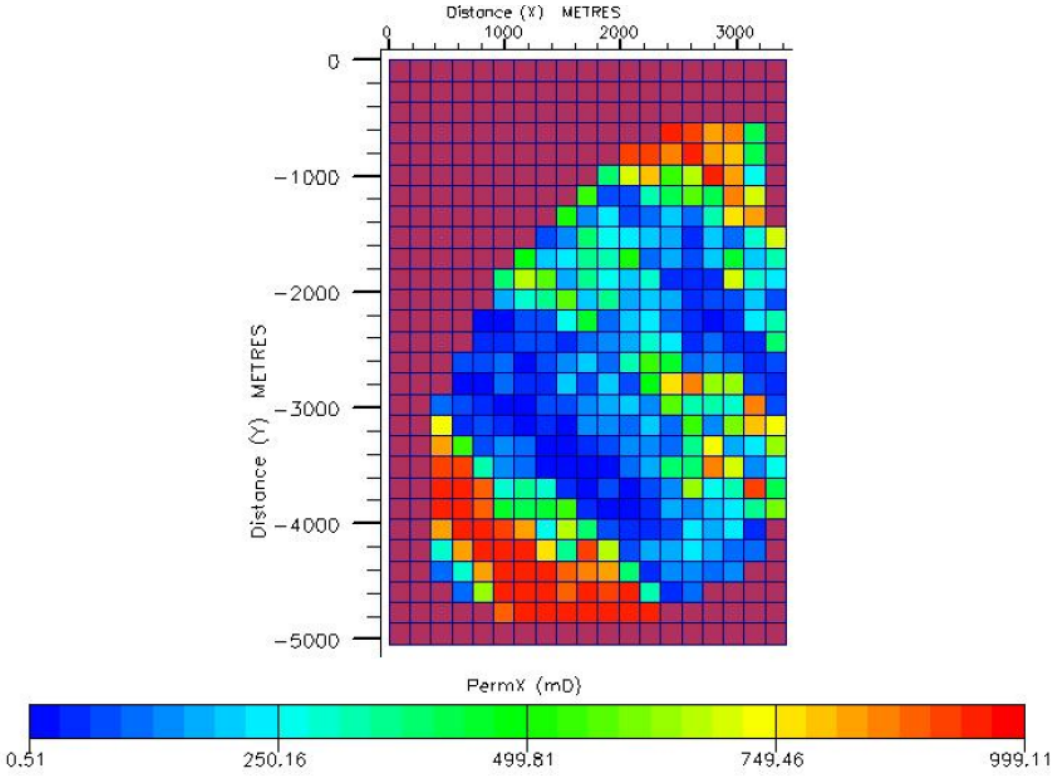

Fig. 17 - Truth case vertical permeability of Layer 3

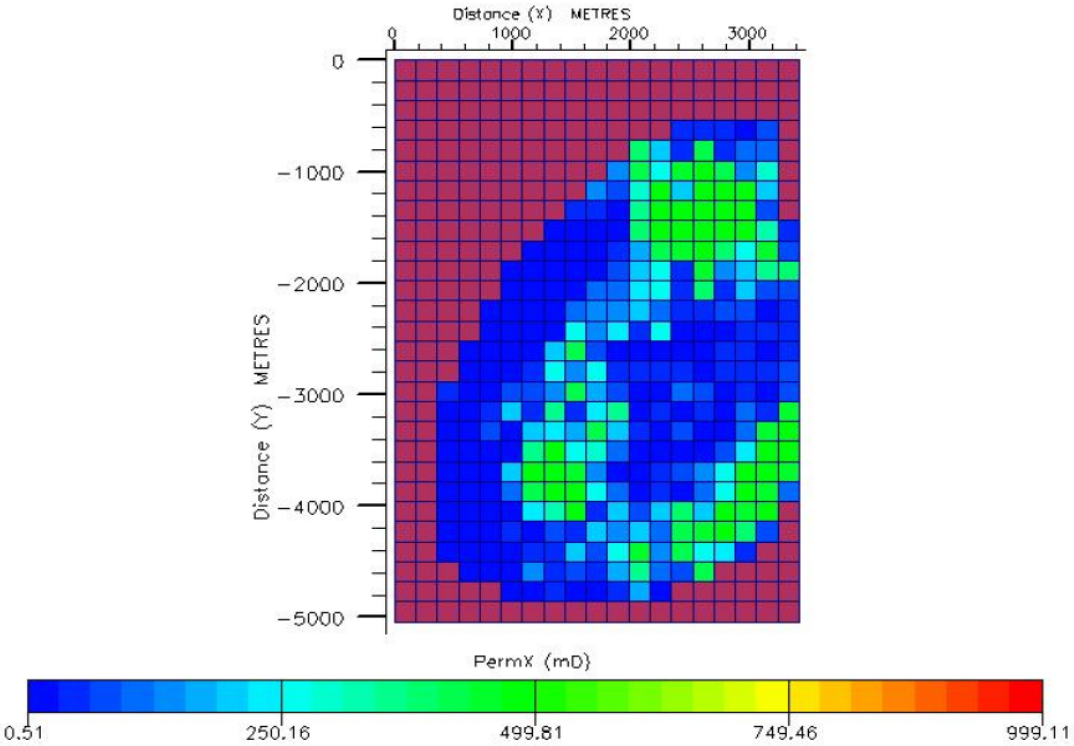

Fig. 18 - Truth case vertical permeability of Layer 4

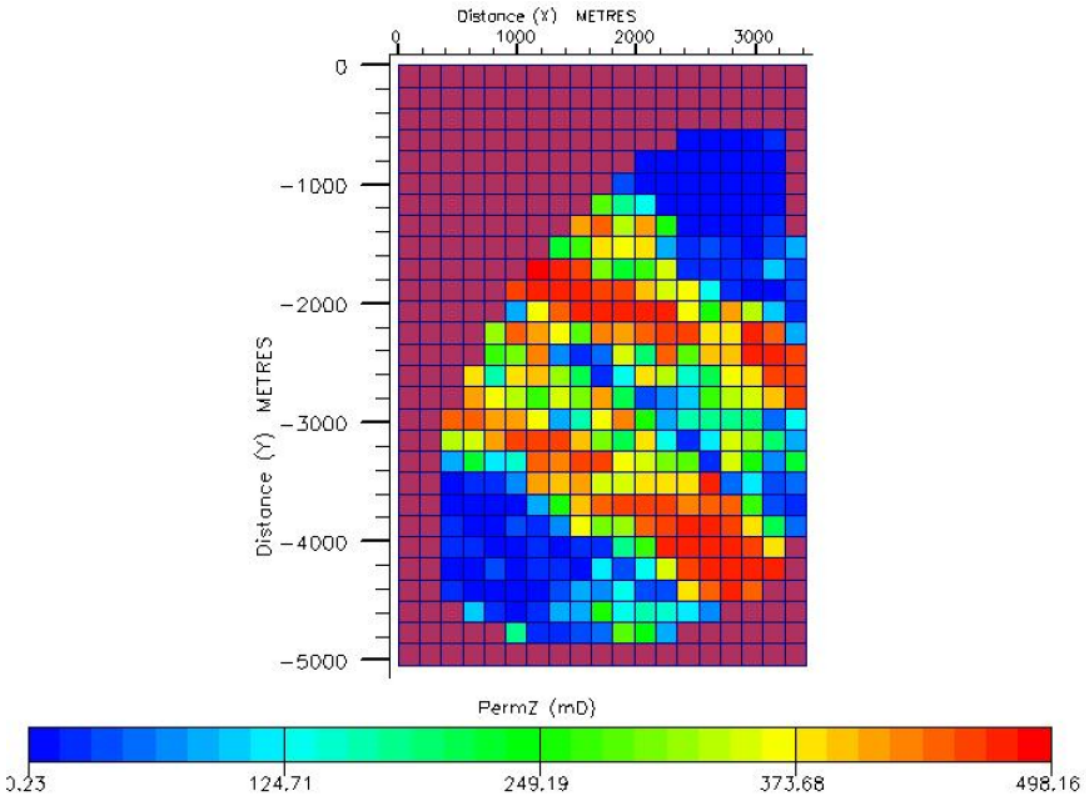

Fig. 19 - Truth case vertical permeability of Layer 5

We use the average values of porosity in each layer from well data to generate our prior porosity. **Table 1** (Gu and Oliver 2004) gives the actual porosity values at well locations and **Table 2** shows the average porosity value of each layer.

Table 1 - Porosity values at well locations for PUNQ-S3 reservoir

Well	Layer 1	Layer 2	Layer 3	Layer 4	Layer 5
PRO-1	0.0828	0.0616	0.0982	0.1486	0.2445
PRO-4	0.2192	0.0588	0.1114	0.16	0.2137
PRO-5	0.2346	0.0708	0.2115	0.1498	0.0949
PRO-11	0.0828	0.088	0.2434	0.1342	0.151
PRO-12	0.0751	0.1092	0.1048	0.1808	0.2401
PRO-15	0.2783	0.0966	0.1939	0.1995	0.2753

Table 2 - Average porosity value of each layer for PUNQ-S3 reservoir

Average	Layer1	Layer2	Layer3	Layer4	Layer5
Porosity	0.17	0.08	0.17	0.16	0.19

The relation between porosity and permeability is shown in **Eqs. 6** and **7** (Gu and Oliver 2004),

$$\log_{10}(k_h) = 9.02\phi + 0.77 \quad \text{..... (6)}$$

$$k_v = 0.31k_h + 3.12 \quad \text{..... (7)}$$

Since we know the mean values of porosity and log-permeability correlates with porosity as in **Eq. 6,** the mean of $\log_{10}(k_h)$ can be calculated. The average value of horizontal permeability can be determined from **Eq. 8.** Based on the horizontal permeability and **Eq. 7**, the mean of vertical permeability can also be calculated. **Table 3** is a summary that shows what permeability should be used in the prior model.

$$E(k_h) = e^{\left(\ln(10)\mu_{\log_{10}^{k_h}} + \frac{\left(\ln(10)\sigma_{\log_{10}^{k_h}}\right)^2}{2} \right)} \quad \text{..... (8)}$$

Table 3 - Average permeability value of each layer for PUNQ-S3 reservoir

Average	Layer1	Layer2	Layer3	Layer4	Layer5
Horizontal permeability	432md	33md	432md	196md	654md
Vertical permeability	137md	13md	137md	64md	205md

Uncertainty Parameters

Review of the geological description indicates the reservoir is marked by wide southeast-trending high-quality streaks. As a result, I parameterized the PUNQ-S3 model using six homogenous regions per layer rather than using rectangular regions. The defined regions approximate the representation of the shape of these streaks (**Fig. 20)**. Five layers times 6 regions per layer times three properties (porosity, vertical permeability and horizontal permeability) yields 90 multipliers that need to be updated each iteration.

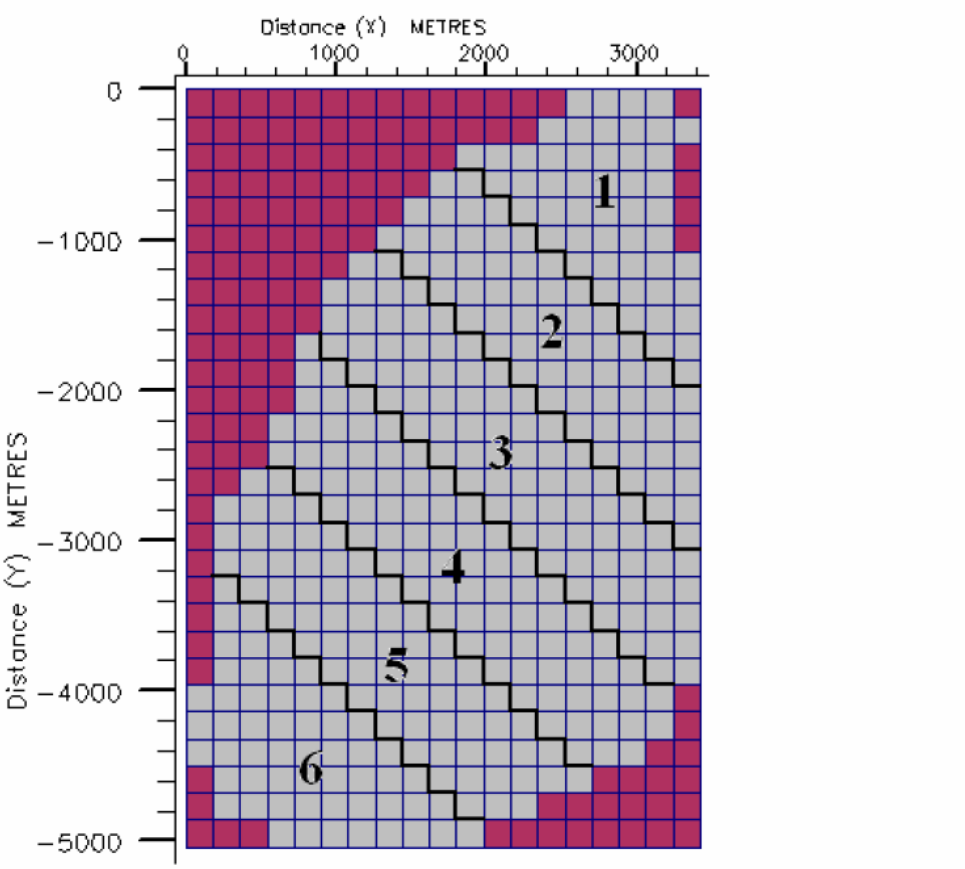

Fig. 20 - Multiplier regions

The Prior Distribution

The porosity adheres to a normal distribution and permeability adheres to a log-normal distribution, which is consistent with practical experience and other research done on the PUNQ model. Udating the multipliers indirectly is identical with updating permeability and porosity directly. As shown by **Eq. 9**, ϕ' denotes the constant porosity value in our base map, X_ϕ denotes the porosity multiplier random variable. ϕ is our final porosity value in the realization.

$$\phi = X_\phi \phi' \quad \text{..... (9)}$$

Eq. 9 shows a linear relationship between porosity multiplier and porosity. So, X_ϕ should follow a normal distribution in order to make our porosity follow a normal distribution. The mean of our porosity multipliers were chosen to be 1. This is reasonable because the prior distribution is built up based on our initial model. This means that the average porosity of each layer should be the most likely realization without any impact by the observed data. Additionally, the variance and standard deviation of porosity are shown by **Eq. 10** and **Eq. 11**. **Table 4** (Barker et al. 2001), shows the mean and standard deviation value of porosity in each layer. According to the values in **Table 4**, the standard deviation on porosity values should be set to 30% of the mean(an average value). As a result, the standard deviation of our porosity multiplier should be chosen as 0.3.

$$Var(\phi) = \phi'^{2} Var(X_\phi) \quad \text{.....} \quad (10)$$

$$std(\phi) = \phi' std(X_\phi) \quad \text{.....} \quad (11)$$

Table 4 - Porosity distribution factors of initial model

layer	Mean	Std	Std/Mean
1	0.17	0.06	0.352941
2	0.08	0.02	0.25
3	0.17	0.06	0.352941
4	0.16	0.03	0.1875
5	0.19	0.06	0.315789

The permeability is not as straightforward because we should use a multiplier that applies to log-normal distribution. This is because our prior permeability follows a log-normal

distribution. The log-normal distribution was chosen based on Craig et al.'s (2005) use of the log-normal distribution for permeability with layered reservoirs. In order to determine the standard deviation of each permeability distribution, **Eq. 12** is used here to show how we can get the variance of our horizontal permeability with known mean and variance of our log horizontal permeability. Then, based **Eq. 12** on **Eqs. 6-8**, the permeability distribution factors can be calculated (**Table 5-7)**.

$$Var(k_h) = \left(e^{(\ln(10)\sigma_{\log k_h})^2} - 1 \right) e^{2(\ln(10)\mu_{\log k_h}) + (\ln(10)\sigma_{\log k_h})^2} \quad \text{..... (12)}$$

Table 5 - Log horizontal permeability distribution factors of initial model

Layer	Mean(md)	Std(md^2)	Std/Mean(md)
1	2.3	0.54	0.234783
2	1.49	0.18	0.120805
3	2.3	0.54	0.234783
4	2.21	0.27	0.122172
5	2.48	0.54	0.217742

Table 6 - Horizontal permeability distribution factors of initial model

Layer	Mean(md)	Std(md^2)	Std/Mean(md)
1	432.232	830.6076	1.921671
2	33.67456	14.57834	0.432918
3	432.232	830.6076	1.921671
4	196.7566	135.1522	0.686901
5	654.2096	1257.176	1.921671

Table 7 - Vertical permeability distribution factors of initial model

Layer	Mean(md)	Std(md^2)	Std/Mean(md)
1	137.1119	257.4884	1.877943
2	13.55911	4.519284	0.333302
3	137.1119	257.4884	1.877943
4	64.11453	41.89719	0.653474
5	205.925	389.7244	1.892555

Because permeability multiplier applies to a log-normal distribution whose mean is different from the median, the median of our permeability multiplier is chosen as 1 instead of choosing the mean to be 1. The standard deviation on permeability values was set to 135% of the mean (an average value of “Std/Mean” from **Table 5-7**) of initial permeability, since we only use one prior distribution to characterize the whole reservoir. Thus, the standard deviation of our log-normal permeability multiplier should be chosen as 1.35.

So far, all the important factors of our prior distribution have been determined. In order to prevent extreme and unrealistic values of permeability, the multiplier distribution is

capped on the upper end at a value of 4 and the lower end at 0. For the same reason, porosity was capped with a maximum value of 2.28 and minimum value of 0. **Fig. 21** and **Fig. 22** show histograms of our prior porosity multiplier distribution and permeability multiplier distribution. This sample size is 20,000 points. Also, the cumulative distribution functions are shown by **Fig. 23** and **Fig. 24**.

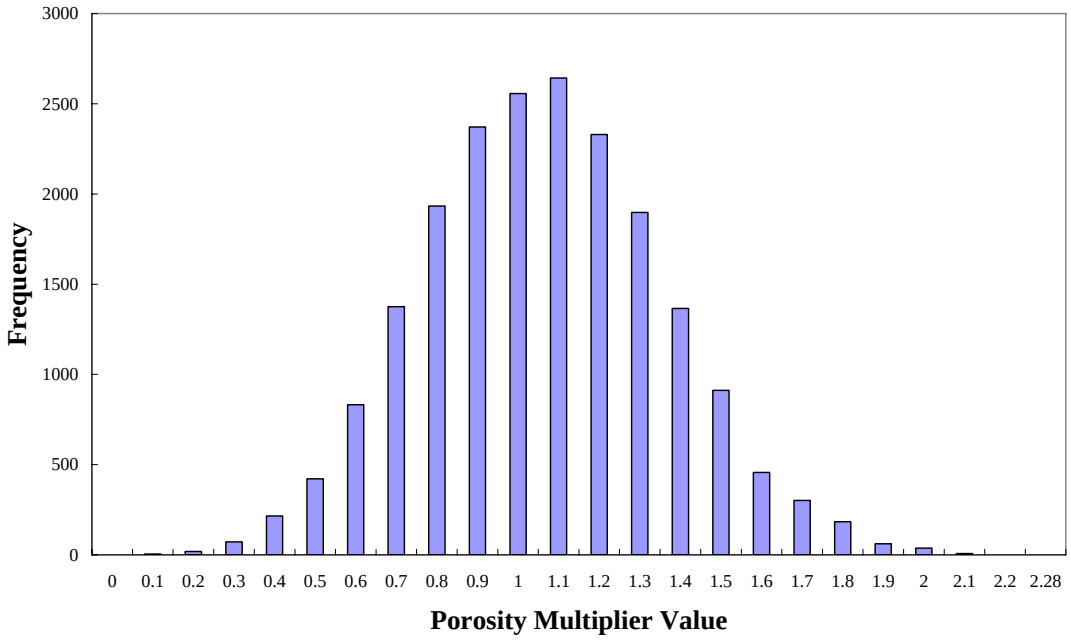

Fig. 21 - Histogram of prior porosity multiplier distribution

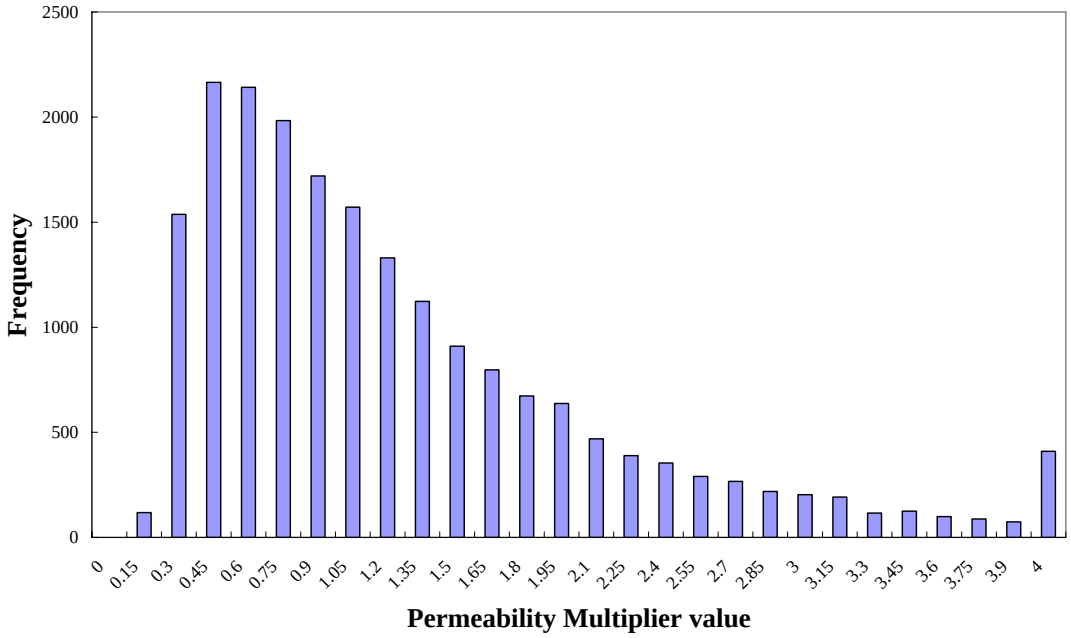

Fig. 22 - Histogram of prior permeability multiplier distribution

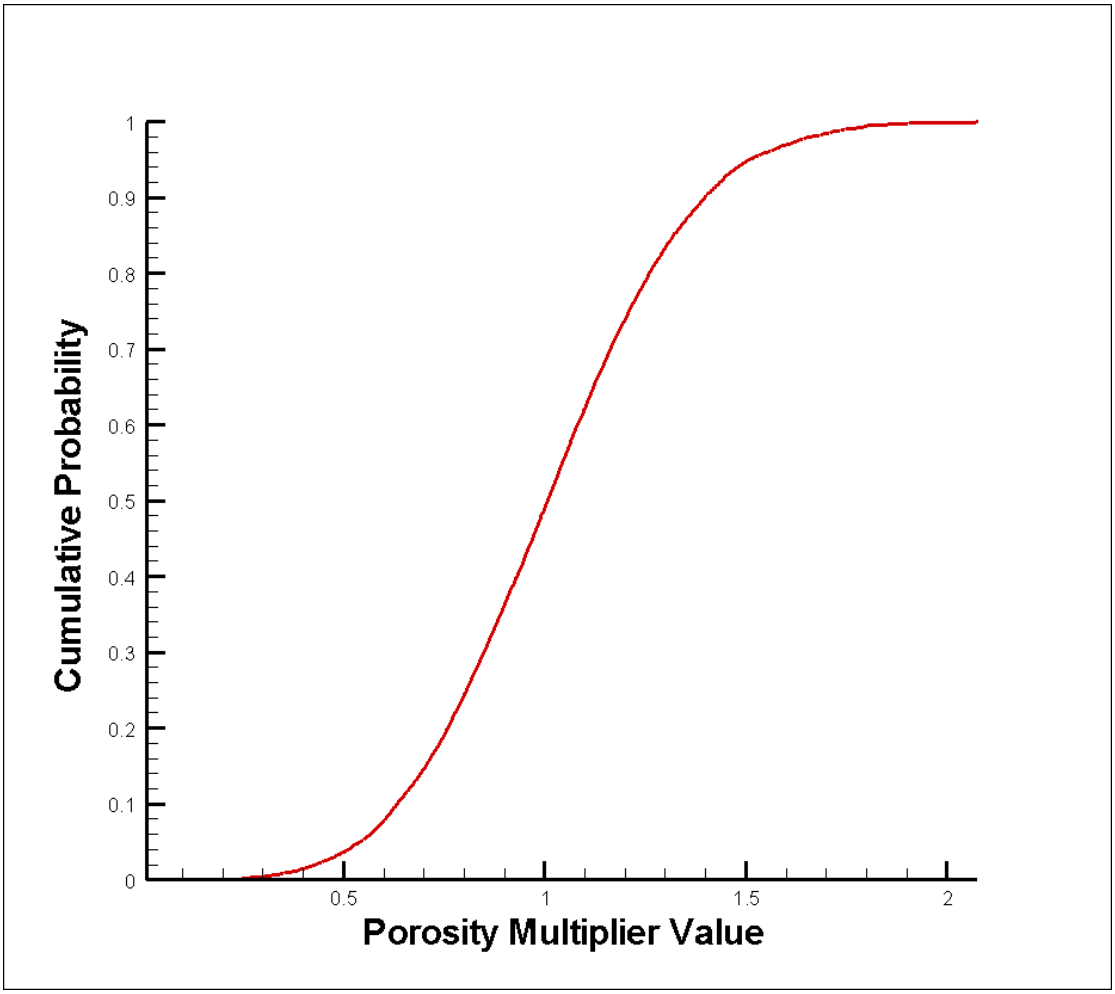

Fig. 23 - CDF of prior porosity multiplier

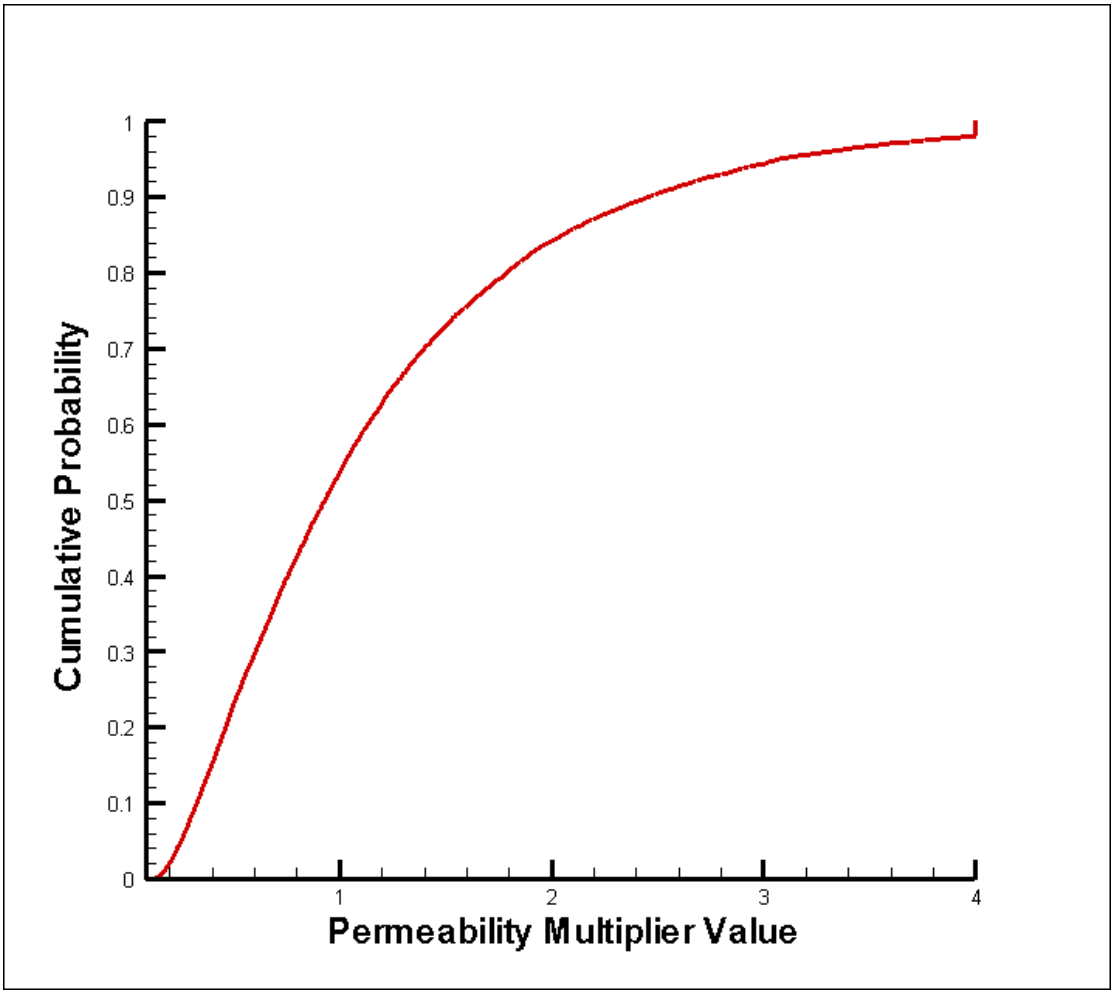

Fig. 24 - CDF of prior permeability multiplier

In order to simplify the equation derivation for the log-normal permeability multiplier, in the MCMC history match process, the permeability multiplier was transferred back to a logarithm form in order to be consistent with porosity multiplier which follows a normal distribution. With the known $Median(X_k)$ as 1 and $Var(X_k)$ as 1.35^2 and **Eqs. 13-14**, the mean and standard deviation for the logarithm form permeability multiplier can be calculated as $\mu_{\log X_K} = 0$, $\sigma_{\log X_k} = 0.354$. Together with the porosity multipliers, the prior 90 parameters distribution is shown by **Eq. 15**.

$$Median(X_k) = e^{(\ln(10)\mu_{\log X_k})} \quad \text{..... (13)}$$

$$Var(X_k) = \left(e^{(\ln(10)\sigma_{\log X_k})^2} - 1\right) e^{2(\ln(10)\mu_{\log X_k}) + (\ln(10)\sigma_{\log X_k})^2} \quad \text{..... (14)}$$

$$P(X) \propto \exp\left(-\frac{1}{2}(X-\mu)^T C_x^{-1}(X-\mu)\right) \quad \text{..... (15)}$$

$$X = \begin{bmatrix} \log X_{k1} \\ \log X_{k2} \\ . \\ . \\ . \\ \log X_{k60} \\ X_{\phi 1} \\ X_{\phi 2} \\ . \\ . \\ . \\ X_{\phi 30} \end{bmatrix} \quad \text{..... (16)}$$

Where $\log X_k$ is the logarithm multiplier of permeability and X_ϕ is the multiplier of porosity. The total number of parameters is 90. C_x is a diagonal matrix shown below because each multiplier is considered independent in our study.

$$C_x = \begin{bmatrix} \sigma_{\log X_k}^2 & & & & & & & \\ & \sigma_{\log X_k}^2 & & & & & & \\ & & \cdot & & & & & \\ & & & \cdot & & & & \\ & & & & \cdot & & & \\ & & & & & \sigma_{\log X_k}^2 & & \\ & & & & & & \sigma_{X_\phi}^2 & \\ & & & & & & & \sigma_{X_\phi}^2 \end{bmatrix} \text{.....(17)}$$

With known $\mu_{\log X_K}$, $\sigma_{\log X_k}$, μ_{X_ϕ} and σ_{X_ϕ}, our final expression of the prior distribution becomes

$$P(X) \propto \exp\left(-\frac{1}{2}\left(\sum\left(\frac{\log X_{k_i} - \mu_{\log X_k}}{\sigma_{\log X_k}}\right)^2 + \sum\left(\frac{X_{\phi_i} - \mu_{X_\phi}}{\sigma_{X_\phi}}\right)^2\right)\right) \text{..... (18)}$$

STATIC RESERVOIR STUDY

Overview

With the prior distribution defined as described above, the first test was carried out by using the static MCMC method. This method is similar to the traditional application of the MCMC method in a one-time study in which there is no adding of new dynamic data during the history matching process. There are two main reasons for doing the static test on the PUNQ-S3 model. First, we can compare our results with other previous work done on this model. This is done in order to verify that our reservoir model was constructed correctly and the prior distribution was chosen properly. Second, it lays the foundation for doing the continuous case.

The likelihood function is also needed in order to construct our posterior distribution. Using the MCMC method to explore the parameter space in our posterior distribution, we can make a cumulative oil production forecast with all sampled models. I will describe the details below.

The Likelihood Function

The definition of the likelihood function relies on the specification of a model for the uncertainty around the observed production (Bos 1999). In our study, the measurement errors are assumed to be an independent Gaussian distribution. Thus, our likelihood

function becomes

$$P(d_{obs}|X) \propto \exp\left(-\frac{1}{2}[d_{sim}-d_{obs}]^T C_D^{-1}[d_{sim}-d_{obs}]\right) \quad \text{(19)}$$

where X represents the multipliers we are trying to update and d_{obs} is a vector that represents the observed data. Here in the static case, we use all the observed history data for the entire 9-year period, which included the BHP, GOR and WCT data listed in **Table 8**. The total number of observed data points is 117. d_{sim} represents the simulated data, and is also a vector including 117 values. We assume that the measurement errors are independent Gaussian distributions, where the C_D here is a diagonal matrix. The value of each diagonal element is consistent with the PUNQ-S3 project report (Bos 1999). The noise level on the shut-in pressures was 3 times smaller than the flowing pressure (respectively 1 bar and 3 bar), to reflect the more accurate shut-in pressures. The noise level on the GOR was set at 10% before gas breakthrough and 25% after gas breakthrough, reflecting the difference between the solution and the free gas situation. Similarly, WCT noise of 2% before and 5% after water breakthrough was used. Our likelihood function can be shown as **Eq. 20** due to the diagonal form of our C_D.

Table 8 - Observed data in static case

Times(days)	WBHP(BARSA)	WGOR(Sm^3/Sm^3)	WWCT(Sm^3/Sm^3)
1.01	6	-	-
91	6	-	-
182	6	-	-
274	6	-	-
366	6	-	-
1461	6	-	-
1642	-	1	-
1826	6	5	-
1840	6	-	-
1841	-	1	-
2008	-	2	-
2192	6	4	-
2206	6	-	-
2373	-	2	-
2557	6	4	-
2571	6	-	-
2572	-	-	1
2738	-	2	1
2922	6	4	6
2936	6	-	-

$$P\left(d_{obs}\middle|X\right)\propto \exp\left(-\frac{1}{2}\sum_{i=1}^{117}\left(\frac{d_{obs(i)}-d_{sim(i)}}{\sigma_i}\right)^2\right) \quad \text{..... (20)}$$

The Posterior Distribution

Our posterior distribution was constructed under the Bayesian frame based on the prior

distribution and likelihood function described above (**Eq. 18** and **Eq. 20**), and is

$$P(X|d_{obs}) \propto P(d_{obs}|X)P(X)$$

$$P(X|d_{obs}) = C\exp\left(-\frac{1}{2}\left(\left(\sum\left(\frac{\log X_{k_i} - \mu_{\log X_k}}{\sigma_{\log X_k}}\right)^2 + \sum\left(\frac{X_{\phi_i} - \mu_{X_\phi}}{\sigma_{X_\phi}}\right)^2\right) + \sum_{i=1}^{117}\left(\frac{d_{obs(i)} - d_{sim(i)}}{\sigma_i}\right)^2\right)\right)$$

…….. (21)

The objective function is thus

$$O(X) = \left(\sum\left(\frac{\log X_{k_i} - \mu_{\log X_k}}{\sigma_{\log X_k}}\right)^2 + \sum\left(\frac{X_{\phi_i} - \mu_{X_\phi}}{\sigma_{X_\phi}}\right)^2\right) + \sum_{i=1}^{117}\left(\frac{d_{obs(i)} - d_{sim(i)}}{\sigma_i}\right)^2 \text{ ……. (22)}$$

Parameter Space Search

The parameter search process was carried out using the MCMC sampling method. First, we randomly sampled the set of multipliers from our prior distribution and regarded this as our first model in the chain. Then, we independently perturbed a portion of multipliers to get our next set of multipliers, which will be our next model in the chain. Because of the prior distributions defined, all parameter values were capped by maximum values (4 for permeability multiplier and 2.28 for porosity multiplier) and a minimum value of 0 to prevent extreme and unrealistic values. Whether or not the new model can be accepted into the chain, after it is generated, is determined by the ratio R (**Eq. 23**). It is the ratio of the posterior distribution values between the new and previous model.

$$R = \frac{\exp\left\{-\frac{1}{2}\left(\left(\sum\left(\frac{\log X_{k_i}{}^{t_{i+1}} - \mu_{\log X_k}}{\sigma_{\log X_k}}\right)^2 + \sum\left(\frac{X_{\phi_i}{}^{t_{i+1}} - \mu_{X_\phi}}{\sigma_{X_\phi}}\right)^2\right) + \sum_{i=1}^{117}\left(\frac{d_{obs(i)}{}^{t_{i+1}} - d_{sim(i)}{}^{t_{i+1}}}{\sigma_i}\right)^2\right)\right\}}{\exp\left\{-\frac{1}{2}\left(\left(\sum\left(\frac{\log X_{k_i}{}^{t_i} - \mu_{\log X_k}}{\sigma_{\log X_k}}\right)^2 + \sum\left(\frac{X_{\phi_i}{}^{t_i} - \mu_{X_\phi}}{\sigma_{X_\phi}}\right)^2\right) + \sum_{i=1}^{117}\left(\frac{d_{obs(i)}{}^{t_i} - d_{sim(i)}{}^{t_i}}{\sigma_i}\right)^2\right)\right\}}$$

…….. (23)

With a known R, we randomly draw a number from the uniform distribution U(0,1). If the random number is smaller than R, we accept this new model and add this new model to the chain. Otherwise, we reject the new model and add the previous model to the chain again. This completes one iteration of the MCMC sampling process. Returning to the perturbing step, we continue adding models to the chain. The posterior distribution can be built up with a sufficient number of models in the chain. The steps are summarized as follows:

1. Randomly sample a set of multipliers from **Eq. 16**, denoted as X^{t_1} .
2. From state t_i to state t_{i+1}, $X^{t_{i+1}} = X^{t_i} + \sigma\varepsilon$

   ε is a 90-dimensional standard normal random variable. σ is a scale factor.
3. $R = \dfrac{P\left(X^{t_{i+1}} \middle| d_{obs}{}^{t_{i+1}}\right)}{P\left(X^{t_i} \middle| d_{obs}{}^{t_i}\right)}$
4. Randomly draw a number y from uniform distribution between 0 and 1. If $y \le R$, accept $X^{t_{i+1}}$ in chain. If $y > R$, put X^{t_i} in chain again.
5. Go back to step 2

In using this MCMC sampling process, it is very important to choose the scalar σ properly and to decide how many parameters are perturbed each iteration. They directly affect if our chain could mix well or converge fast with a reasonable acceptance rate. In order to show how the acceptance rate affects the sampled distribution, tests were carried out on the porosity multiplier of our prior distribution with a number of 10,000-sample models. If the acceptance rate of the whole chain is too high, all the samples would almost have the same values, which means the parameter space is only partially explored. **Fig. 25** shows the histograms comparison between a high acceptance rate (99.7%) chain and the truth case, which illustrates this point. On the other hand, if the acceptance rate of the whole chain is too low, the chain will be stuck on the same model for a long time. The histogram cannot reproduce the shape of the probability density function with just a few accepted models. **Fig. 26** shows the histograms comparison between a low acceptance rate chain (3.2%) and the truth case. In some experiments, we set the perturb scalar as 0.1 and perturbed 10 parameters at each time, obtaining an acceptance rate of approximately 80%. With these MCMC parameters, our prior histogram reproduced the truth case much closer (**Fig. 27)**.

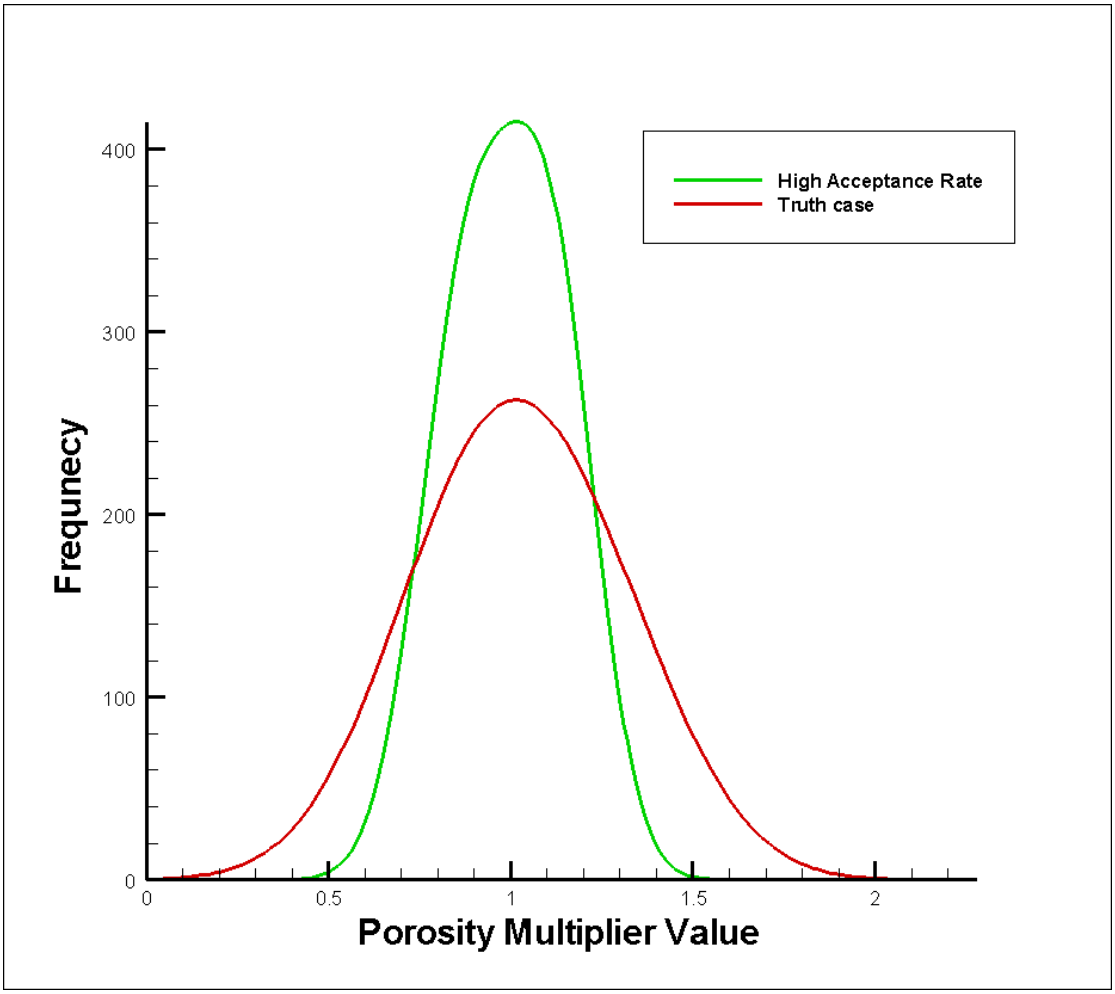

Fig. 25 - Histogram comparison between high acceptance rate chain and the truth

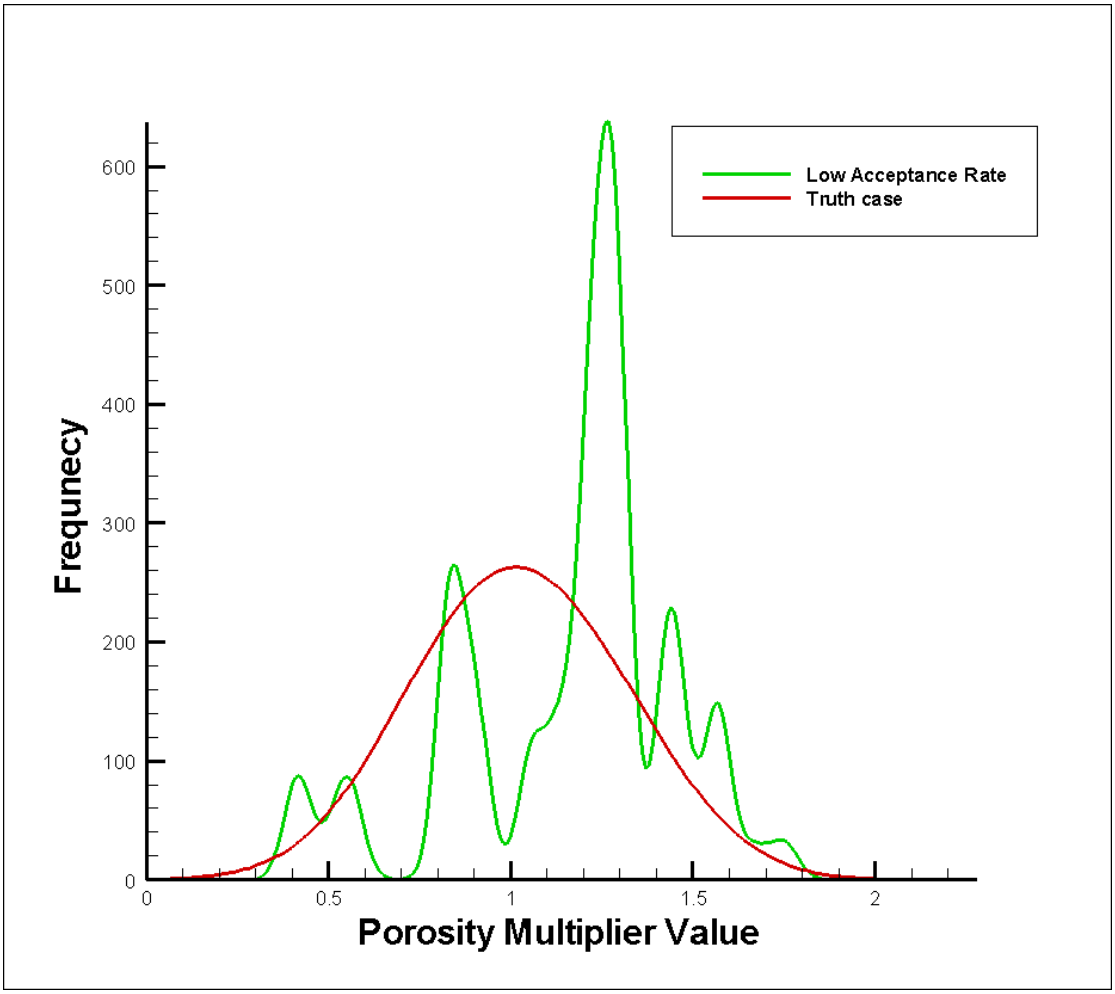

Fig. 26 - Histogram comparison between low acceptance rate chain and the truth

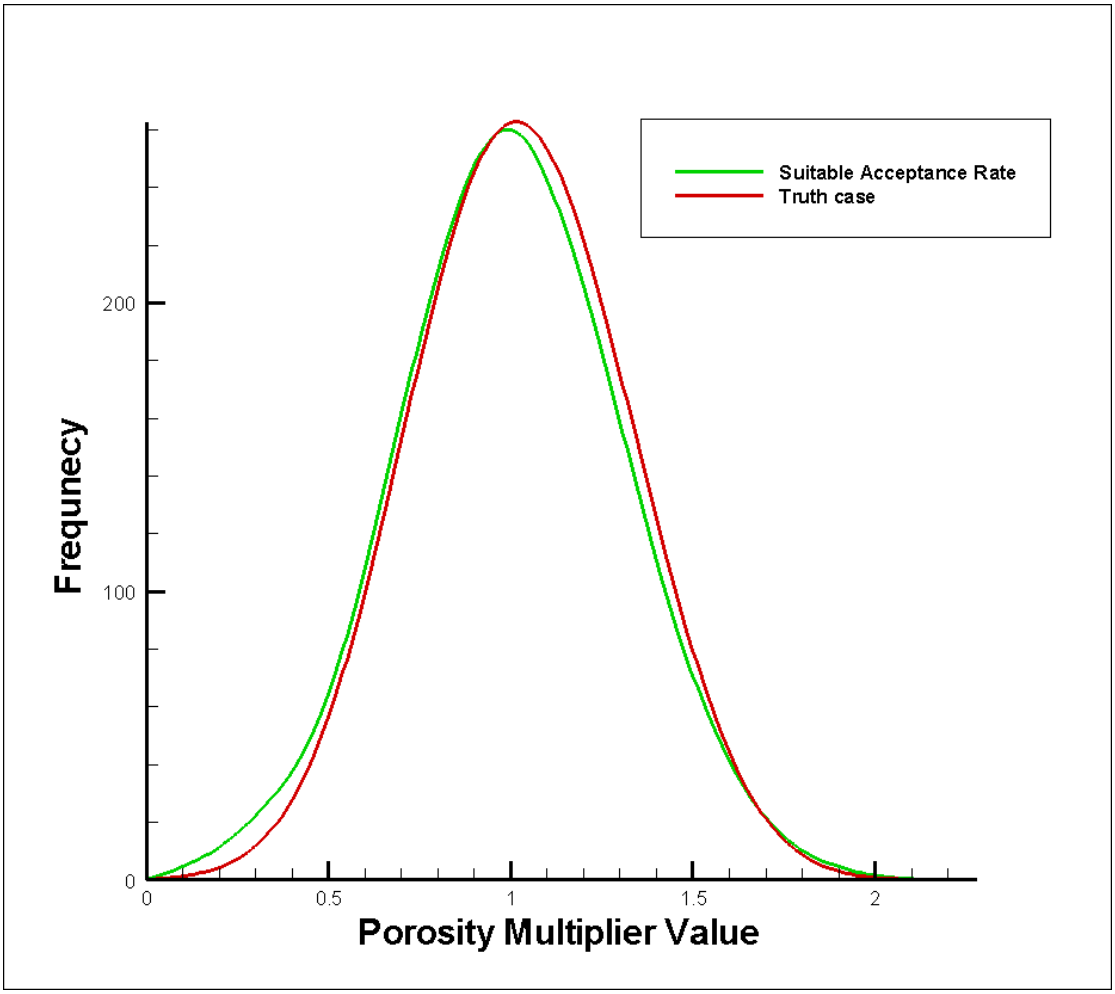

Fig. 27 - Histogram comparison between proper acceptance rate chain and the truth

Forecast

With the determined scalar value and a proper perturbation size of parameters, we can now start to sample our models from a posterior distribution (**Eq. 19**). The acceptance rate of the chain is approximately 40% when the likelihood term is included. This is also a reasonable acceptance rate to ensure a well mixed chain (Givens and hoeting 2005). The objective function value of the whole chain is shown by **Fig. 28.** The program is run to get 17,400 samples, where we determine by observation that the chain is stable and long enough to build up the posterior distribution. The first 7,000 models are determined visually to be in the burn-in period and are eliminated from the chain. We use the rest of the models to forecast the cumulative oil production at 16.5 years. **Fig. 29** shows the objective function value of all mixed-well models used to forecast. The forecast histogram and cumulative distribution function are shown in **Fig. 30** and **Fig. 31,** respectively. **Fig. 32** shows our results compared to previous published results.

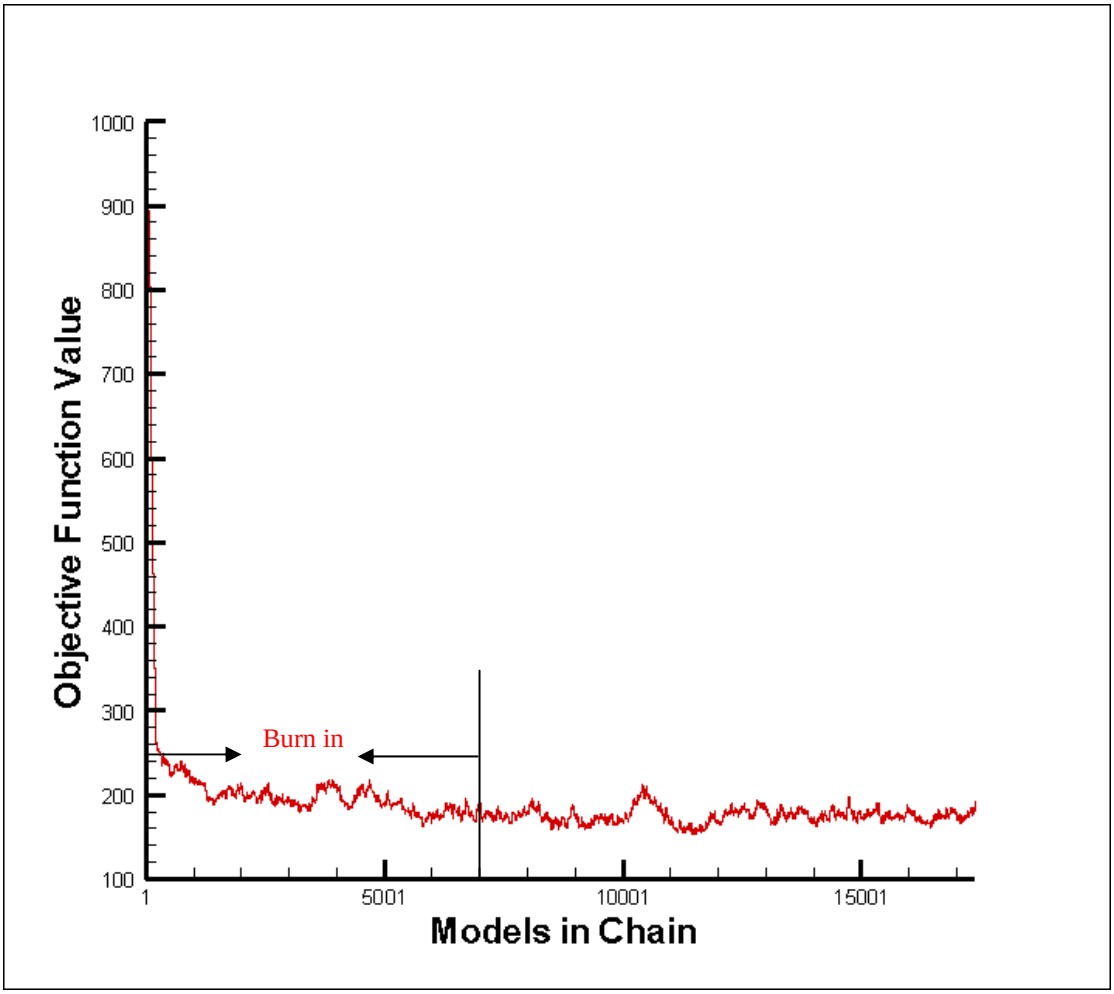

Fig. 28 - Objective function value vs. model number (static case)

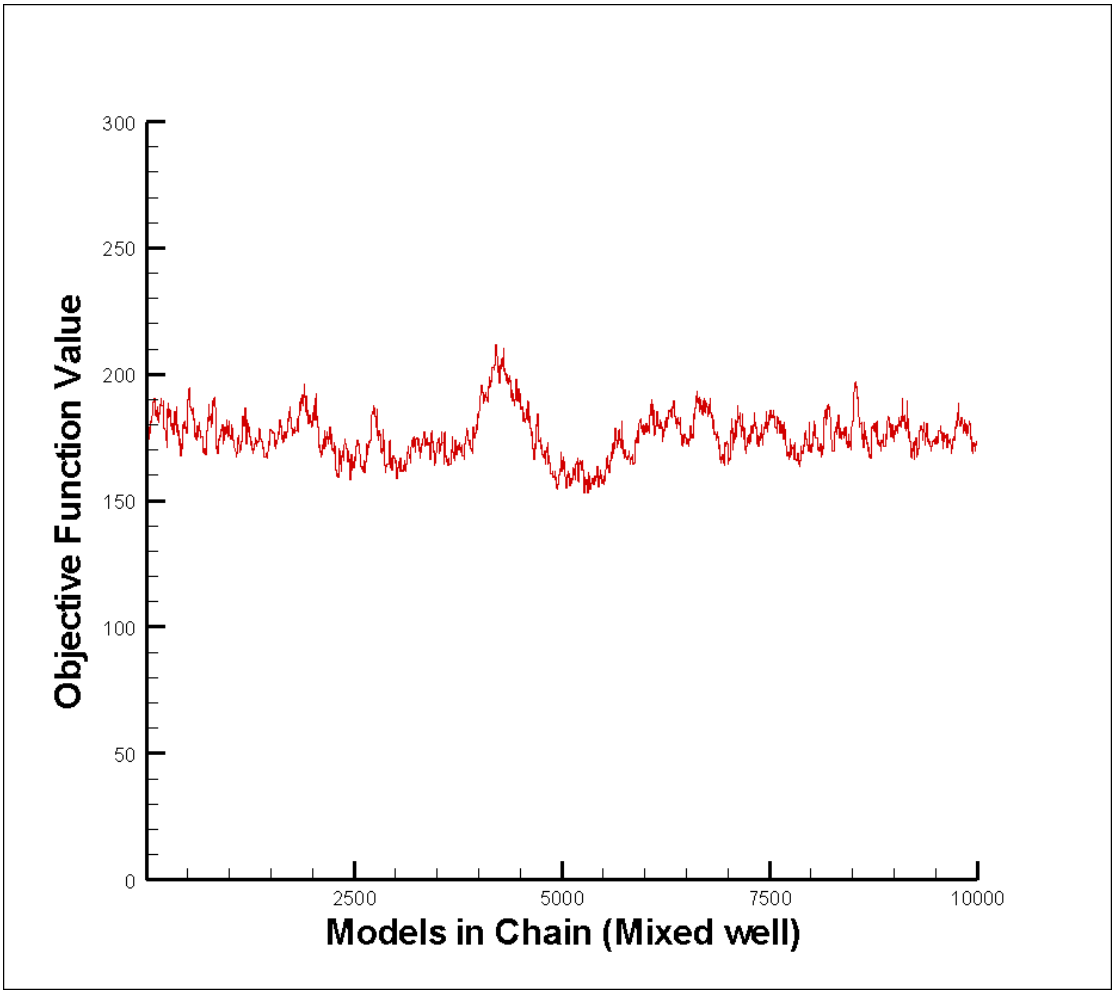

Fig. 29 - Mixed well objective function value vs. model number (static case)

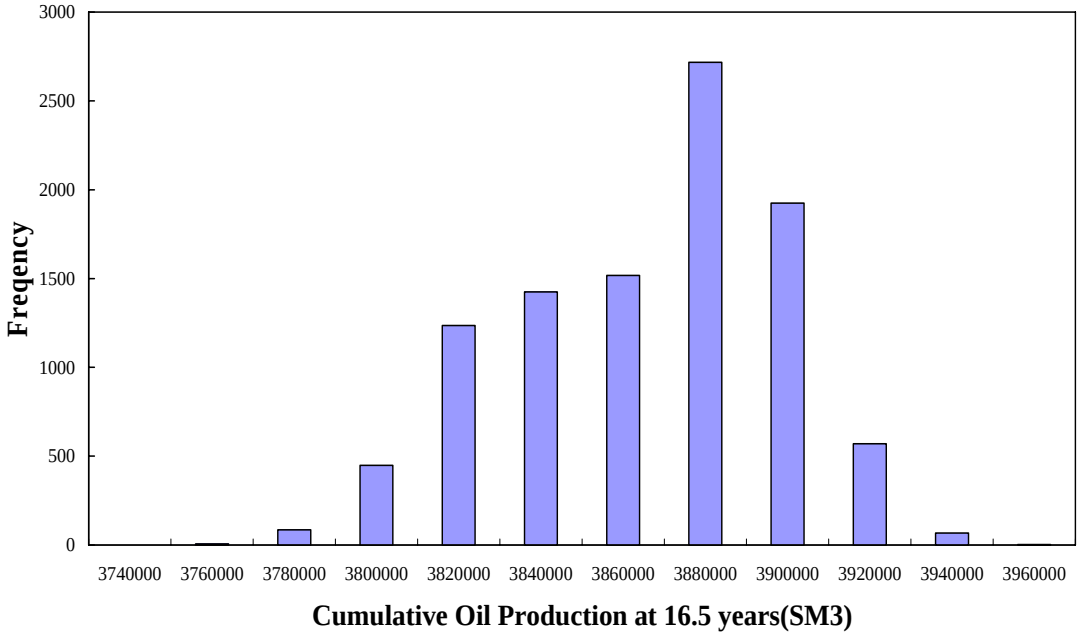

Fig. 30 - Histogram of cumulative oil production made by static case

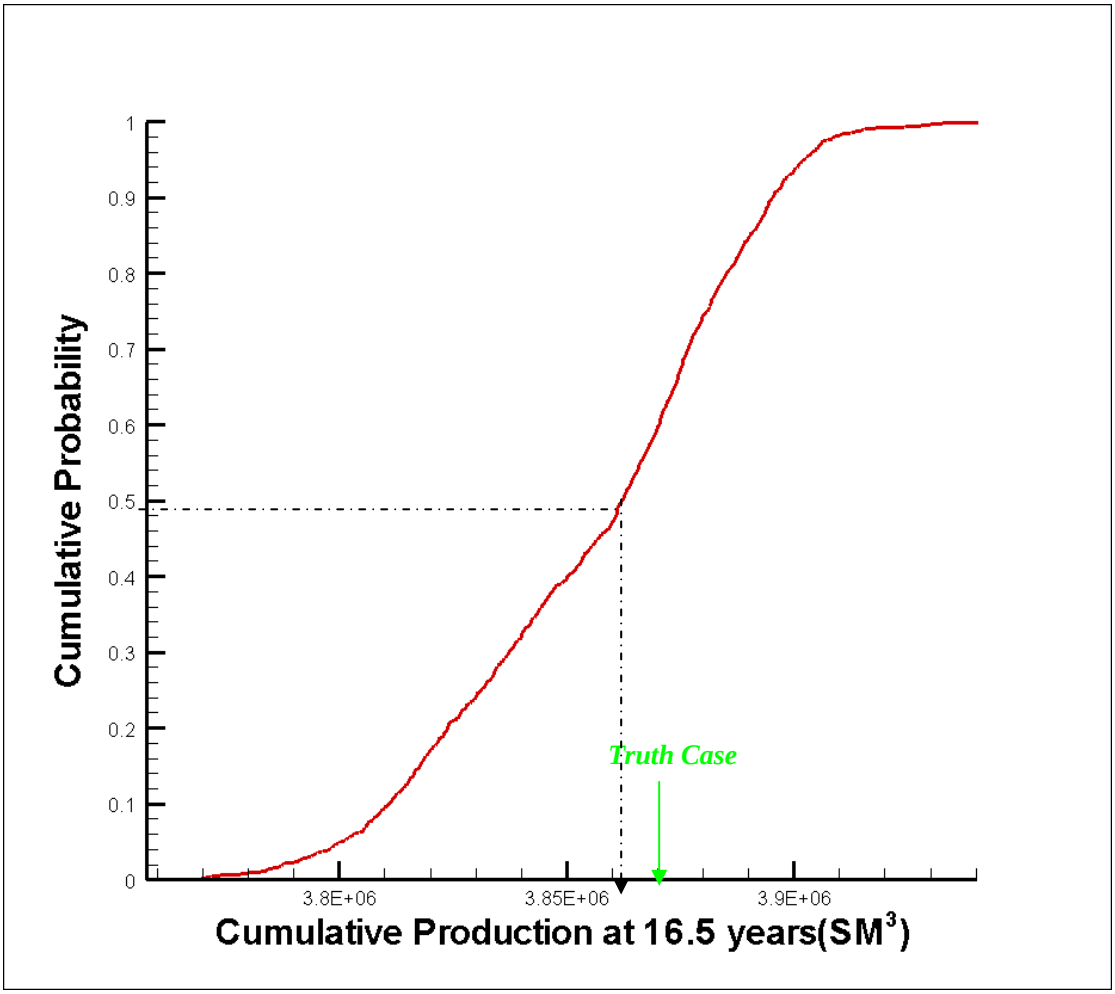

Fig. 31 - CDF of cumulative production by mixed well models in static case

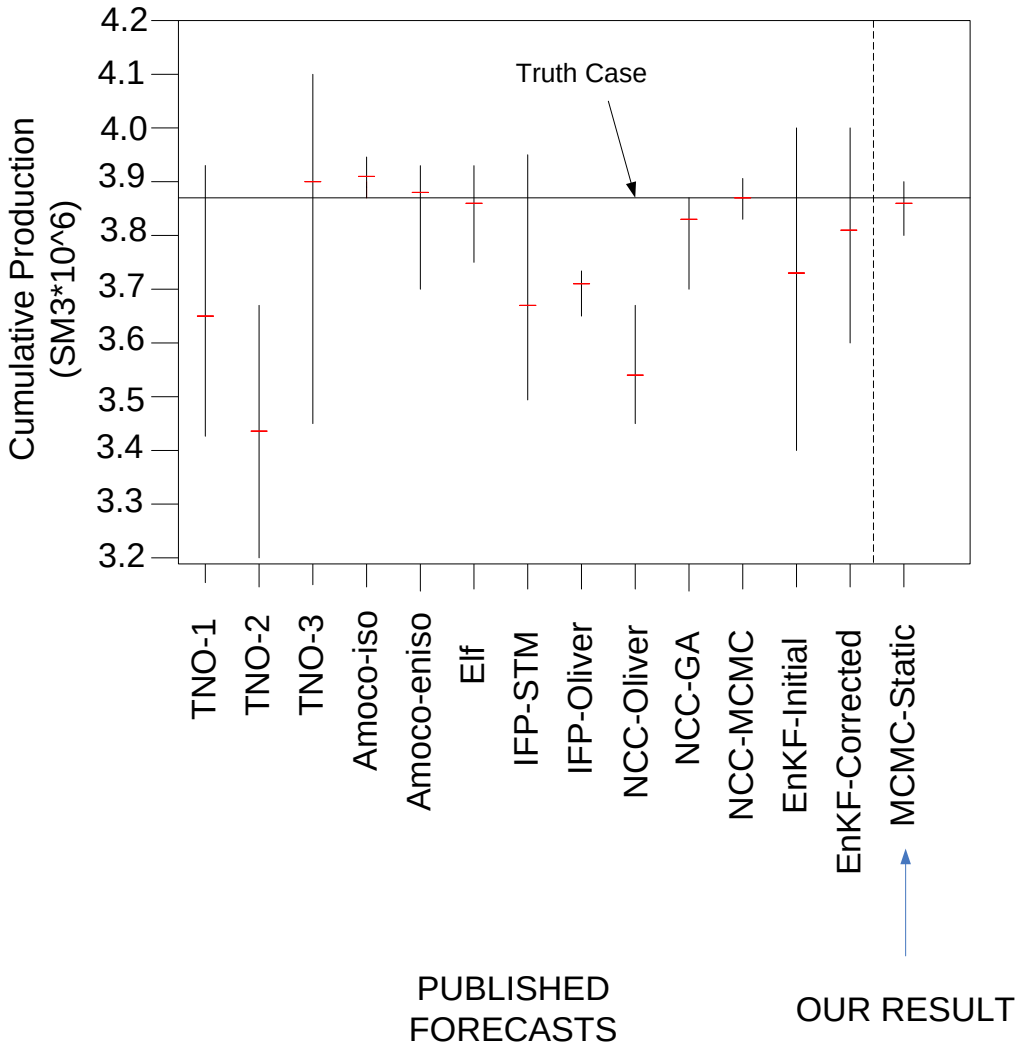

Fig. 32- Synthetic test forecast compared. A comparison of forecasts from the synthetic static test to published forecast for the PUNQ reservoir

The truth cumulative oil production at 16.5 years is $3.87\times10^{6}\,Sm^{3}$ and our P_{50} (median) model among all the samples is about $3.86\times10^{6}\,Sm^{3}$. This is much closer to the truth case than our prior model (about $3.44\times10^{6}\,Sm^{3}$). **Fig. 33** shows a comparison of the cumulative oil production forecast at 16.5 years between the prior distribution and the posterior distribution. The picture clearly proves that the MCMC history matching process leads to a production forecast that comes closer to the truth case. We also observe

that our uncertainty range narrows significantly after doing the history matching process (**Fig. 33**). The P_{10} model among all samples is about $3.80\times10^{6}Sm^{3}$ and the P_{90} model is about $3.90\times10^{6}Sm^{3}$.

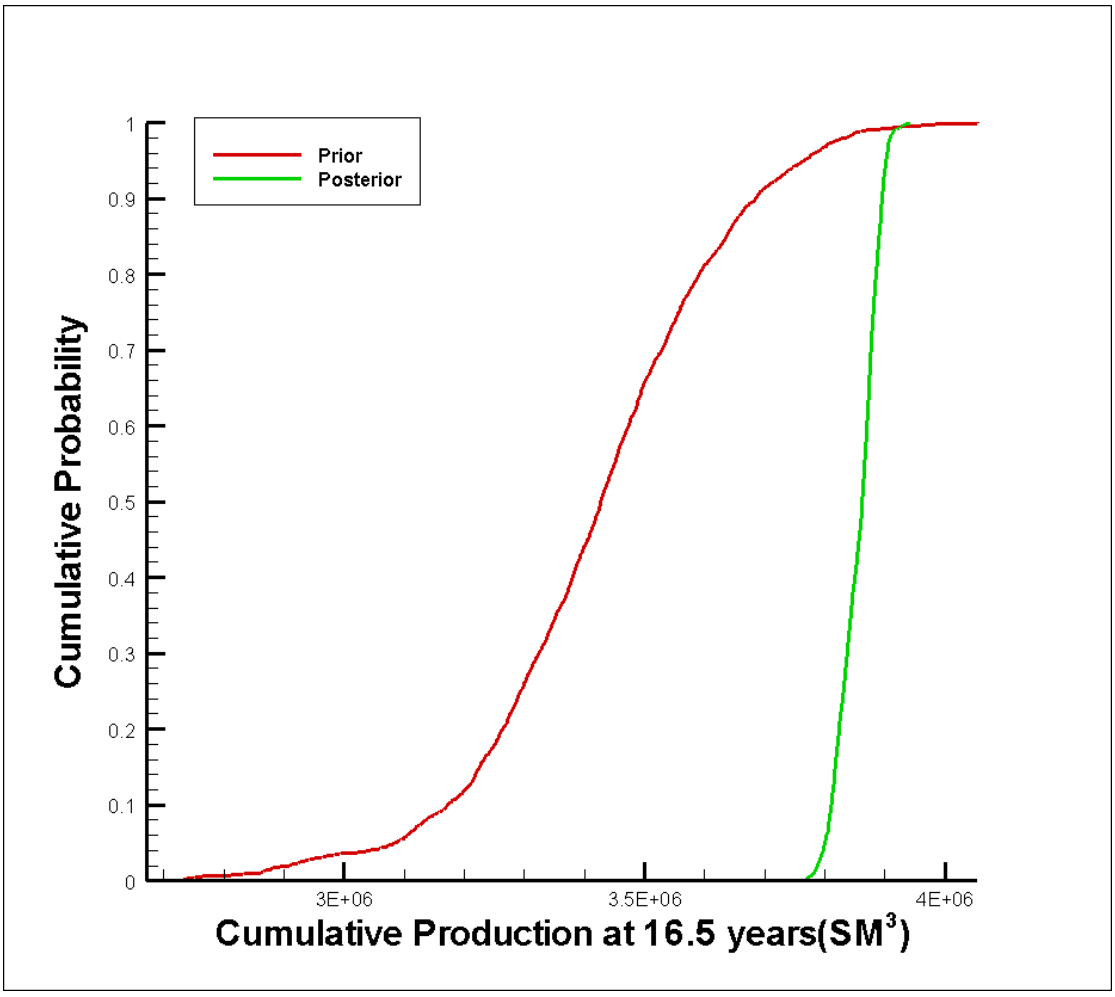

Fig. 33 - CDF comparison between prior and posterior (static case)

In addition to providing probabilistic forecasts, we can also provide a probabilistic assessment of reservoir properties by building up the multiplier distribution from our sampled models. Such information could be valuable in routine reservoir management tasks, such as infill drilling. In layers and regions where wells were completed, and thus more dynamic data were available, the posterior distributions of parameters varied significantly from the prior distribution. In layers and regions where wells were not completed, the posterior distribution deviated only slightly from the prior distribution. This is illustrated in **Fig. 34**, which shows the prior and posterior distributions of the horizontal permeability multiplier in layer 1, region 1 (no wells) and layer 4, region 4 (where a well is completed). The posterior distribution of layer 4, region 4, deviates significantly from the prior. Meanwhile, the posterior distribution in layer 1, region 1, is quite similar to the prior distribution. This behavior is typical of the other regions in the reservoir. Thus, the history matching process allows us to refine and narrow our assessments of reservoir properties in only those regions and layers in which wells are present and in which we have dynamic data available.

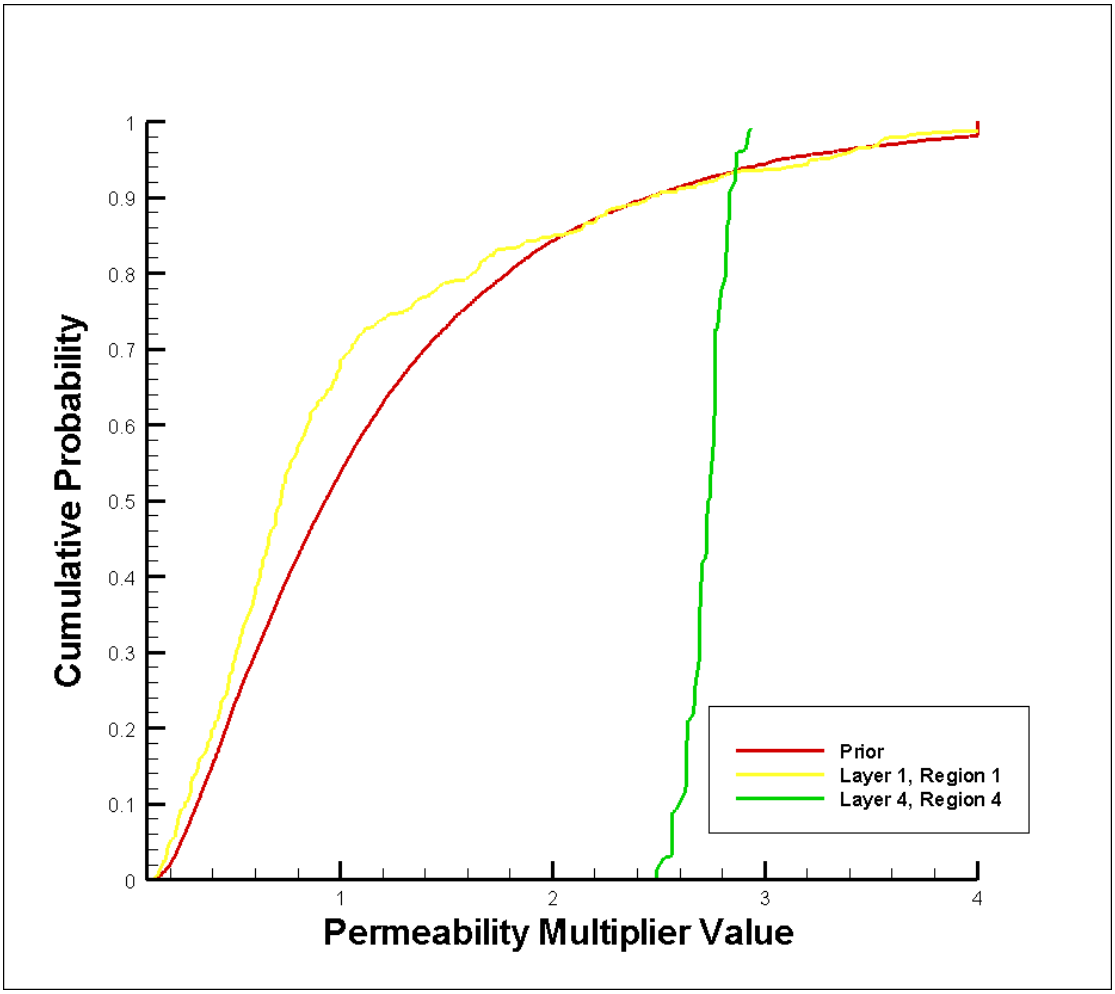

Fig. 34 - Posterior permeability assessments (static case)

Summary of Results

Close agreement between our static test forecast and the truth case demonstrates that the initial model and prior distributions were set up properly. The difference between the prior and posterior CDFs of the cumulative production forecast demonstrates the value of the MCMC history matching process. The narrower uncertainty range after the history match demonstrates that more information leads to less uncertainty. In addition, the test shows that we can improve our assessments of reservoir properties. The static case also provides a base for comparison for the continuous case discussed in the next section.

CONTINUOUS RESERVOIR STUDY

Overview

The second test was conducted on the PUNQ-S3 synthetic reservoir by using the continuous MCMC method. An objective of developing this continuous technology is to include the new observed data as soon as it becomes available, which could lead to a better estimation of the underlying reservoir.

In this continuous history matching process, the simulation runs were also matched against observed data for 9 years. The forecasts were made to 16.5 years of production. The difference is that the PUNQ-S3 model was continuously simulated, starting from year 4.5 and continuing through the end of year 9, making forecasts to 16.5 years. During the test, the history data were added in sequence at the 5^{th}, 6^{th}, 7^{th}, 8^{th} and 9^{th} years. For the first half year (4.5 to 5 years), 4,500 models were sampled and the number of sampled models was 9,000 per year for the remaining years. As a result, the total number of simulation samples was 49,500. All of this assumes that 9000 model runs can be made in a year of actual time. This equates to about one run per hour, which is not atypical in the petroleum industry today for fieldwide simulation runs. Thus, the comparisons to be made in this section are between static and continuous simulations at the end of year 10, one year after the acquisition of the last observed data at the end of year 9.

In this continuous study, our uncertain parameters are also the 90 porosity and

permeability multipliers. The initial model and prior multiplier distribution are the same as we used in our static test. As we add in the observed data sequentially, our likelihood function (**Eq. 19**) changes when the new observed data are included. Compared to the sampled models prior to adding in the new data, the later sampled models' posterior distribution would include more observed and simulated data. Results of these runs were combined into probabilistic forecasts at the time points corresponding to the addition of new observed data.

The Likelihood Function

In the continuous MCMC test, the history data are divided into six parts and the sampling process starts in year 4.5. The new history data are added in sequentially; at the 5^{th}, 6^{th}, 7^{th}, 8^{th} and 9^{th} years. **Table 9** shows how we divided the history data.

Table 9 - Observed data in the continuous case (each color sequence corresponds to a different data assimilation)

Time(days)	WBHP(BARSA)	WGOR(Sm^3 / Sm^3)	WWCT(Sm^3 / Sm^3)
1.01	6	-	-
91	6	-	-
182	6	-	-
274	6	-	-
366	6	-	-
1461	6	-	-
1642(before 4.5 year)	-	1	-
1826(before 5 year)	6	5	-
1840	6	-	-
1841	-	1	-
2008	-	2	-
2192(before 6 year)	6	4	-
2206	6	-	-
2373	-	2	-
2557(before 7 year)	6	4	-
2571	6	-	-
2572	-	-	1
2738	-	2	1
2922(before 8 year)	6	4	6
2936(before 9 year)	6	-	-

Recall that **Eq. 20** shows the likelihood function with all history data in the static case. Here, **Eqs. 24-29** represent the likelihood functions used in 4.5^{th}, 5^{th}, 6^{th}, 7^{th}, 8^{th} and 9^{th} years, respectively.

$$P\left(d_{obs}\middle|X\right) \propto \exp\left(-\frac{1}{2}\sum_{i=1}^{37}\left(\frac{d_{obs(i)}-d_{sim(i)}}{\sigma_i}\right)^2\right) \quad \text{..... (24)}$$

$$P\left(d_{obs}\middle|X\right) \propto \exp\left(-\frac{1}{2}\sum_{i=1}^{48}\left(\frac{d_{obs(i)}-d_{sim(i)}}{\sigma_i}\right)^2\right) \quad \text{..... (25)}$$

$$P(d_{obs}|X) \propto \exp\left(-\frac{1}{2}\sum_{i=1}^{67}\left(\frac{d_{obs(i)}-d_{sim(i)}}{\sigma_i}\right)^2\right) \quad \text{..... (26)}$$

$$P(d_{obs}|X) \propto \exp\left(-\frac{1}{2}\sum_{i=1}^{85}\left(\frac{d_{obs(i)}-d_{sim(i)}}{\sigma_i}\right)^2\right) \quad \text{.....(27)}$$

$$P(d_{obs}|X) \propto \exp\left(-\frac{1}{2}\sum_{i=1}^{111}\left(\frac{d_{obs(i)}-d_{sim(i)}}{\sigma_i}\right)^2\right) \quad \text{..... (28)}$$

$$P(d_{obs}|X) \propto \exp\left(-\frac{1}{2}\sum_{i=1}^{117}\left(\frac{d_{obs(i)}-d_{sim(i)}}{\sigma_i}\right)^2\right) \quad \text{..... (29)}$$

The Posterior Distribution

Due to the changes we have made in the likelihood function, the posterior distributions in different years also differ from each other. **Eq. 21** shows the posterior distribution with all 9 year's history data in the static case. Here, **Eqs. 30-35** represent the posterior distribution used in 4.5th, 5th, 6th, 7th, 8th and 9th years, respectively.

$$P(X|d_{obs}) = C\exp\left(-\frac{1}{2}\left(\left(\sum\left(\frac{\log X_{k_i}-\mu_{\log X_k}}{\sigma_{\log X_k}}\right)^2+\sum\left(\frac{X_{\phi_i}-\mu_{X_\phi}}{\sigma_{X_\phi}}\right)^2\right)+\sum_{i=1}^{37}\left(\frac{d_{obs(i)}-d_{sim(i)}}{\sigma_i}\right)^2\right)\right)$$

..... (30)

$$P(X|d_{obs}) = C\exp\left(-\frac{1}{2}\left(\left(\sum\left(\frac{\log X_{k_i}-\mu_{\log X_k}}{\sigma_{\log X_k}}\right)^2+\sum\left(\frac{X_{\phi_i}-\mu_{X_\phi}}{\sigma_{X_\phi}}\right)^2\right)+\sum_{i=1}^{48}\left(\frac{d_{obs(i)}-d_{sim(i)}}{\sigma_i}\right)^2\right)\right)$$

..... (31)

$$P(X|d_{obs}) = C\exp\left(-\frac{1}{2}\left(\left(\sum\left(\frac{\log X_{k_i}-\mu_{\log X_k}}{\sigma_{\log X_k}}\right)^2+\sum\left(\frac{X_{\phi_i}-\mu_{X_\phi}}{\sigma_{X_\phi}}\right)^2\right)+\sum_{i=1}^{67}\left(\frac{d_{obs(i)}-d_{sim(i)}}{\sigma_i}\right)^2\right)\right)$$

..... (32)

$$P(X|d_{obs}) = C\exp\left(-\frac{1}{2}\left(\left(\sum\left(\frac{\log X_{k_i} - \mu_{\log X_k}}{\sigma_{\log X_k}}\right)^2 + \sum\left(\frac{X_{\phi_i} - \mu_{X_\phi}}{\sigma_{X_\phi}}\right)^2\right) + \sum_{i=1}^{85}\left(\frac{d_{obs(i)} - d_{sim(i)}}{\sigma_i}\right)^2\right)\right)$$

…… (33)

$$P(X|d_{obs}) = C\exp\left(-\frac{1}{2}\left(\left(\sum\left(\frac{\log X_{k_i} - \mu_{\log X_k}}{\sigma_{\log X_k}}\right)^2 + \sum\left(\frac{X_{\phi_i} - \mu_{X_\phi}}{\sigma_{X_\phi}}\right)^2\right) + \sum_{i=1}^{111}\left(\frac{d_{obs(i)} - d_{sim(i)}}{\sigma_i}\right)^2\right)\right)$$

…… (34)

$$P(X|d_{obs}) = C\exp\left(-\frac{1}{2}\left(\left(\sum\left(\frac{\log X_{k_i} - \mu_{\log X_k}}{\sigma_{\log X_k}}\right)^2 + \sum\left(\frac{X_{\phi_i} - \mu_{X_\phi}}{\sigma_{X_\phi}}\right)^2\right) + \sum_{i=1}^{117}\left(\frac{d_{obs(i)} - d_{sim(i)}}{\sigma_i}\right)^2\right)\right)$$

…… (35)

Parameter Space Search

As mentioned above, 49,500 simulation runs were made corresponding to a 5.5-year period during history matching. In order to continuously simulate during a significant percentage of the reservoir's life, the test was performed in such a way that time was "accelerated". **Fig. 35** shows the cumulative number of runs made versus the producing time of the reservoir. The new data are added in at the end of every year. The additional data were included in the objective function calculation at the corresponding time in the reservoir's life. Care must be taken when making comparisons between runs made at different points in time because the objective function value changes with time. One must also make sure that the new sampled models have the possibility to be accepted. The last model is added is accepted into the chain again with the new posterior distribution value. The steps are as follows:

1. Randomly sample a set of multiplier from **Eq. 18**, denoted as X^{t_1} .

2. From state t_i to state t_{i+1}, $X^{t_{i+1}} = X^{t_i} + \sigma\varepsilon$

   ε is a 90-dimensional standard normal random variable. σ is a scalar factor.

3. $R = \dfrac{P\left(X^{t_{i+1}} \middle| d_{obs}{}^{t_{i+1}}\right)}{P\left(X^{t_i} \middle| d_{obs}{}^{t_i}\right)}$

4. Randomly draw a number y from uniform distribution between 0 and 1. If $y \le R$, accept $X^{t_{i+1}}$ in chain. If $y > R$, put X^{t_i} in chain again.

5. Check to see if new observed data are available. If yes, recalculate the last model in the chain with the new posterior distribution function and go to step 2. If no, go directly to step 2.

Additionally, in order to make the chain converge fast and mix well, the scalar and perturbation size used in the continuous case are the same as those used in the static case.

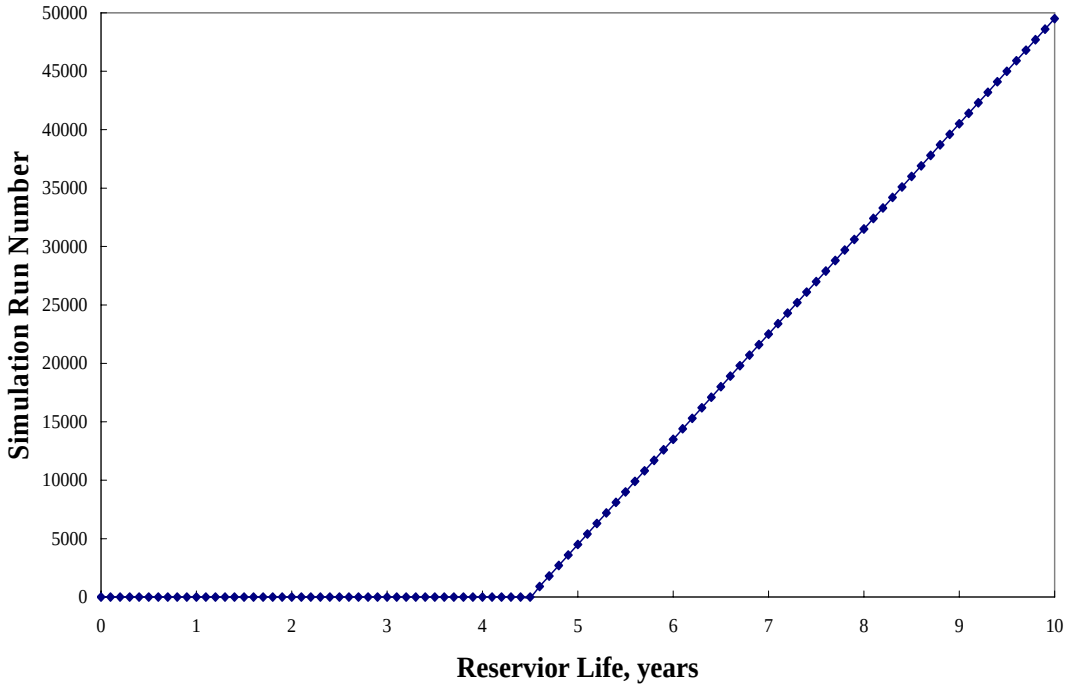

Fig. 35 - Continuous test run number by time. Run number versus point in reservoir life for the continuous test

Forecast

The sampling process starts at year 4.5 with the fixed scalar and perturbation size, and runs up to the end of the 10th year. **Fig. 36** shows the objective function values for all runs made in this test, listed by time in the reservoir's life. We see that there are several points in the process where the objective function values shift. These shifts are caused by adding new data and thus changing the objective function definition. Forecasts were made at 5, 6, 7, 8, 9 and 10 years using sampled models in the chain available at the respective times. These probabilistic forecasts were created by taking only the runs made over the past year (or half year at 5 years). In **Fig. 36** we do not see an early-time portion in which the objective function decreases significantly, as opposed to the static case where we saw a burn-in time of about 7000 models. There is no significant shift and subsequent decline at data assimilation points, such as at model 40,501 where we added in the new history data between the 8th and 9th years. For this reason, we used all the models since the last assimilation to build up our forecast distributions at the different times. Each run was given equal weight in the forecasts. **Figs. 39-42** show the forecast histograms using interval sampled models. For instance, **Fig. 42** is the forecast done by using 9,000 models between the 9th and 10th years. The cumulative distributions of these forecasts are shown together in **Fig. 43**.

Fig. 44 shows all the forecast uncertainties made by various methods including our static and continuous MCMC, as well as the PUNQ-S3 forecasts published in Barker et al. (2001) and forecast ranges generated using the EnKF method (Gu and Oliver 2004). All the published forecasts were made using all the data through year 9, including the EnKF,

except for the continuous MCMC yearly forecasts with different history data. The median of our forecast made between the 9^{th} and 10^{th} years, which includes all the history data, is pretty close to the truth case. Also, from **Fig. 44,** we can tell our continuous result is comparable to NCC-MCMC method because of the similar uncertainty rage. This happens as well as the traditional MCMC method.

We can draw some general conclusions from **Fig. 44**. First, we see the medians of our forecasts are moving from the median of the prior distribution ($3.44\times10^{6}Sm^{3}$ made by the initial model) towards the truth case. This happens year by year while adding in more yearly history data. This is because the likelihood term in our posterior distribution is assuming more weight with more observed data, which will lead the forecast result from prior model to the truth case by involving more history information. Second, we see that as time progresses, the uncertainty range narrows and shifts. This shows the newly observed data are of value because they alter our assessments. The narrowing and shifting are more obvious in the early years' forecasts, which also seems reasonable. Early on, the observed data set included in our posterior distribution is smaller and, thus, each new available data point will have a larger impact on the posterior distribution. As the data set becomes larger, the impact of new available data during the later year decreases. The uncertainty range narrows as more data are assimilated. This makes sense, as we would expect the uncertainty to decrease as we acquire more information about the reservoir.

Fig. 44 shows the production forecasts with all the history data made by the static and continuous cases (between the 9^{th} and 10^{th} years). Even though both are similar and close

to the truth case, the comparison is not quite fair because the static case is using many more sampled models to build up the uncertainty range as opposed to the continuous case. In the static case, we ran 17,400 models and used the last 10,400 models to forecast the uncertainty, considering the first 7000 models to be the burn-in period. In our continuous case, we simply used all 9,000 models sampled from the beginning of the 9^{th} year. This saved almost a year's worth of simulation runs and yielded a slightly better forecast (smaller uncertainty) than the static case. If we want to compare forecasts at the end of the 10^{th} year, we can only make a fair comparison by using the 9,000 models sampled from the continuous case and the first 9,000 models from our static case (assuming only 9000 simulation runs can be made in year). **Fig. 45** shows the objective function comparison for these two cases, while **Fig. 46** shows the cumulative production vs. model number. **Fig. 47** shows the CDFs of static case and continuous case by using 9,000 models.

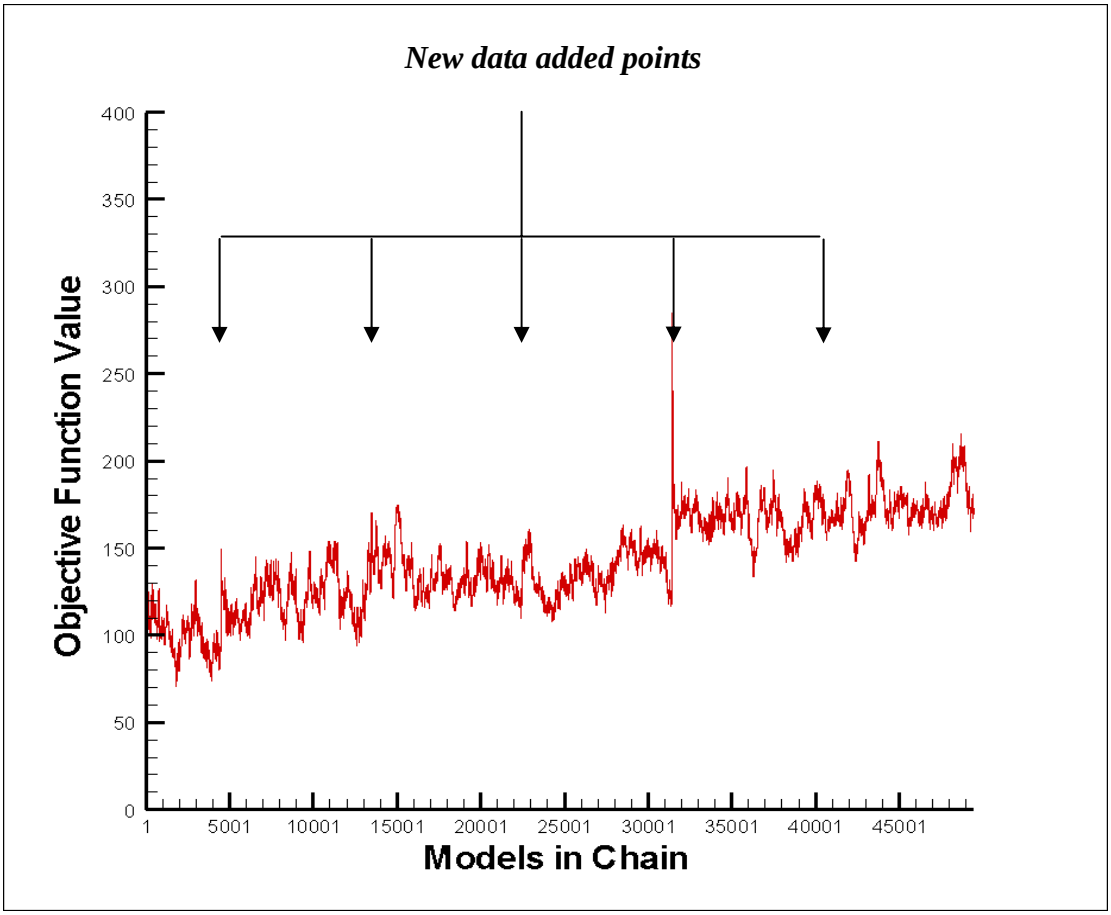

Fig. 36 - Objective function value vs. model number in continuous case

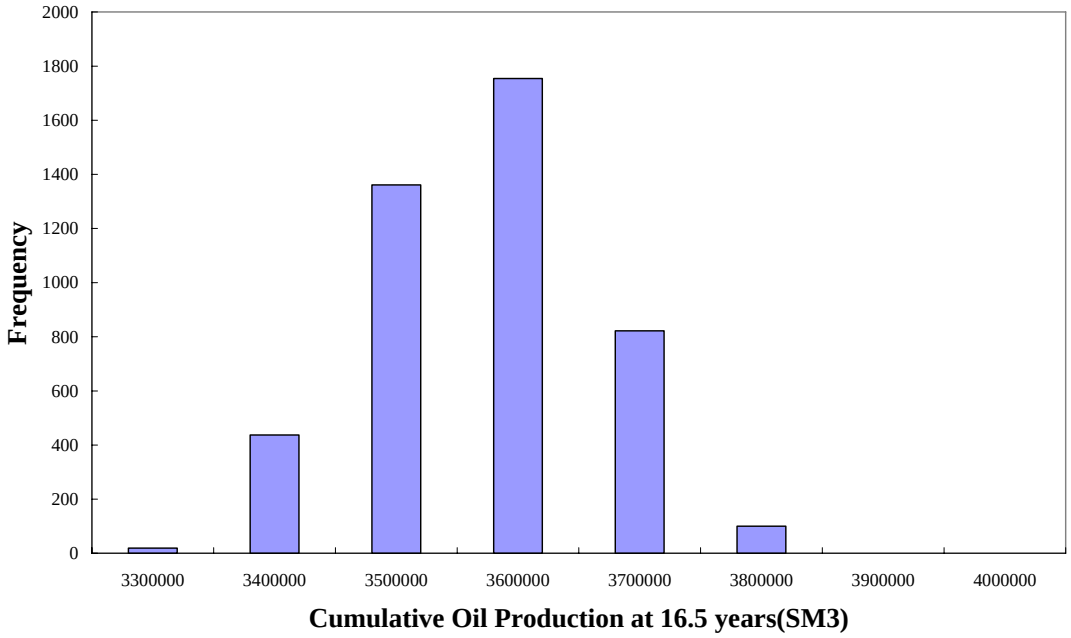

Fig. 37 - Synthetic test forecast using model between 4.5 to 5 years (runs 1-4,500)

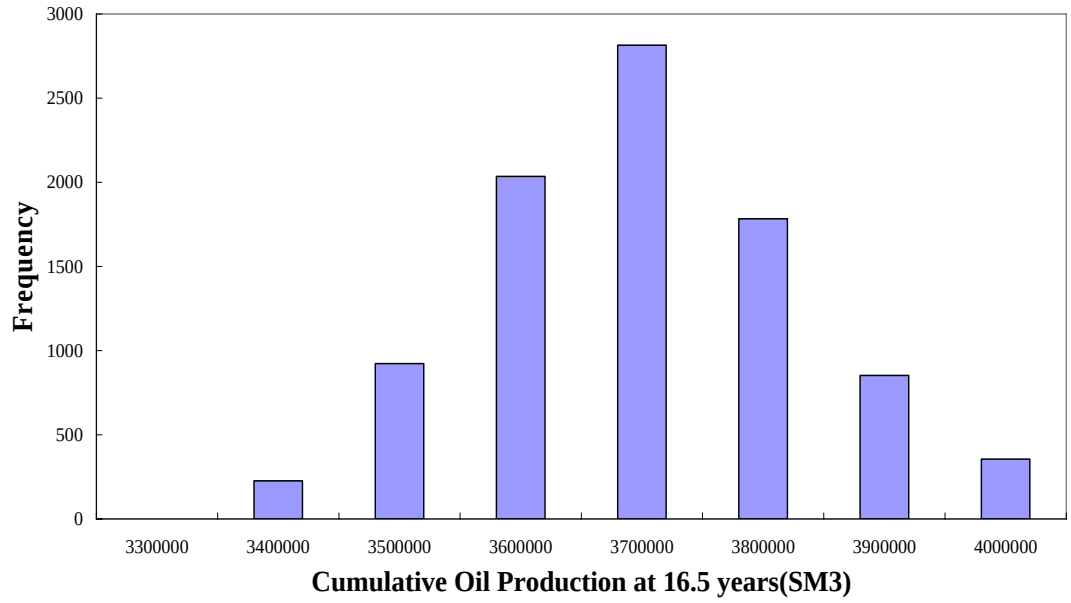

Fig. 38 - Synthetic test forecast using model between 5 to 6 years (runs 4,501-13,500)

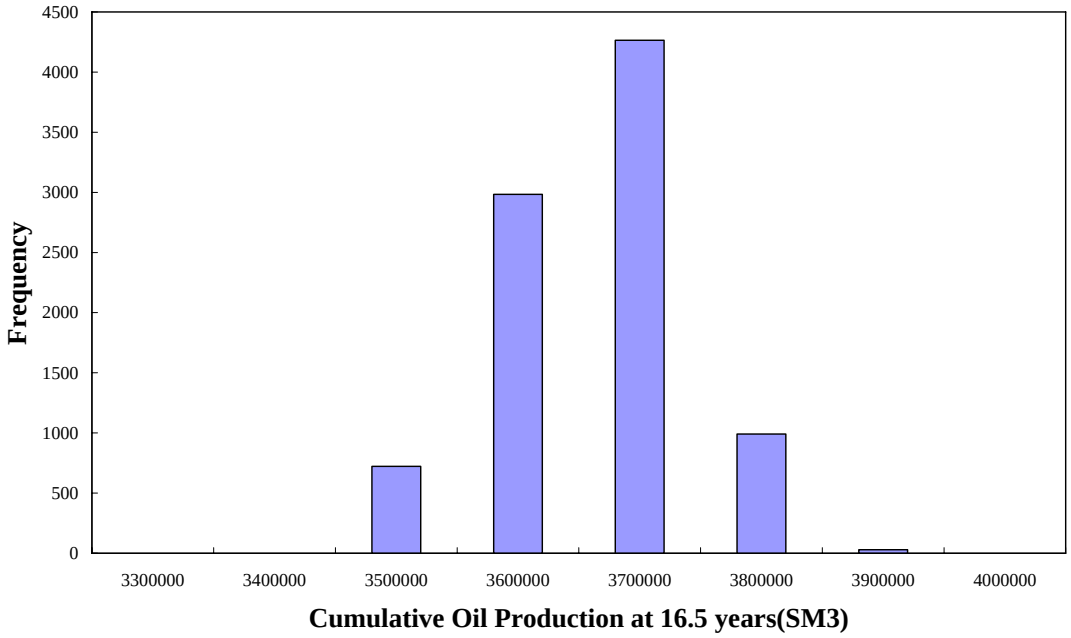

Fig. 39 - Synthetic test forecast using model between 6 to 7 years (runs 13,501-22,500)

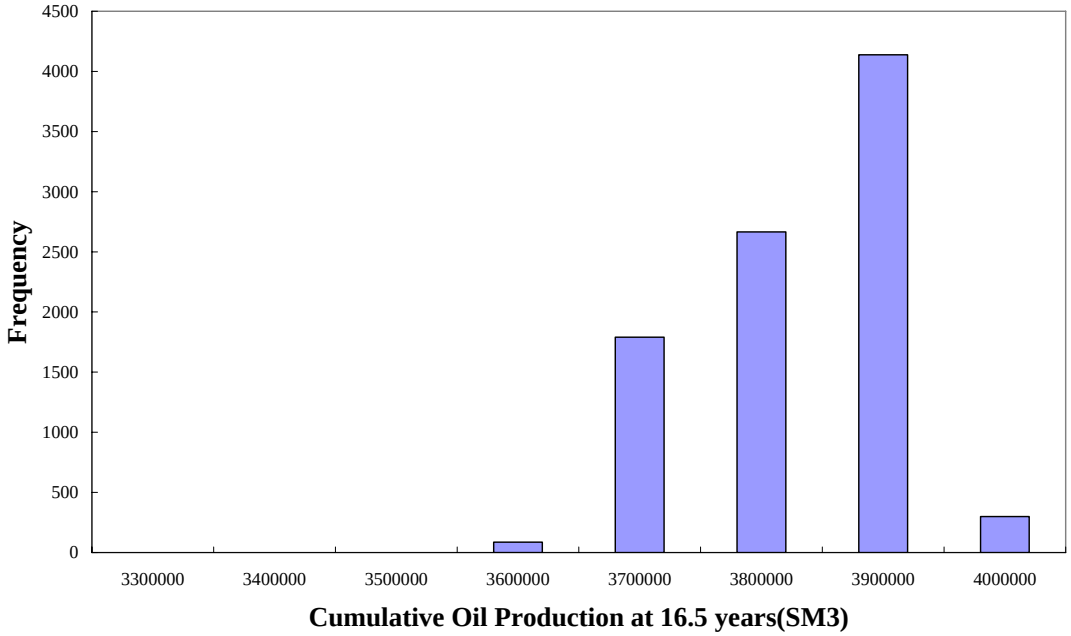

Fig. 40 - Synthetic test forecast using model between 7 to 8 years (runs 22,501-31,500)

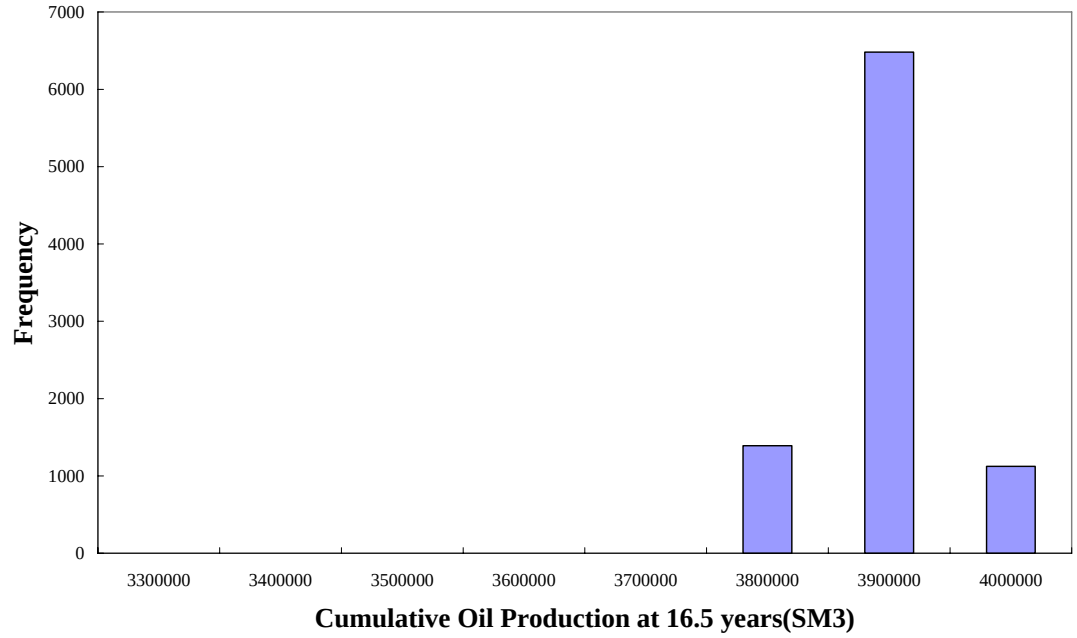

Fig. 41 - Synthetic test forecast using model between 7 to 8 years (runs 31,501-40,500)

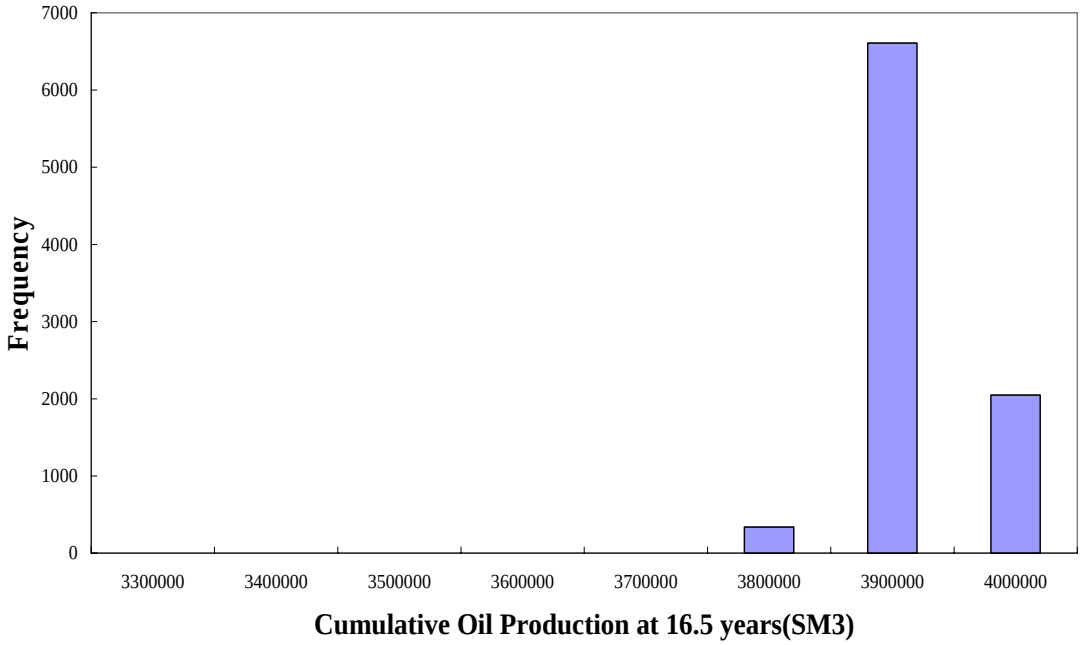

Fig. 42 - Synthetic test forecast using model between 7 to 8 years (runs 40,501-49,500)

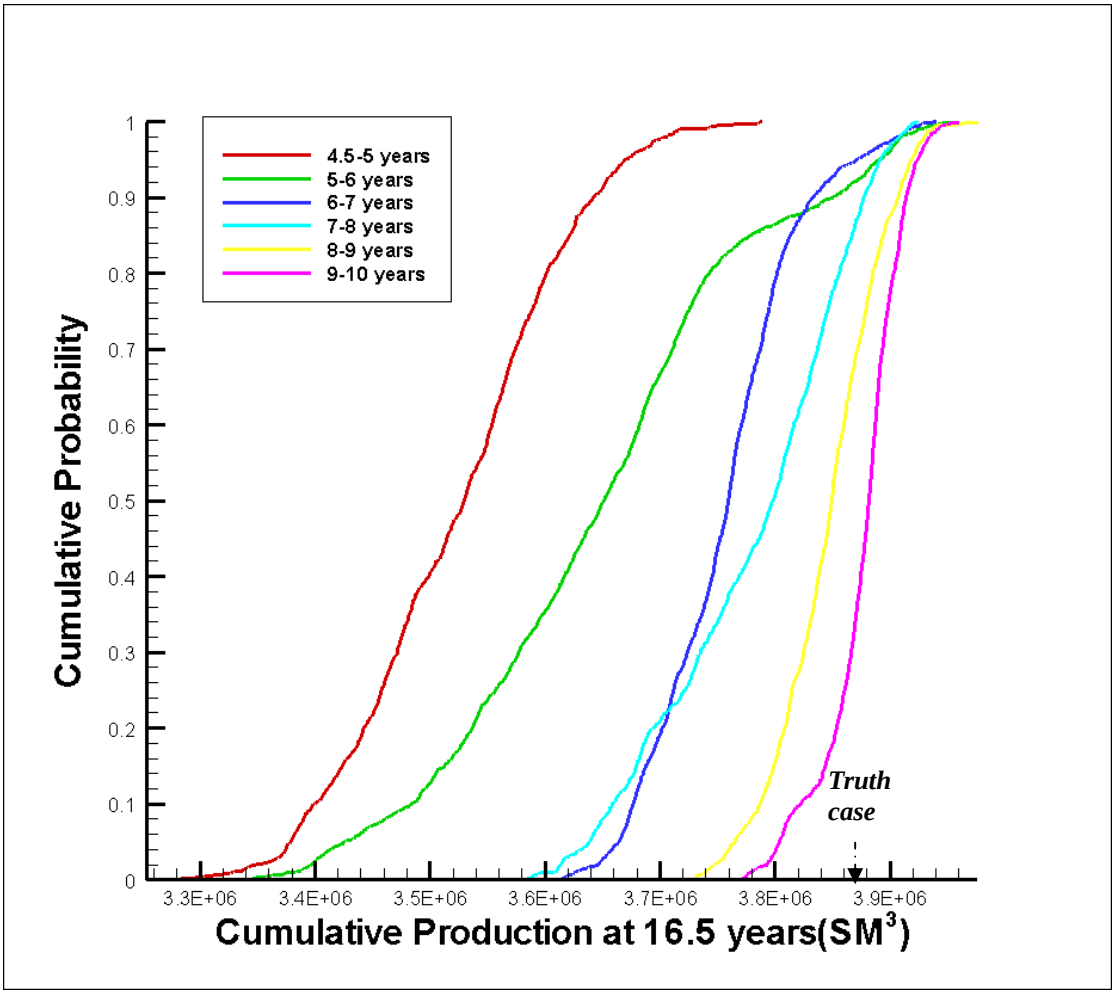

Fig. 43 - Continuous test forecast CDFs. A comparison of the cumulative distribution functions for various forecasts made during each year (or half year)

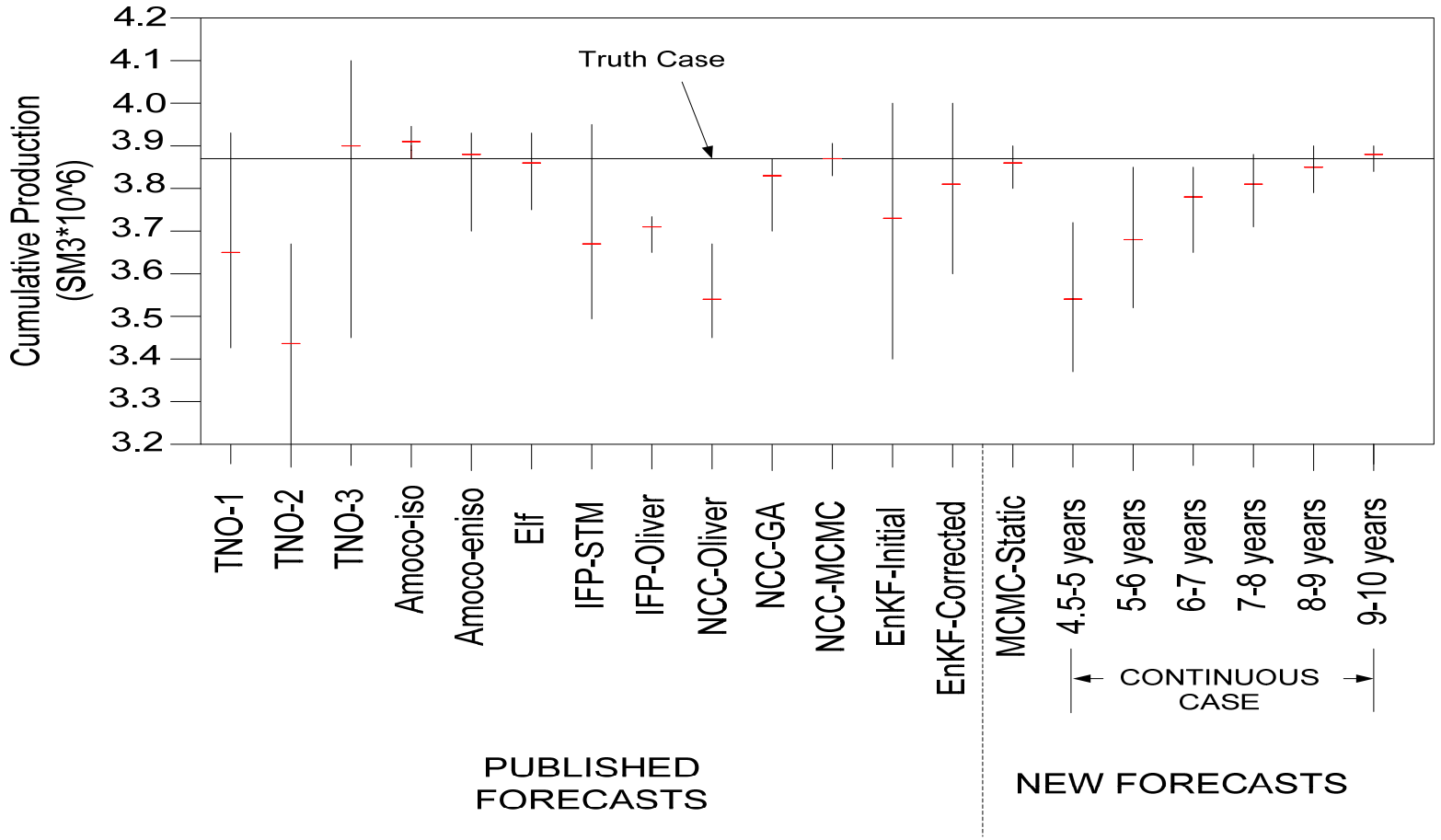

Fig. 44 - Synthetic test forecast compared. A comparison of forecasts from the synthetic continuous test to published forecast for the PUNQ reservoir

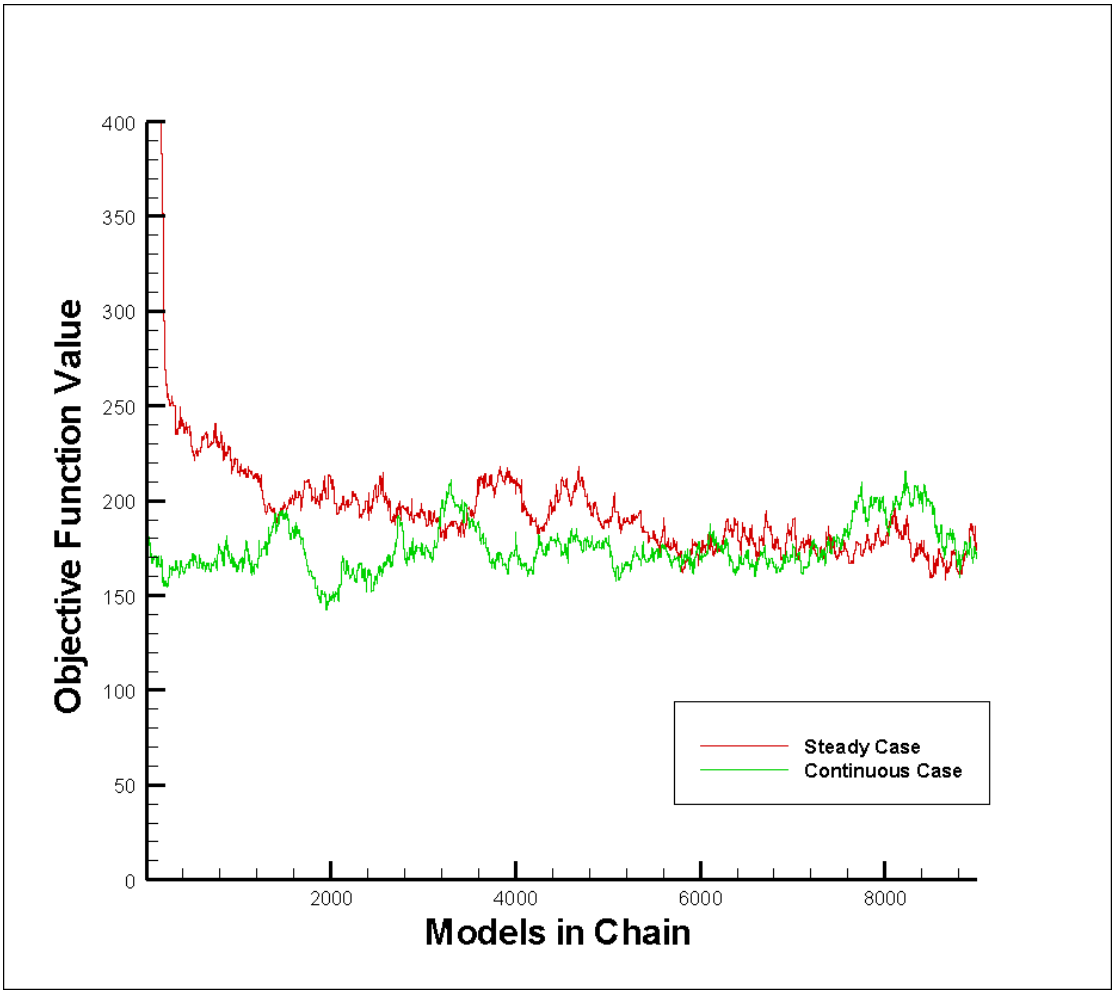

Fig. 45 - Comparison of objective function value between static case and continuous case, with 9,000 models made between years 9 and 10

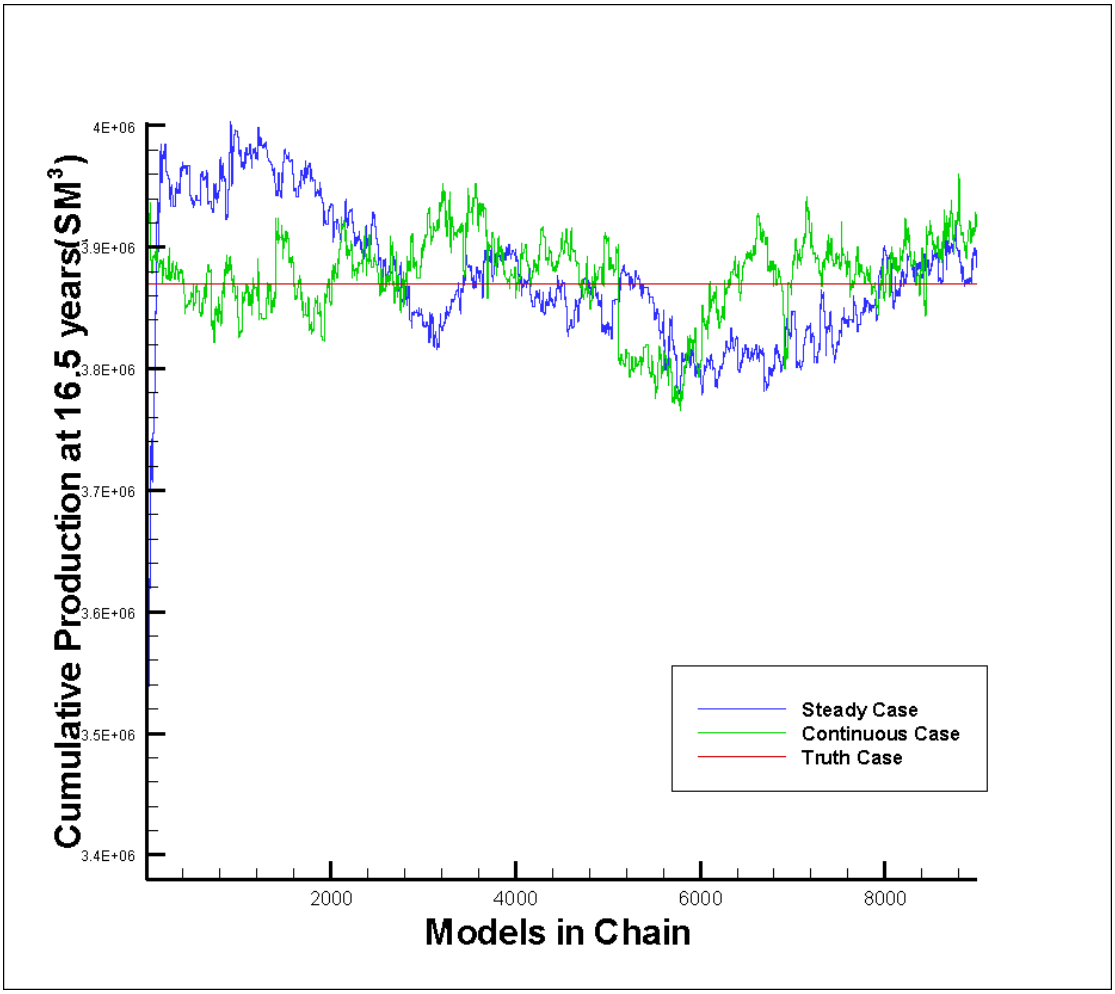

Fig. 46 - Comparison of forecasts between static case and continuous case, with 9,000 models made between years 9 and 10

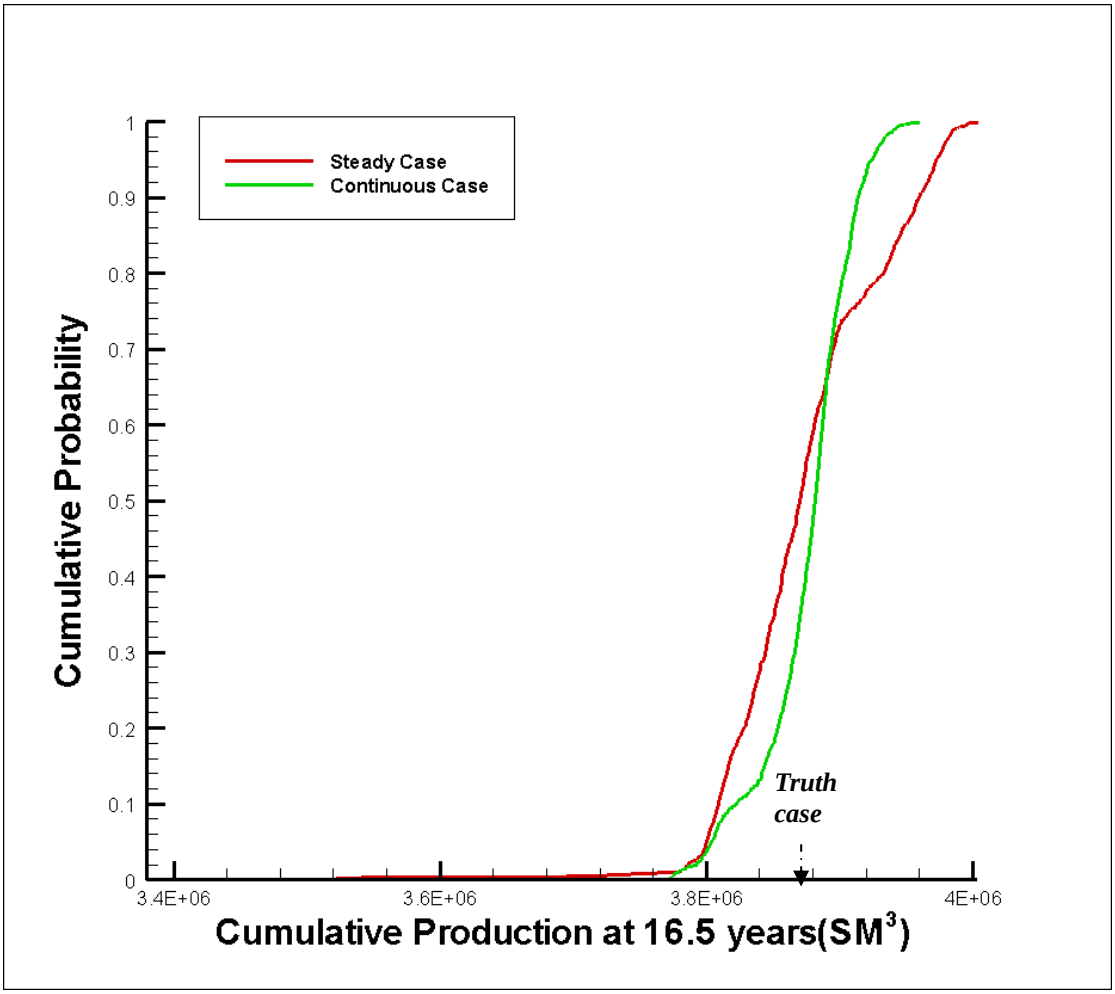

Fig. 47 - Comparison of cumulative production CDFs between static case and continuous case, with 9,000 models made between years 9 and 10

We can provide a probabilistic assessment of reservoir properties with all mixed-well sampled models in the continuous case, as was done in the static case. **Fig. 48** shows the CDFs of multipliers in certain regions. The posterior distribution of our parameter changes a lot from the prior in layer 4, region 4, where a well was completed. Without any well in layer 1, region 1, our posterior distribution is close to the prior because of little impact from the observed data. The improvement here is similar to the static case but with many fewer sampled models.

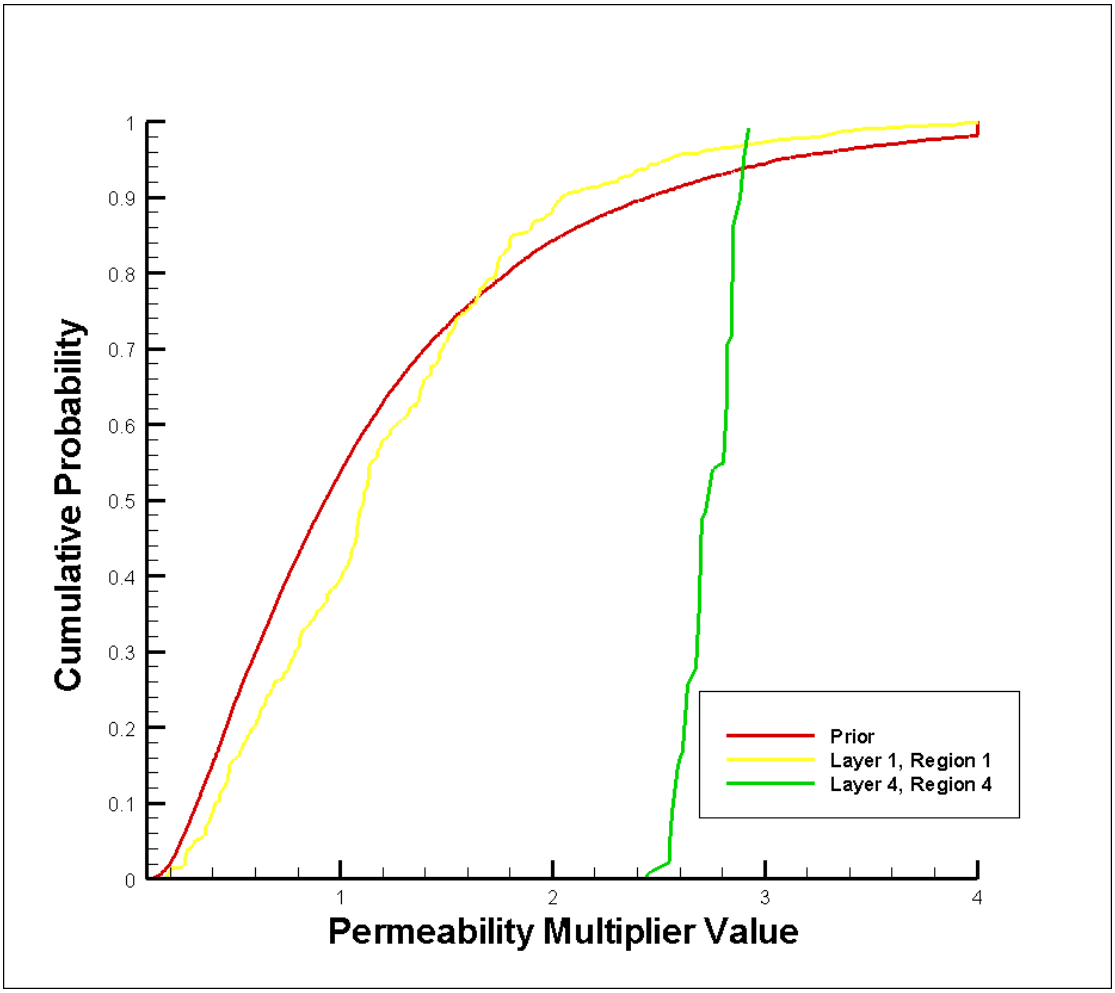

Fig. 48 - Posterior and prior distribution of permeability assessments (Continuous case)

Consider a more practical problem, one in which we want to generate a forecast CDF at a time when we do not have enough samples available since the data assimilation. There is more like what the continuous simulation process will be like in an actual field application, where the data acquisition rate is likely to be higher than the once per year assumed in the tests described thus far. In this situation, since the chain will likely not be long enough to build up the correct distribution, we will have to also rely on models sampled from previous years to build up the distribution. **Fig. 49** shows the CDFs obtained by combining two years of sampled models together. We can see the truth case still falls in the range of forecasts in the later years and the distributions move toward the truth case and narrow as in the forecasts obtained using only one year of models. Since the distributions were built up with samples over two years, models are sampled with different objective functions. **Fig. 50** shows an extreme case where the CDFs are obtained using all models from previous years for each forecast. Though the truth case falls in the range except for the first half year, the uncertainty range does not narrow as much over time because we retain all the uncertainty from all the previous years. In actual field applications where the data assimilation rate is much higher than we have assumed, the question remains of how many models back should be retained to generate reasonable posterior distributions. This will require a balance between retaining many samples (resulting in longer chains) versus retaining fewer samples (more uniform objective function definition).

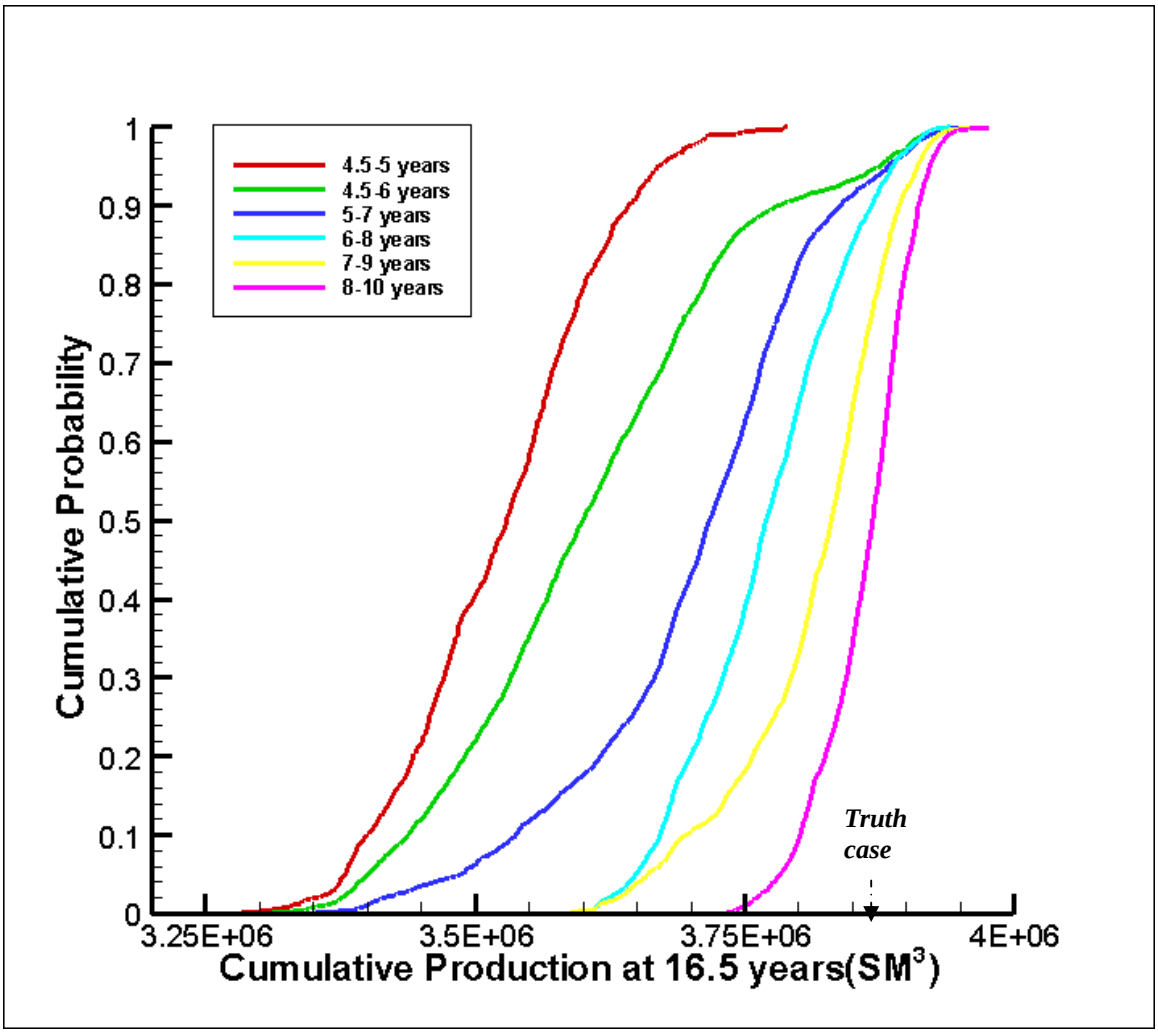

Fig. 49- Continuous test forecast CDFs. A comparison of the cumulative distribution functions for various forecasts made using two years of samples

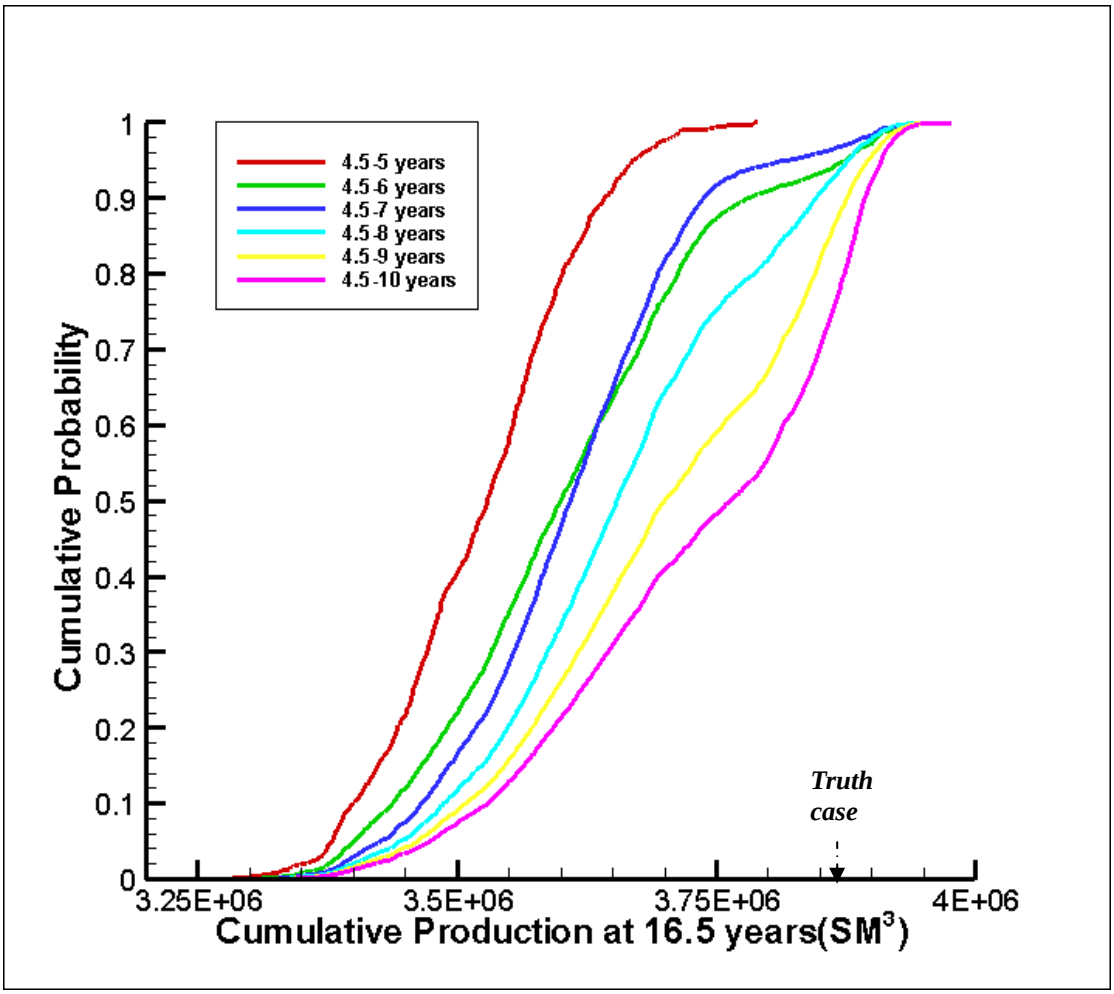

Fig. 50- Continuous test forecast CDFs. A comparison of the cumulative distribution functions for various forecasts made using all the models in previous years

Calibration of Uncertainty Estimates

Referring back to **Fig. 44**, we see that the first three forecasts failed to bracket the truth case, and the forecast made between 4.5 and 5 years is particularly far off. Thus, the uncertainty is underestimated in the early years. This could be due to either an underestimation of uncertainty in the prior distribution, or an underestimation in the error in the observed data. We would like to correctly quantify the uncertainty at all times, even when there is not much dynamic data available. In order to increase the uncertainty,

we can use a larger standard deviation in either our prior distribution or the observed data, or both. I increased the standard deviations of our prior multipliers in order to overcome this drawback. The permeability multiplier standard deviation was increased from 0..354 to 1 and the porosity multiplier standard deviation was increased from 0.3 to 0.5. **Figs. 51-56** show the forecasts generated using one year's worth of models and the enlarged prior distributions, while **Fig. 57** shows the CDFs of cumulative production for all the forecasts. **Fig. 58** summarizes the uncertainty ranges and compares them to the forecasts with the original prior distribution. Compared to the forecasts with the original prior, the enlarged prior standard deviation yields larger uncertainty ranges in the early year which bracket the truth case (between 4.5 and 5 years and between 5 and 6 years). The forecasts in the later years, however, are similar because of the larger impact of the likelihood function (observed data) in later years.

These results suggest another benefit of the continuous simulation approach – calibration of uncertainty estimates. However, our test was a synthetic test in which we know the truth case. Since we know the truth case, we could adjust the prior distribution until all the forecasts bracketed the truth case. How could this work in an actual field application in which we do not know the correct answer? The solution is suggested in **Fig. 58**. With the original prior, the posterior distributions shift in addition to narrowing. Subsequent distributions are not bracketed by previous distributions. In the enlarged prior case, however, subsequent distributions are essentially bracketed by all previous distributions, which is what we should expect to see in practice. To effect this in a continuous simulation application, one must monitor the posterior distributions generated over time.

If they shift in addition to narrowing, then this indicates uncertainty is being underestimated somewhere and either prior or data standard deviations should be increased. The previous posterior distributions can be regenerated with increasing standard deviations until they essentially bracket all subsequent posterior distributions.

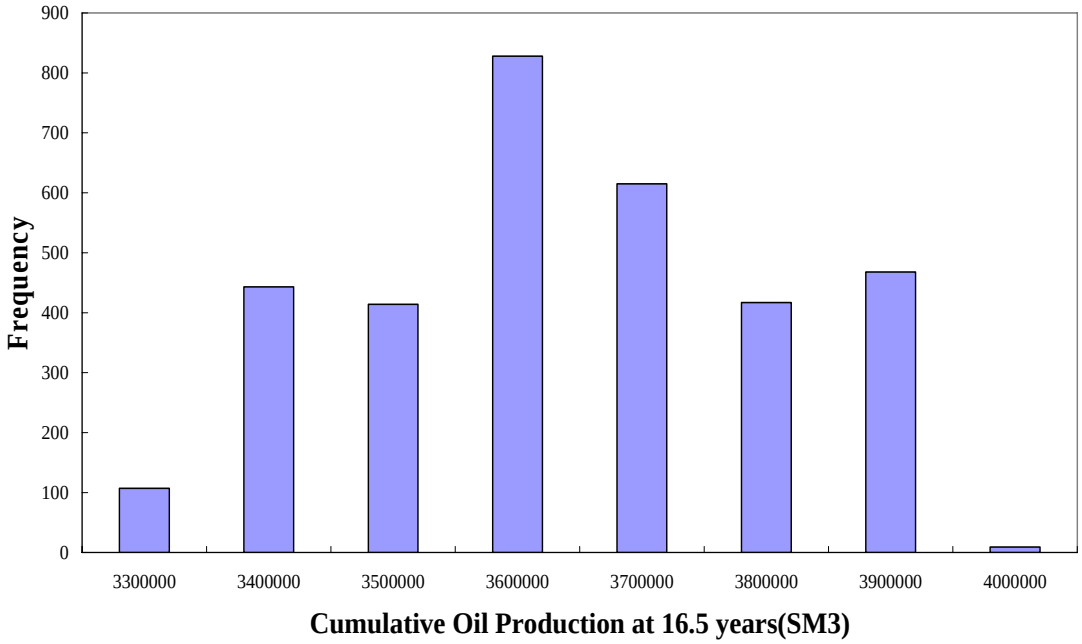

Fig. 51 - Continuous test forecast using model between 4.5 to 5 years (runs 1-4,500) with enlarged prior distribution

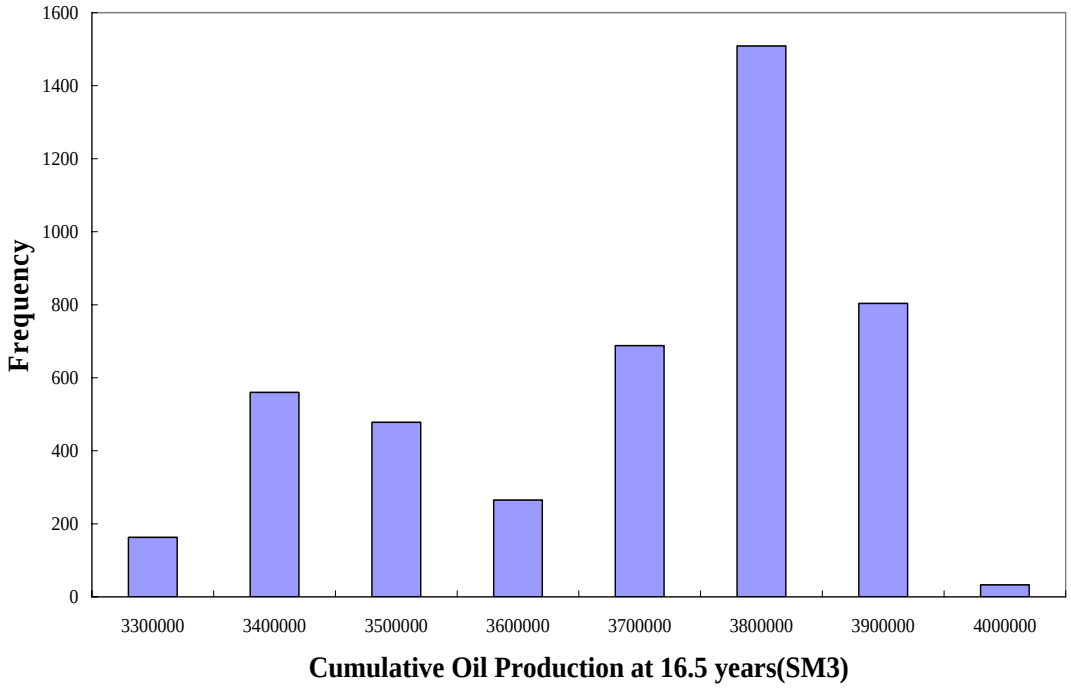

Fig. 52 - Continuous test forecast using model between 5 to 6 years (runs 4,501-13,500) with enlarged prior distribution

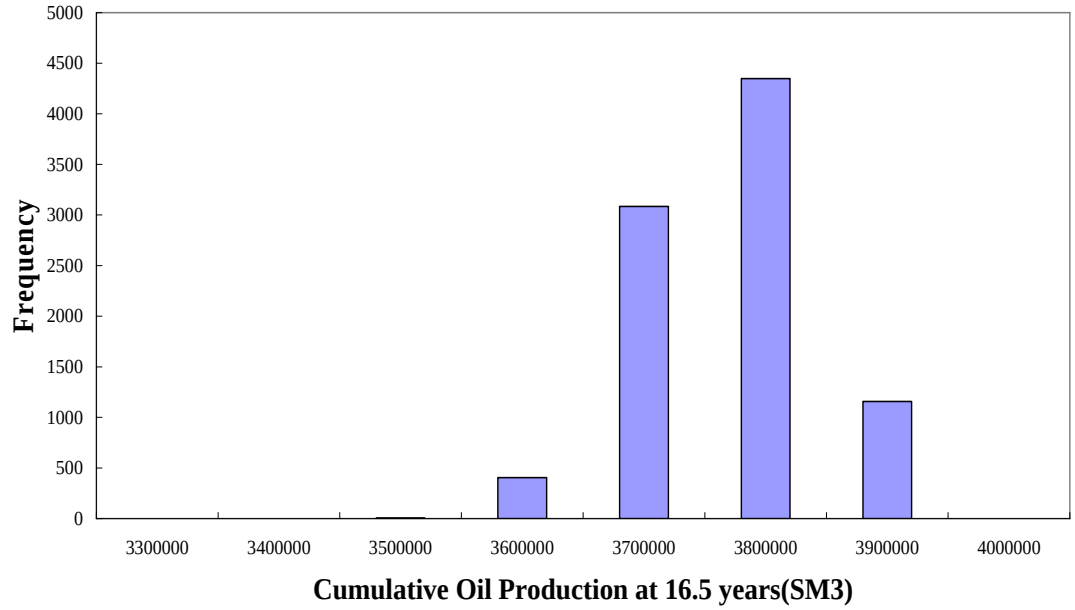

Fig. 53 - Continuous test forecast using model between 6 to 7 years (runs 13,501-22,500) with enlarged prior distribution

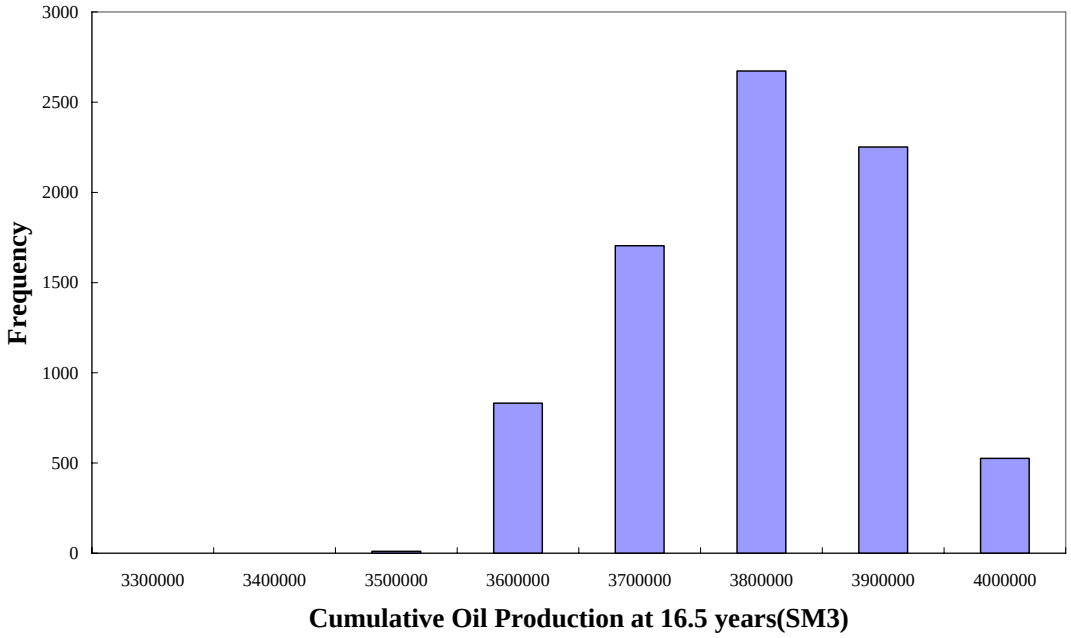

Fig. 54 - Continuous test forecast using model between 7 to 8 years (runs 22,501-31,500) with enlarged prior distribution

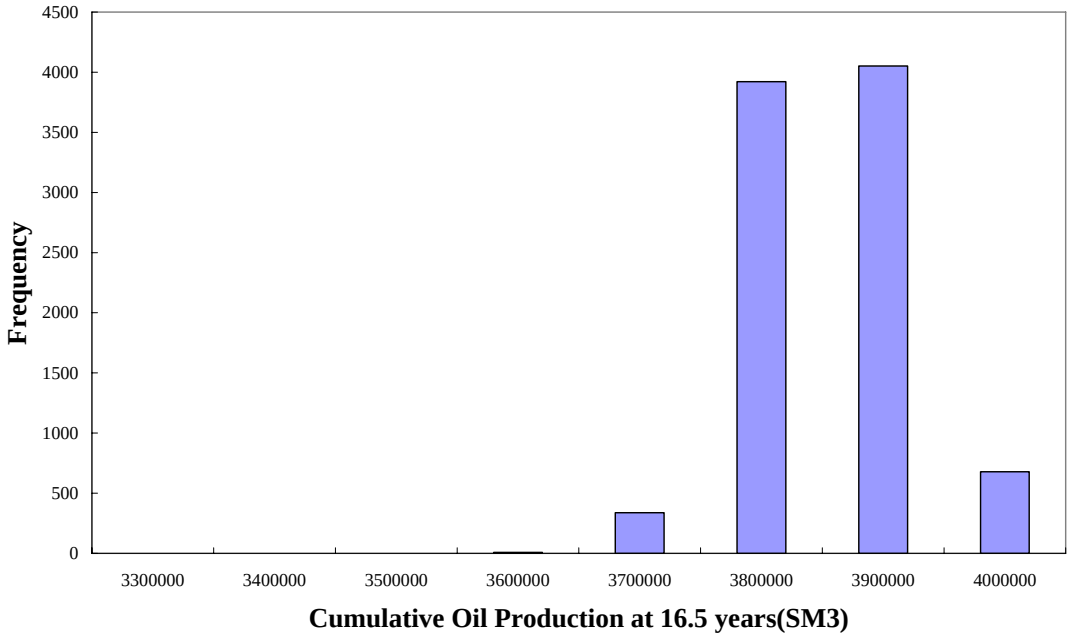

Fig. 55 - Continuous test forecast using model between 8 to 9 years (runs 31,501-40,500) with enlarged prior distribution

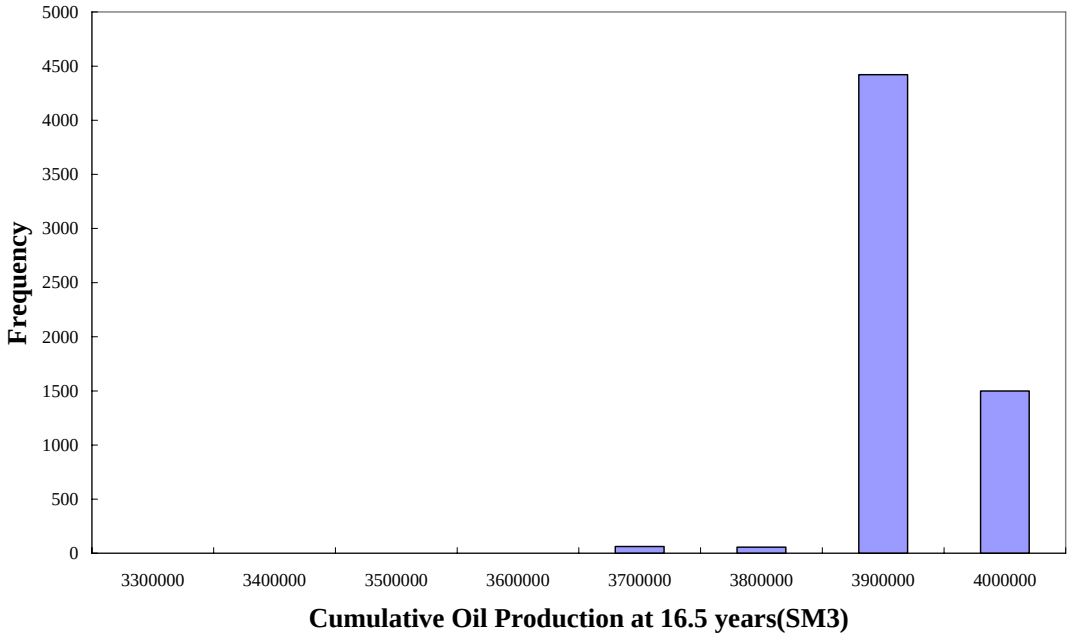

Fig. 56 - Continuous test forecast using model between 9 to 10 years (runs 40,501-49,500) with enlarged prior distribution

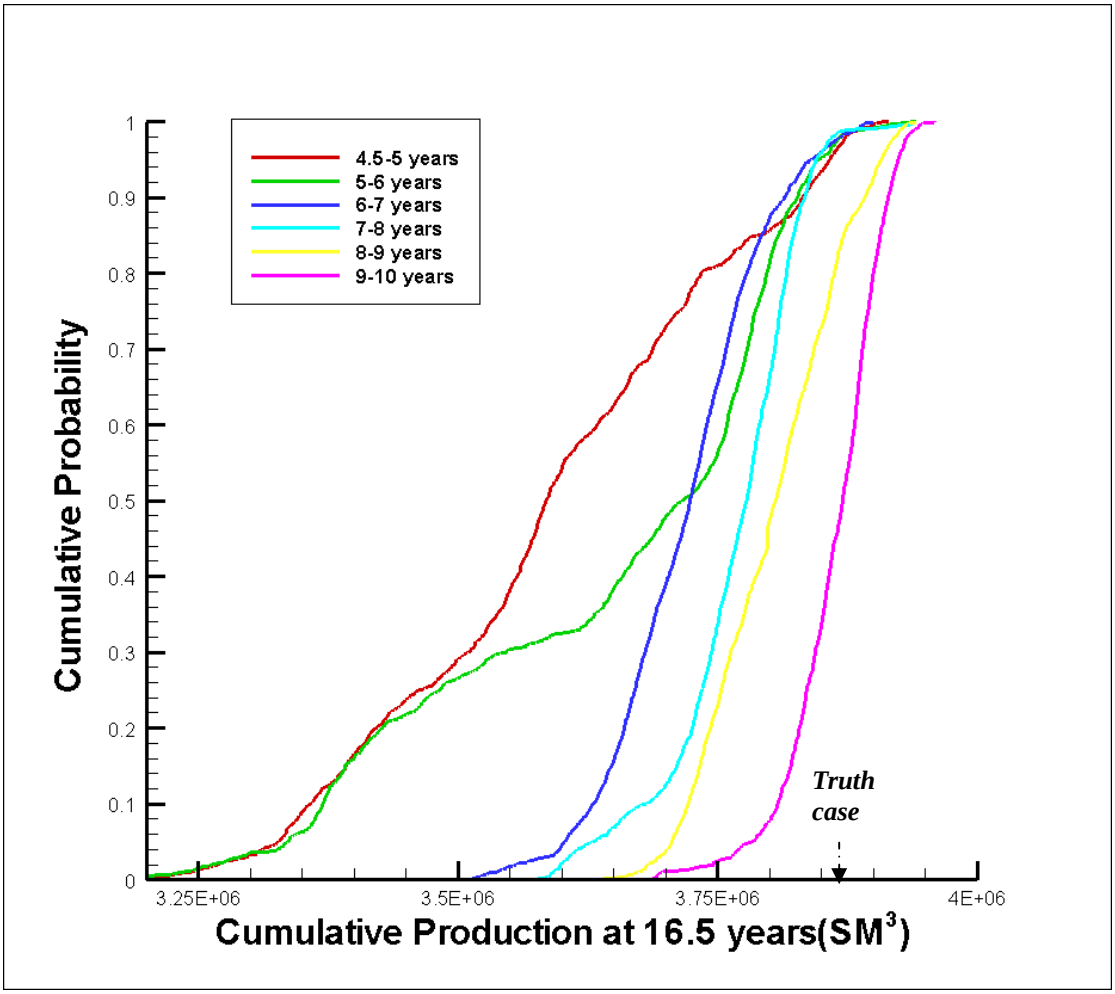

Fig. 57 - Continuous test forecast CDFs with enlarged prior. A comparison of the cumulative distribution functions for various forecast made during each year (or half year)

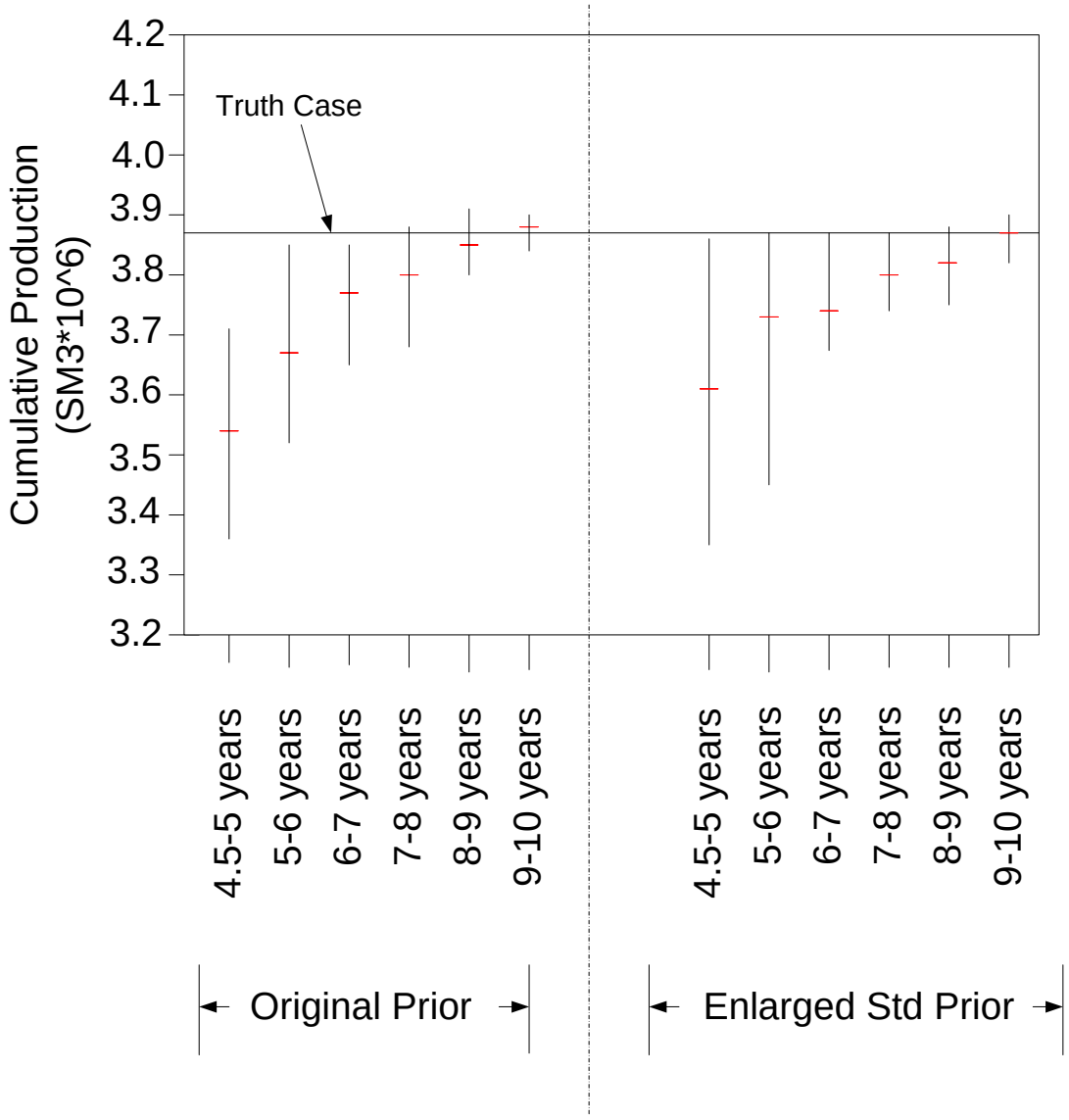

Fig. 58 - Continuous test forecasts compared. A comparison of forecasts between the original prior distribution and enlarged prior distribution

Summary of Results

By history matching continuously over the life of a reservoir, we see the uncertainty range narrowing with time and increased observation data. Compared to the static case, the continuous approach allows us to generate a reasonable forecast in a much shorter time (fewer models). This advantage should also allow us to consider more uncertain parameters in our parameterization, which should result in more reliable forecasts. In addition, in order to avoid the biased forecasts made in the early years, the continuous simulation approach provides a way of calibrating uncertainty estimates over time.

CONCLUSIONS AND RECOMMENDATIONS

Conclusions

The MCMC method is a strong tool for history matching and quantifying uncertainty. To the best of my knowledge, the work presented here is the first implementation of this continuous MCMC history matching process. We can draw the following conclusions from the tests described above:

1. The static study was consistent with the truth case in forecasts and consistent with results presented in the literature, demonstrating that a proper initial model and prior distribution were used. The uncertainty ranges narrow over time, as more information leads to less uncertainty. In addition, the test shows that we can make improvements to our assessments of reservoir properties.
2. The continuous study indicates that we can shorten the time to make a reasonable forecast compared to our static case, by continuing the chain with models that include more history information as new data are added over time. The continuous approach allows a more thorough exploration of the parameter than the static case by reducing the burn-in time of the MCMC process.
3. In the continuous case, the uncertainty ranges shift in addition to narrowing as time progresses. The continuous simulation approach provides a mechanism for calibrating uncertainty estimates over time. If it is observed that posterior distributions generated over time shift in addition to narrowing, then we can either enlarge the standard deviation of our prior distribution or our observed data to increase the uncertainty.

Adjustments should be made until subsequent posterior distributions are bracketed by all previous distributions.

Recommendations for Future Work

In conducting this study, several additional areas for future work were identified:

1. In my research, the tests were carried out on a synthetic model (PUNQ-S3). Even though the results demonstrate the benefit of a continuous simulation approach, it would be helpful to test this method on a live field.
2. Based on the numerous sampled models, it would be useful to withdraw a small set number of diverse models which represent the posterior distribution reasonably well. These models could then be used to generate probabilistic forecasts for other reservoir management decisions (for instance, where and when to drill a new well).
3. In this study, we used the random walk method to get the next sampling candidate. This method could be replaced by other improved methods which may generate a better set of samples, especially when the target distribution is multi-modal.
4. Making simulation runs continuously produces a large quantity of output data. Techniques for storing and managing this data will be necessary in order to run this process for long periods of time in actual field applications.

NOMENCLATURE

d_{obs} = Observed data

m = Uncertain parameters

μ = Prior mean

$P(m)$ = Prior probability distribution

$P(d_{obs}|m)$ = Likelihood function

$P(m|d_{obs})$ = Posterior distribution

$g(m)$ = Simulated reservoir response

C_m = Parameter covariance matrix

C_D = Data covariance matrix

$\pi(m)$ = Distribution function

m_n = Uncertainty parameters value at state n

$q(m|m_n)$ = Proposal distribution

R = Acceptance ratio

L = Likelihood function

y^{calc} = Calculated data from the simulator

y^{obs} = Observed data

c = Constant factor

$O(m)$ = Objective function

k_v = Vertical permeability

k_h = Horizontal permeability

ϕ = Porosity

ϕ' = Porosity value of base map

$\mu_{\log k_K}$ = Mean of log-normal horizontal permeability

$\sigma_{\log k_K}$ = Standard deviation of log-normal horizontal permeability

X_ϕ = Uncertainty multiplier of porosity

X_k = Uncertainty multiplier of permeability

$\mu_{\log X_K}$ = Prior mean of log-normal permeability multiplier

$\sigma_{\log X_k}$ = Prior standard deviation of log normal permeability multiplier

$P(X)$ = Prior multiplier distribution

C_x = Prior multiplier covariance matrix

μ_{X_ϕ} = Prior mean of normal porosity multiplier

σ_{X_ϕ} = Prior standard deviation of normal porosity multiplier

σ_i = Standard deviation of observed data

$P(d_{obs}|X)$ = Likelihood function of multiplier

$P(X|d_{obs})$ = Posterior distribution of multiplier

$O(X)$ = Objective function of multiplier

t_i = State i

t_{i+1} = State $i+1$

ε = 90-dimensional standard normal random variable

σ = Scale factor

REFERENCES

Barker, J.W., Cuypers, M. and Holden, L. 2001. Quantifying Uncertainty in Production Forecasts: Another Look at the PUNQ-S3 Problem. *SPE Journal* 6 (4): 433-441. SPE-74707-PA.

Bianco, A., Cominelli, A., Dovera, L., Naevdal, G. and Valles, B. 2007. History Matching and Production Forecast Uncertainty by Means of the Ensemble Kalman Filter: A Real Field Application. Paper SPE 107161 presented at the EUROPEC/EAGE Conference and Exhibition, London, U.K., 11-14 June.

Bos,C.F.M. *et al*. 1999. Production Forecasting with Uncertainty Quantification (PUNQ). Final report, Contract No. NITG 99-225 A (December).

Capen, E.C. 1976. The Difficulty of Assessing Uncertainty. *JPT* 28 (8):843-850. SPE-5579.

Craig, David P., Eberhard, Mike J. and Odegard, Chad E. 2005. Permeability, Pore Pressure, and Leakoff-Type Distributions in Rocky Mountain Basins. *SPE Production & Facilities* 20 (1): 48-59.

Devegowda, Deepak, Arroyo-Negrete, Elkin, Datta-Gupta, Akhil and Douma, S.G. 2007. Efficient and Robust Reservoir Model Updating Using Ensemble Kalman Filter With Sensitivity-Based Covariance Localization. Paper SPE 106144 presented at the SPE Reservoir Simulation Symposium, Houston, Texas, 26-28 February.

Floris, F.J.T., Bush, M.D., Cuypers, M., Roggero, F. and Syversveen, A-R. 2001. Methods for Quantifying the Uncertainty of production Forecasts: A comparative Study. *Petroleum Geoscience* 7: 87-96.

Gelman, Andrew and Rubin, Donald B. 1992. Inference from iterative simulation using multiple sequences(with discussion). *Statistical Science* 7 (4):457-472.

Givens, Geof H. and Hoeting, Jennifer Ann 2005. *Computational Statistics*. New Jersey: John Wiley & Sons Inc.

Goldberg, D.E. 1989. *Genetic Algorithms in Search, Optimization, and Machine Learning.* New York city: Addison-Wesley Publishing Co.

Greenberg, E. and Chib, S. 1995. Understanding the Metropolis-Hastings algorithm. *The American Statistican* 49 (4): 327-335.

Gu, Yaqing and Oliver, Dean S. 2004. History Matching of the PUNQ-S3 Reservoir Model Using the Ensemble Kalman Filter. Paper SPE 89942 presented at the SPE Annual Technical Conference and Exhibition, Houston, Texas, 26-29 September.

Hastings, W. K. 1970. Monte Carlo Sampling Methods Using Markov Chains and Their Applications. *Biometrika* 57 (1): 97-109.

Holden, L. 1998. Adaptive chains. Technical Report. Norwegian Computing Center (November 1998).

Holmes, Jay C., McVay, Duane A. and Senel, O. 2007. A System for Continuous Reservoir Simulation Model Updating and Forecasting. Paper SPE 107566 presented at the Digital Energy Conference and Exhibition, Houston, Texas, 11-12 April.

Howard, R.A. 2005. Decision Analysis, class notes, Department of Management Science and Engineering, Stanford University, Stanford,CA.

Liu, Ning and Oliver,Dean S. 2003. Evaluation of Monte Carlo Methods for Assessing Uncertainty. *SPE Journal* 8 (2): 188-195. SPE- 84936.

Ma, X., Al-Harbi, M., Datta-Gupta, Akhil and Efendiev, Y. 2006. A Multistage Sampling Method for Rapid Quantification of Uncertainty in History Matching Geological Models. Paper SPE 102476 presented at the SPE Annual Technical Conference and Exhibition, San Antonio, Texas, 24-27 September.

Nævdal, Geir, Johnsen, Liv Merethe, Aanonsen, Sigurd Ivar, Hydro, Norsk and Vefring, Erlend H. 2003. Reservoir Monitoring and Continuous Model Updating Using Ensemble Kalman Filter. Paper SPE 84372 presented at the SPE Annual Technical Conference and Exhibition, Denver, Colorado, 5-8 October.

Thakur, G.C. 1996. What is reservoir management? *JPT* 48 (6):520-525.

Thomas, G.W. 1986. The Role of Reservoir Simulation in Optimal Reservoir Management. Paper SPE 14129 presented at the SPE International Meeting on Petroleum Engineering, Beijing, 17-20 March.

Vose, D. 2000. *Risk Analysis: A Quantitative Guide*. Second edition, New York city: John Wiley&Sons Inc.

VITA

Name:	Chang Liu
Address:	Harold Vance Department of Petroleum Engineering 3116 TAMU, College Station, TX 77843-3116
Email Address:	chang.liu@pe.tamu.edu
Education:	B.A., Applied Mathematics, Peking University, 2006 M.S., Petroleum Engineering, Texas A&M University, 2008